LOW-COST GPS SYSTEMS FOR INTERMEDIATE SURVEYING AND MAPPING ACCURACY APPLICATIONS

MUSTAFA D. SUBARI

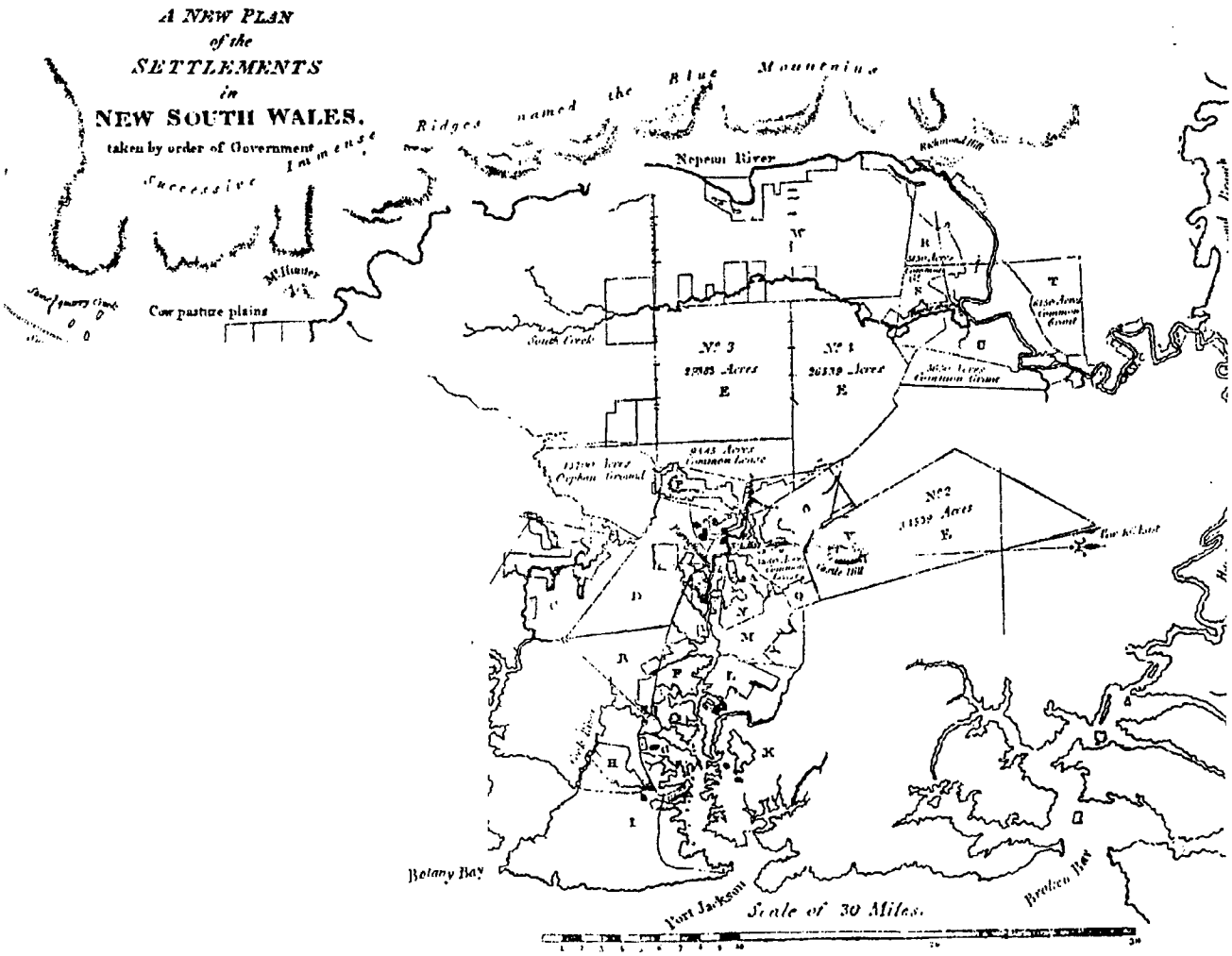

UNISURV S-50, 1997

Reports from

SCHOOL OF GEOMATIC ENGINEERING

THE UNIVERSITY OF NEW SOUTH WALES SYDNEY NSW 2052 AUSTRALIA

UNISURV REPORT S-50, 1997

LOW-COST GPS SYSTEMS FOR INTERMEDIATE SURVEYING AND MAPPING ACCURACY APPLICATIONS

MUSTAFA D. SUBARI

Received: December, 1996
Accepted: August, 1997

SCHOOL OF GEOMATIC ENGINEERING
UNIVERSITY OF NEW SOUTH WALES
SYDNEY NSW 2052
AUSTRALIA

National Library of Australia

Card No. and ISBN 0 85839 075 2

ABSTRACT

GPS for high and ultra-high surveying accuracy applications is now a mature and established technology. System requirements, field procedures and data processing strategies to achieve these high accuracies have been standardised. However, in the intermediate accuracy range such specifications are not available. As a result, there is a tendency within the surveying community to use a high accuracy system for all types of surveying applications, regardless of the accuracy requirement. This practice results in a high investment cost for GPS technology, even if intended for intermediate accuracy surveying applications. Hence, this constraints the adoption of GPS by surveying practices.

Realising the important of this issue, investigations were carried out on options for low-cost GPS systems and their performance characteristics, which are more appropriate for use in the intermediate accuracy applications. In particular, benchmarking tests have been carried out to establish the achievable accuracy of these systems, and the level of reliability associated with this accuracy, with respect to some observational conditions and constraints.

For the purpose of evaluating a GPS system, a performance benchmarking procedure has been designed and implemented in these investigations. Results from the tests have been able to identify the performance characteristics of these systems.

TABLE OF CONTENTS

LIST OF TABLES

LIST OF FIGURES

ACKNOWLEDGEMENTS

Alhamduli'Llah, praise be to Allah Subhanahu Wata'ala that finally, I was able to finished my work.

Next, I sincerely thank my supervisor, Prof. C. Rizos, for his guidance and help in the warmest way. Indeed I have learned from him many more things beside GPS. I also like to thank the Survey Navigation And Positioning (SNAP) Group in the School, in particular to Mr. B. Hirsch, for his wonderful help on the computer hardware and software, as well as the entire past and present members, and also to all the staff of the School of Geomatic Engineering (formerly the School of Surveying).

I would also like to express my thanks to colleagues at the Department of Geodesy, Institut Teknologi Bandung, Indonesia, for their help and assistance in the first field campaign. Colleagues at the Department of Geodesy and Space Study, Universiti Teknologi Malaysia, who helped me in the second campaign, I thank you. My employer, Universiti Teknologi Malaysia and the Government of Malaysia are acknowledged for the study leave and financial support they granted throughout this period. The Malaysian Student Department in Sydney is also acknowledged for their help and support, especially in the last period of our stay in Australia. Not forgetting our friends in all-over Australia, that helps making our stay in this foreign land, a meaningful one.

Last, but not least, my special thank goes to my wife, Nor Yani Md Tan, who substituted my absent for my children Wardah, Salwa, Ahmad and Shakir. Their sacrifices have indeed made this struggle a worth full one. Finally, I thank my beloved mother, for the constant prayers she offered for us.

Chapter 1

INTRODUCTION

1.1 GPS Positioning and Mapping Applications

The NAVSTAR Global Positioning System (GPS) is a passive, all-weather, satellite-based radio navigation and positioning system operated by the U.S. Department of Defense. Initially developed to support military navigation requirements for a point positioning capability based on the use of transmitted code measurements, the system has found ever increasing usage by civilians. A recent study by the U.S. National Academy of Public Administration reports that nine out of ten GPS receivers today are being purchased by civilian users (GPS World, 1995a).

The applications of GPS are growing rapidly, with new applications being identified on a daily basis. The "GPS World" magazine sponsors a competition for new and novel GPS applications every year, attracting hundreds of entries. One general classification of GPS uses (apart from the military) is the following (Rizos, 1996);

- *Surveying and Mapping* - on land, at sea and from the air. The applications are of relatively high accuracy, in both the stationary and moving (or kinematic) mode.
- *Land, Sea and Air Navigation* - including enroute as well as precise navigation, vehicle tracking, cargo monitoring, etc.
- *Search and Rescue Operations* - including collision avoidance and rendezvous functions.
- *Spacecraft operations* - spacecraft navigation, positioning and manoeuvre.
- *Recreational use* - on land, at sea and in the air.
- *Other specialised uses* - time transfer, automatic and continuous operations guidance, etc.

This research has focused only on the use of GPS in the *surveying and mapping* application area.

For surveying and mapping applications, the advantages of GPS as a positioning tool, compared to traditional surveying methods, have now been widely recognised and thus boosted the acceptance of GPS for surveying. In fact, the surveying community can be considered the pioneers in developing GPS for higher accuracy positioning. Among the advantages of GPS for surveying and mapping are (Ibid, 1996);

- Intervisibility between stations is not necessary, hence
- points can be chosen where they are required (and not restricted to mountain tops, to satisfy intervisibility requirements of traditional surveys), thus offering greater flexibility in network design.
- The system is independent of weather conditions, and
- the service is available 24 hours a day, hence there is no restriction to the "effective" working period.
- Position accuracy is largely a function of interstation distance and not of network "shape" or "geometry".
- Provides three-dimensional information.
- Generally less field-data-collection-time is required to "cover" a given distance or area.
- High homogeneous accuracy can be obtained with relatively little effort.
- Easy interconnectability to other survey points or networks, even on a global scale.

1.1.1 GPS Positioning Accuracy

GPS positioning can be carried out in two modes: (1) absolute or point positioning, and (2) differential or relative positioning. **Absolute positioning** requires the determination of the position of an object in relation to a well-defined reference system; in the case of GPS it is the WGS84 (World Geodetic System 1984) reference frame. **Relative positioning**, on the other hand, is concerned with the determination of the position of an object relative to another object. The dynamics of the object being positioned can also be classified according to whether it is static or kinematic. Survey monuments are an example of a static object, while positioning a moving ship is a kinematic example.

GPS was explicitly developed for low to moderate accuracy real-time kinematic positioning, utilising the pseudo-ranges codes modulated on the signals. Two levels of services were provided: (a) the Precise Positioning Service (PPS) reserved for the military and designed to offer 10-20 m accuracy; and (b) a lower level Standard Positioning Service (SPS), freely available to all users. The accuracy of SPS was intended to be an order of magnitude worse than the PPS, however, after extensive

testing it was found to be significantly more accurate than expected, achieving accuracies of a few decametres. A deliberate policy known as "Selective Availability" was then introduced (Georgiadou & Doucet, 1990), whereby the U.S. Department of Defense intentionally degraded the accuracy of the SPS. The accuracy level was first set to approximately 500m in the horizontal (at the 95% confidence level), and subsequently changed (in July 1990) to 100m horizontal and 150m vertical, at the 95% confidence level. Note that such a policy is aimed at the real-time (that is navigation) capability of the system, and has marginal effect on other users. At the time of preparation of this thesis (April, 1996), this is the assured positioning accuracy since the declaration of GPS Full Operational Capability in April 1995.

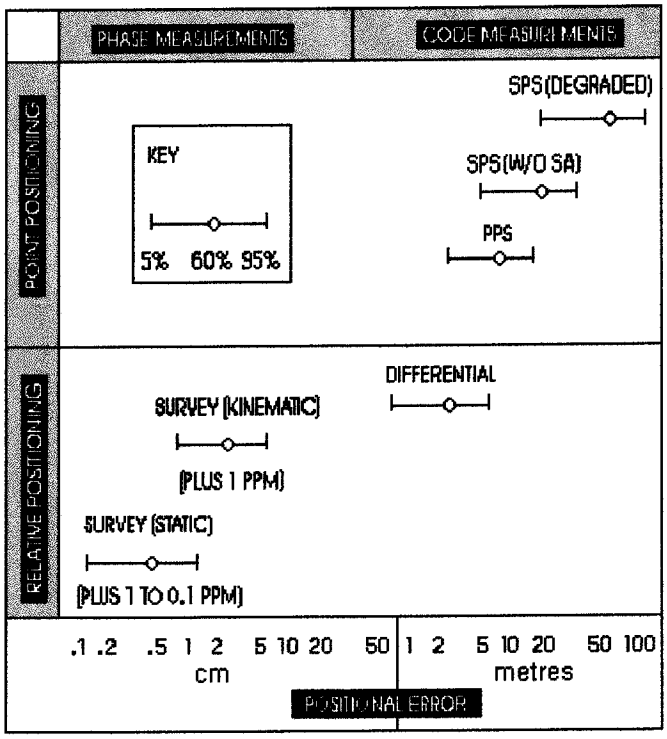

Note: SA - Selective Availability, SPS - Standard Positioning Service, PPS - Precise Positioning Service, ppm - parts per million.

Figure 1.1: GPS Positioning Accuracies (after Rizos, 1996)

In the relative positioning mode GPS has proven to be able to give positioning accuracy better than conventional surveying methods (see Figure 1.1), even long before the full satellite constellation was launched. Relative positioning accuracies of few parts per million were reported about 10 years ago (e.g., Bock et al.,1985; Goad,1985; Beutler et al., 1987b), and these days, special techniques deliver even a few parts per 100 million

(e.g., Blewitt, 1989). (Part-per-million, or ppm, is the ratio of the error to one millionth of the baseline length, for example 10 ppm translates into 10 mm for a 10 km baseline).

1.1.2 Mapping Accuracy Requirements

One convenient classification scheme for surveying and mapping applications is in terms of their accuracy requirements. Three classes of applications can be distinguished on this basis, for which the range of relative accuracies are assumed to be from low-moderate to ultra-high accuracies (Table 1.1, adapted from Rizos, 1996).

Table 1.1: Class of Activity and Mapping Accuracy

Class	Type of work	Accuracy
Class A	Scientific	better than 1 ppm
Class B	Geodetic	1 to 10 ppm
Class C	General surveying	lower than 10 ppm

Class A surveys primarily encompass those surveys undertaken for precise engineering, deformation analysis and geodynamic applications. Class B surveys include geodetic surveys undertaken for the establishment, densification and maintenance of control networks to support mapping. Class C surveys primarily encompass lower accuracy surveys, primarily undertaken for urban, cadastral, geophysical prospecting, Geographic Information System (GIS) data capture and other general purpose mapping applications.

Hence the **intermediate accuracy range** is considered here as the positioning accuracy in the range of sub-decimetre (few cm) to one or two metres, for baseline lengths up to about 10 kilometres. In terms of relative positioning, it refers to somewhere between 10 to 100 ppm. The positioning and mapping applications in this accuracy range is very wide, and includes the very important GIS data capture activity.

GPS as the new tool for surveying has proven to be able to address all types of surveying applications. The high and ultra-high accuracy classes have in fact driven phase-based GPS technology development. System requirements, field procedures and data processing algorithms have become, to a large extent, standardised. Unfortunately, in the intermediate to low-accuracy class of applications, GPS has been introduced in "free-for-all" fashion, with hardly any standardisation or guidelines. One example is the adoption of GPS as a "real-world-digitiser" for GIS (Masters et al., 1993; 1994), which has been

driven mainly by the GPS and GIS vendor-product developers, rather than by objective standards and specifications for the positioning task. There is therefore a need to develop some standards and specifications for the use of the GPS technology for this class of surveying and mapping applications.

1.2 Motivations for the Investigations

(a) Dual-Frequency Paradigm

Survey activity using single-frequency GPS receivers are restricted due to the major limitation of single frequency instrumentation, the inability to account for the ionospheric delay (Seeber, 1993; Leick, 1995; Rizos, 1996). Dual-frequency receivers on the other hand, are able to eliminate the ionospheric signal delay and also provide a distinct advantage in carrier-phase ambiguity resolution which, is the key to precise positioning in rapid static or kinematic modes, albeit at a relatively high cost (Hofmann-Wellenhof et al.,, 1994; Rizos et al., 1995). Single-frequency receivers are therefore generally considered to be unsuitable for most high accuracy surveying applications. To some extent, however, the attitude of the GPS surveying community nowadays is to insist on using dual-frequency receivers for all positioning tasks. This research seeks to study the extent to which inexpensive C/A-code single-frequency GPS systems can be used for survey applications, and in particular their "performance characteristics". A special focus therefore has been the low-cost GPS hardware systems.

(b) The Full Operational Capability of GPS

On April 27, 1995, GPS was given the 'Full Operation Capability' status, implying that with the 24 Block II satellites in orbit, the system met all the requirements specified in several formal performance and requirements documents (GPS World, 1995b). However, for applications other than those satisfied with standard point positioning (using the SPS or PPS), it would be necessary for the user to carry out "bench-marking" tests of the system, in order to determine the performance characteristics.

(c) GPS Systems Specifically Intended for the Intermediate Accuracy Applications

High precision surveying (1-10 ppm accuracy) is generally addressed using top-of-the-line GPS hardware and software (Hofmann-Wellenhof et al., 1994), while low precision positioning (100 metre accuracy, e.g., in support of most navigation requirements) has been addressed by inexpensive 'navigation-type' GPS receivers (Rizos et al., 1995). Differential GPS system (DGPS), on the other hand, delivers accuracies in the range of 2-5 metres (Ackroyd & Lorimer, 1990; Kalafus, 1991). However, between the systems intended for DGPS and high precision surveying applications, that is, those intended to

address accuracies in the subdecimetre to metre level range, no clear guidelines on instrumentation and procedures are available (Subari and Rizos, 1995b). This is the accuracy range that these investigations have focused on.

(d) GPS System Cost

The cost of a standard GPS surveying system involving dual-frequency hardware is relatively high (Subari & Rizos, 1995a; Rizos et al., 1995). Yet there are many low-cost instruments, some classified as being intended for navigation applications, others not so clearly 'labelled', which can measure phase, or phase-related data. These measurements, which hold the key to high accuracy positioning, also have the potential for use in the low to intermediate accuracy applications area. Given 'moderately' sophisticated data processing software, a suitable hardware-software system can be developed. This research project proposes several hardware-software configurations for such low to intermediate accuracy systems.

(e) Intermediate Accuracy GPS Applications

Although the focus of GPS for surveying and mapping applications are generally concerned with the high accuracy ones, there is an expanding interest GPS to satisfy those applications that require only intermediate accuracy. An example is 'GPS for GIS', a relatively "new" GPS application, for which standards and specifications concerning the appropriate systems to use for specific tasks have not been developed. This research project seeks to establish specifications for low-cost GPS systems which are intended to address this intermediate accuracy range.

(f) Improvements in the C/A-Code Observations

C/A-code pseudo-range data is used for point positioning in navigation, but not in surveying. One investigation of the use of C/A-code data for surveying was reported by Lukac and Zhuang (1989), but only reported obtaining positioning accuracy of about 7 metres. Recent developments of 'narrow-correlator' C/A-code tracking technology, enabling high precision C/A-code measurements, reports that submetre accuracy is achievable (Cannon & Lachapelle, 1992; Lachapelle et al., 1992, 1993). The NovAtel GPSCard Series are the first implementation of this technology (Fenton et al.,1991). With this hardware, C/A-code pseudo-range measurements might be useful for low and intermediate accuracy surveying, as well as for navigation use. This research project investigates the utility of such 'narrow-correlator' data.

(g) The High Cost of RSP Systems

Most of the commercially available rapid-static-positioning (RSP) systems employ dual-frequency GPS hardware, such as Leica's SR299 and SR399 receiver, Ashtech Z-12, and the Trimble Surveyor^{tm} based on the 4000SSi receiver (Philips Business Information, 1995). RSP systems based on single-frequency GPS receivers (RSP-L1) are rare. This research investigates the capabilities of a low-cost RSP-L1 system based on single-frequency GPS receivers.

Research Statement

The objective of this research is to investigate the performance characteristics of several low-cost GPS systems. In particular it is intended to study how variable the positioning accuracy is as a function of parameters over which the observer have little control, such as: satellite geometry, multipath and other signal disturbances. It is intended to determine the relationship(s) between accuracy and reliability on the one hand, and operational issues such as baseline length, observation session lengths, etc., on the other hand.

1.3 Methodology and Scope of the Research

The performance of a low-cost GPS system will depend on factors such as; (1) the system configurations, (2) the signal disturbances, and (3) the operational conditions (Figure 1.2). System configuration consist of two elements; the hardware and the software. The hardware, i.e., the GPS receiver, will determine the type of measurement, and hence the precision of the observation data. The software, i.e., the data processing algorithm, will determine the level of treatment of the biases in the observation data. Signal disturbances which will affect the quality of the observation data includes the atmospheric biases, i.e., the ionospheric and the tropospheric delays, and the multipath. The operational conditions, on the other hand, are issues such as; Selective Availability, satellite geometry, baseline length, and length of observation session.

In these investigations, the performance of several low-cost GPS systems are studied in relations to parameters which includes; observation session length, baseline length, satellite geometry and the atmospheric effect. The multipath effect is not studied.

In order to facilitate the performance investigations, seven low-cost GPS system configurations have been identified in this research. Each system is identified according to the type of measurement and data processing algorithm used. Two low-cost GPS

receivers were used; (1) NovAtel GPS receiver, a GPSCard Performance Series Model NR915; and (2) Trimble SVeeSix GPS receiver.

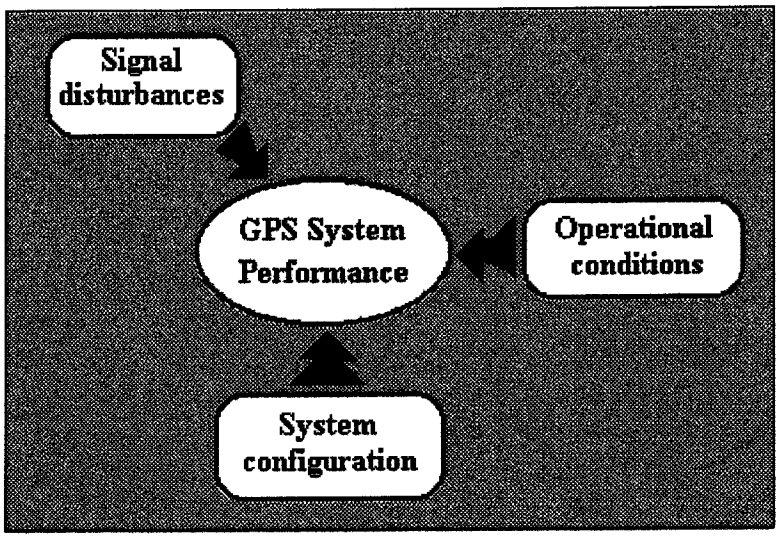

Figure 1.2: Factors affecting GPS system performance.

Two field campaigns have been observed. The first campaign was done in Bandung, Indonesia, involving seven baselines ranging in length from 1.9 to 16.5km. The second campaign was done in Johor Bahru, Malaysia, involving three baselines ranging in length from 5.5 to 34.9km. The baseline lengths were chosen to represent the likely 'scale' of most medium accuracy mapping applications. Furthermore, the baselines have been observed in view of accommodating the implementation of the low-cost GPS system as a stand-alone system, i.e., low-cost receiver - low-cost receiver baseline, or using it with a standard system, i.e., low-cost receiver - standard surveying receiver baseline. Both campaigns were purposely selected to be on the tropical and equatorial locations, with the aim to carry out the tests in the 'worst' ionospheric affected area, a condition that was expected in this region.

The observation has been carried out for 24 hour span in order to sample all satellite distribution geometry, as well as varying atmospheric contributions.

A baseline computation package, BASEPACK, has been developed by the author to process the data according to each system configuration. Varying observation length, namely; single-epoch, 1, 2, 5, 10, 30 and 60 minute spans have been processed.

Results of the baseline solution were then used to analyse the performance characteristics of these low-cost GPS systems.

1.4 Research Objectives

The objectives of this investigation are therefore:

- *To investigate the achievable accuracy of several low-cost GPS systems,*
- *To investigate the variability of the accuracy performance of these systems,*
- *To investigate the factors influencing baseline accuracy and its reliability.*

1.5 Outline of the Dissertation

This dissertation consists of nine chapters.

Chapter 1 introduces the research topic, the background studies and the motivation for the research, describes the research objectives, and the anticipated contributions from it.

Chapter 2 discusses the Global Positioning System and the achievable positioning accuracy. Factors influencing the positioning accuracy are reviewed and the options for addressing them for single-frequency users are discussed.

Chapter 3 addresses the intermediate surveying and mapping accuracy applications. Issues concerning the accuracy standards and requirements are discussed vis-a-vis the use of the Global Positioning System.

Chapter 4 describes the low-cost GPS system configurations, which includes the hardware and software. A case study concerned with the technicalities of mixing a low-cost GPS receiver and a standard surveying GPS receiver is also included.

Chapter 5 describes the data reduction algorithms suitable for use with low-cost GPS systems. The algorithms are restricted to those appropriate for single-frequency observables.

Chapter 6 introduces the data processing algorithm for the Rapid Static Positioning using single-frequency data.

Chapter 7 describes the two field campaigns that have been carried out for this research, and the low-cost GPS system configurations tested in these investigations.

Chapter 8 describes procedures of the analyses, results of the two campaigns, and the analyses made on the results.

Chapter 9 summarises the investigations, draws conclusions on the findings, and makes recommendations.

1.6 Contributions of this Research

The contributions of this research can be summarised as follows:

i. A comprehensive analysis of low-cost GPS positioning systems has been carried out.

ii. The characteristics of GPS systems able to satisfy accuracy requirements in the range of sub-decimetre to one or two metres have been identified.

iii. Extensive reliability studies of several low-cost GPS systems have been carried out.

Chapter 2

POSITIONING WITH GPS

2.1 Positioning with the Global Positioning System

GPS is a satellite-based *navigation system* which utilises range measurements to multiple satellites. Each GPS satellite transmits a unique signal modulated with several binary codes. Two types of ranging codes are used, the Coarse Acquisition (C/A) code intended for public use under the Standard Positioning Service (SPS), and the Precise (P) code intended to support the military's Precise Positioning Service (PPS). The precise codes are modulated on the two L band carriers, the P1 on the L1 carrier (nominal frequency of 1575.42 Mhz), and the P2 on the L2 carrier (nominal frequency of 1227.60 Mhz). The C/A-code is modulated only on the L1 carrier. The accuracy of horizontal positioning for the SPS and PPS is 100m and 30m, at 2.drms, respectively (Rizos, 1996) (2.drms = 2 x distance root mean square, is a position uncertainty measure, expressed in the form of circle for 2-dimension (2-D), or sphere for 3-dimension (3-D)).

The phases of the L1 and L2 carrier waves can also be measured, with a ten to one hundred fold higher precision than using the codes. This technique is sometimes referred to as "GPS interferometry". However, the problem with carrier phase measurements is that they are essentially ambiguous ranges. Only the fractional component is measured and the accumulated phase counted precisely, but the total integer number of cycles from the satellite to the receiver are unknown. Fortunately, this bias can be handled by appropriate data processing algorithms and observation strategies developed particularly by the precise surveying community.

2.2 GPS Observables

There are three basic GPS observables: code-ranges, carrier-phases and Doppler. These observables can be measured on either of the two carrier waves, L1 and L2. The C/A-code is only available on the L1 carrier, while the P-codes are available on both carrier

waves. Measurements can be made on either or both of the carrier waves itself. Another observable is the instantaneous Doppler measurement, which can also be made on both frequencies. In effect, the GPS observables are "ranges" or "distances" which are deduced from the measurement of time or phase differences obtained from a comparison between the incoming satellite signals and the receiver generated signals (Ibid, 1996).

GPS uses the "one-way" measurement concept whereby two clocks are required to relate the measurement in the GPS Time System, one in the satellite and another one in the receiver. These clocks are not perfectly synchronised, hence the ranges are biased by errors in both clocks, and also by delays caused by the propagation medium through which the signal travels. Consequently these measurements are referred to as *"pseudo-ranges"*.

The **pseudo-range** observable P, can be represented by the following standard model (Ibid, 1996);

$$P = \rho + c.(dT - dt) + I + T + M_P + \varepsilon_P \tag{2.1}$$

where ρ is the slant satellite-receiver range; c is the speed of light in a vacuum; dT is receiver clock bias; dt is satellite clock bias; I is ionospheric delay; T is tropospheric delay; M_P is pseudo-range multipath and ε_P is code observation noise.

The geometric information relating the receiver's coordinate $r = \left(X_r, Y_r, Z_r\right)^T$, and the satellite coordinate $R = \left(X^s, Y^s, Z^s\right)^T$, is contained within the slant satellite-receiver range $\rho = \|R - r\|$.

The **carrier-phase** observable can be represented by a similar relation (Ibid, 1996);

$$\Phi = \rho + c.(dT - dt) - I + T + M_\Phi + N + \varepsilon_\Phi \tag{2.2}$$

with most of the terms being the same as in (equation 2.1) with the exception that the ionospheric bias I of the carrier-phase has the opposite sign to that of the pseudo-range; M_Φ is the carrier-phase multipath; ε_Φ is the carrier-phase observation noise, and it also contain an unknown full-cycles ambiguity of the carrier, N.

In the case of the **Doppler** measurement, or Doppler shift, it is the difference between the transmitted and received signal frequency that is measured. In practice, the changing

difference between the frequency of the received signal f_r and a stable reference frequency f_g generated within the receiver is measured during a given time interval, as the instantaneous value of a frequency cannot be observed directly. Hence "zero-crossings" of the difference or beat frequency (f_g - f_r) are counted, resulting in the integrated Doppler count (Seeber, 1993);

$$N_{jk} = \int_{T_j}^{T_k} (f_g - f_r) dt \tag{2.3}$$

with

f_g the stable reference frequency (generated in the receiver),
f_r the received (shifted) frequency,
T_j, T_k time marks for start and stop of the counting interval,
N_{jk} integrated Doppler count between T_j and T_k.

The Doppler observable can be represented by the following mathematical model (Lu, 1995);

$$\dot{\Phi} = \dot{\rho} + c(d\dot{T} - d\dot{t}) - \dot{I} + \dot{T} + \dot{M}_{\Phi} + \varepsilon_{\dot{\Phi}} \tag{2.4}$$

where

$\dot{\Phi}$ is phase rate measurements (m/s)
$\dot{\rho}$ is the range-rate between the satellite and the receiver
$(\dot{})$ denotes a derivative with respect to time.

In most GPS navigation-type receivers, the Doppler measurement can be considered to be simply the carrier-phase-rate (Hatch, 1986);

$$D(t_n) = \Phi(t_n) - \Phi(t_{n-1}) \tag{2.5}$$

where

$D(t_n)$ is the Doppler measurement at the epoch t_n
$\Phi(t_n)$ is the carrier-phase measurement at epoch t_n
$\Phi(t_{n-1})$ is the carrier-phase measurement at epoch t_{n-1},

with a negative sign (Fu, 1996). In this respect, the raw Doppler shift measured in most GPS receiver is less accurate than the integrated Doppler.

2.3 Factors Influencing Positioning Accuracy

GPS positioning accuracy is influenced by several factors, such as the observation type, the signal biases present, the data processing algorithm used and the operational conditions, as summarised in Table 2.1.

Table 2.1: Factors Influencing GPS Positioning Accuracy

Observation type	C/A or P-code pseudo-ranges or carrier-phases, or Doppler, Single- or dual-frequency measurements, Level of noises in the measurements.
Signal disturbances	Ionosphere, troposphere and multipath.
Processing strategy	Level of treatment of observation errors and biases, Real-time or post-processing.
Operational conditions	Length of observation session, Inter-station separation, Static, rapid-static or kinematic, Point-positioning or differential, Satellite geometry: - Number of satellites, - Location and distributions of satellites.

The *observation type* may be the C/A or Precise pseudo-range, the carrier phase, or the Doppler. Except for the C/A pseudo-range, which is only available on the L1 frequency, all other observations can be made either on the L1 frequency by a single frequency GPS receiver, or on both the L1 and the L2 frequencies using a dual-frequency GPS receiver. The standard C/A-code measurement precision is typically at the few metre level, while the P-code measurement accuracy is at several decimetre level. Some new GPS receivers, utilising the so-called 'narrow-correlator' technology, can give C/A-code measurement to about the same level of precision as the P-code measurements (Lachapelle et al., 1992). *Signal disturbances* include the ionospheric and the tropospheric delays, which introduces systematic measurement biases are mostly beyond the control of users. The *processing strategy* or *algorithm* used to process the data will determine the level of treatment of the biases in the data, and thus the final computed position accuracy. The *operational conditions* include the satellite geometry, the length of the observation session, the mode of operation (such as whether the antenna is static or kinematic), the separation of the antennas, etc.

Assuming a certain measurement precision, and the presence of an 'acceptable' level of residual biases (remaining after the application of a processing algorithm based on double-differencing simultaneously observed GPS data), it is the operational issues that will influence positioning accuracy the most. The operational issues will impact on the quality of the positioning results in several ways, for example: (a) the baseline length will mostly affect the magnitude of the residual biases (the longer the baseline, the larger the residual biases), and (b) the length of the observation session affects the sensitivity of the solution to residual biases, satellite geometry, etc.

2.3.1 Measurement Noise

Measurement or receiver "noise" can be attributed to the mechanisation within the receiver, the signal-to-noise ratio of the signals, and to some extent, the dynamics of the antenna. As a rule-of-thumb, the observation resolution for typical receivers is at about 1% of the signal wavelength (Wells et al., 1986). The typical receiver noise level is indicated in Table 2.2

Table 2.2: Measurement Noises for Different Observation Types

Obs. Type	Wavelength	Measurement Noise
C/A-code	300 m	2-3 m (20-30 cm)
P1-code	30 m	20-30 cm
L1 Carrier-phase	~20 cm	2-3 mm (0.2-0.3 mm)
L1 Doppler	same as L1 carrier-phase	

The latest generation of GPS receivers use 'digital technology', and some have been able to reduce internal noise by a factor of ten, to about 20-30 cm for the C/A-codes and about 0.2-0.3 mm for the carrier-phase (Van Dierendonck et al.,1992).

In practice, as far as data processing is concerned, the observation noise comprises the internal observation noise plus multipath effects, and other unaccounted for residual biases.

2.3.2 Signal Disturbances

Satellite signals travel through the atmosphere before reaching the receiver's antenna. The atmosphere causes a disturbance to the signal. These disturbances introduce systematic biases in the observations, though most of them are beyond the control of the users. The two largest effects are the ionospheric and the tropospheric delays (Figure 2.1). In addition, depending on the antenna construction and surrounding environment, some of the signals arriving at the antenna are not the direct signals from the satellite but are reflected from physical objects such as buildings, trees and even the earth's surface. This type of signal disturbance is known as multipath.

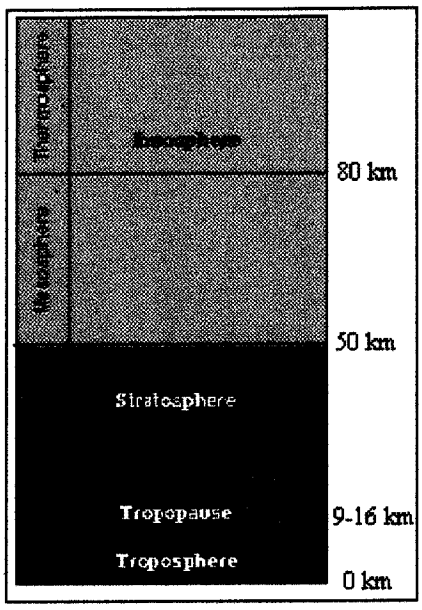

Figure 2.1: The layers of the Atmosphere

2.3.2.1 Tropospheric Delay

Tropospheric delay is caused by the refraction of the GPS signal in the electrically *neutral* (or non-ionised) atmospheric layer called the **troposphere**, extending from the earth surface to about 8 km, as well as the **stratosphere**, extending to an altitude of about 50 km (Figure 2.1). The term "tropospheric delay" will include the effect due to both the troposphere and stratosphere (Rizos, 1996).

Tropospheric delay is essentially a function of the satellite elevation, the altitude of the receiver, the atmospheric pressure, temperature and water vapour (Brunner & Welsh, 1993). The tropospheric delay can be separated into "dry" and "wet" components.

Generally about 90% of the total delay is attributable to the dry component (Wells et al., 1986). The delay is usually expressed as (Hofmann-Wellenhof et al., 1994);

$$d\rho^{trop}(E) = d\rho_d^{trop}(E) + d\rho_w^{trop}(E) \tag{2.6}$$

where

$d\rho_d^{trop}$, $d\rho_w^{trop}$ are the contribution of the dry and the wet troposphere at local zenith, known as the *zenith delay*,

$d\rho_d^{trop}(E)$, $d\rho_w^{trop}(E)$ are the corresponding distribution at elevation angle E.

Tropospheric refraction delays can cause significant range measurement errors of the GPS signal propagation at angles low to the horizon (Figure 2.2). Errors ranging from about 2.3 m for signals that are overhead and increasing to about 20 m or more at a 10° angle (Figure 2.2).

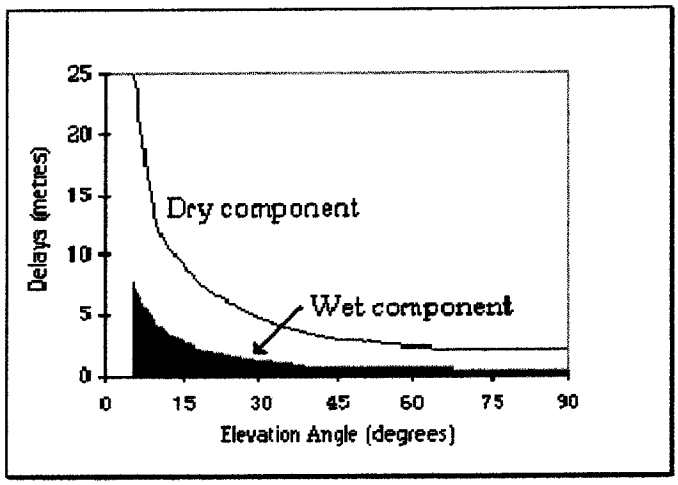

Figure 2.2: Propagation delays of the troposphere, as a function of elevation angle, in terms of the dry component and the wet component (adapted from Brunner & Welsch, 1993)

Handling Tropospheric Delay

Tropospheric effect is independent of signal frequency. Hence, the following options of handling the tropospheric effect are applicable to both single-frequency as well as dual-frequency GPS users (Wells et al., 1986; Rizos, 1996):

1. Ignore the bias. For navigation applications using the standard C/A-code measurement, the tropospheric bias will be within the magnitude of the measurement

noise, but care should be taken to avoid tracking satellites with elevation below 15° or 20°.

2. Correct data using standard tropospheric refraction model (such as Saastamoinen, Hopfield, Black, etc.). This option requires surface meteorological readings, or alternatively standard meteorological values can also be use with the model.

3. Data differencing techniques. This option relies on the spatial correlation of the tropospheric bias at the two sites.

4. Estimate residual tropospheric bias as an additional parameter. This option is use for very high precision result.

In these investigations, where the baseline lengths are short (< 35 km), the tropospheric effect is assumed to be eliminated through between-receiver data differencing.

2.3.2.2 Ionospheric Delay

The ionosphere is a layer of electrons and electrically charged atoms and molecules that surrounds the earth, stretching from a height of about 50 km to about 1000 km or more. It owes its existence primarily to ultraviolet radiation from the sun. The photons making up the radiation possess energy and when they collide with atoms and molecules in the upper atmosphere, the photon's energy breaks some of the bonds that hold the electrons to their parent atoms. The result is a large number of free, negatively charged electrons, and positively charged atoms and molecules called ions. The free electrons in the ionosphere affect the propagation of radio waves. The speed of propagation of a radio wave through the ionosphere is affected by the density of electrons along the ray path. The speed of a carrier, the pure sinusoidal radio wave, is increased by the presence of the electrons. On the other hand, the signal that is modulating the carrier (the pseudo-random codes and the navigation message) is delayed by the ionosphere, and is referred to as the group delay (Klobuchar, 1991). The ionospheric effect is therefore proportional to the Total Electron Content (TEC), which is itself a complex function of solar ionising flux, magnetic activity, sunspot cycle, season of the year, time of day, user location and viewing direction. A first order expression for the group delay in the zenith direction τ_g, is (Wang, 1995);

$$\tau_g = \frac{40.3}{cf^2} TEC \qquad (2.7)$$

where c is the speed of light, f denotes the frequency, and TEC is given in unit of electrons per square metre. Terms neglected in the above equation are only of the order of about 5 cm. For the delay along the line-of-sight, a simple mapping function can be employed, such as inverse of the sine of the elevation angle.

Ionospheric group delays can cause GPS range measurement errors of up to 40 m during daytime and perhaps a few metres during night time (see Table 2.3).

Table 2.3: The Ionospheric Range Errors for L1 in Low-Latitude (after Wang, 1995)

Season (*months*)	**High Solar Activity (1981)**		**Minimum Solar Activity (1986)**	
	Daytime	Night time	Daytime	Night time
Summer (*Nov.,Dec.,Jan.,Feb.*)	25 m	5 m	6 m	< 2 m
Winter (*May, Jun.,Jul.,Aug.*)	25 m	10 m	9 m	< 2 m
Equinoxes (*Mar.,Apr.,Sep.,Oct.*)	40 m	13 m	9 m	< 2 m

Note: Time: Daytime = 11:00 - 17:00 local time
Night time = 23:00 - 05:00 local time

The daily variation of the time delay can reach 50 nsec (15 m) in the zenith direction. The minimum effect can be expected between midnight and early morning, while the maximum is around local afternoon (Klobuchar, 1987).

The activity of the ionosphere is strongly influenced by the eleven-year cycle of sunspot activity (Figure 2.3). When the sunspot activity is low, then the ionosphere is not as active, and the effect on the microwave signals from GPS satellites is similar over a wider area then when the sunspot activity is increased. In 1983 when the sunspot activity was low, single-frequency phase-measuring receivers provided phase measurements which allowed for integer ambiguity to be resolved up to distances of 60 km. At the maximum of the most recent sunspot activity in 1990-1991, integer ambiguities were sometimes difficult to identify even at distances up to 10 km (Goad, 1995).

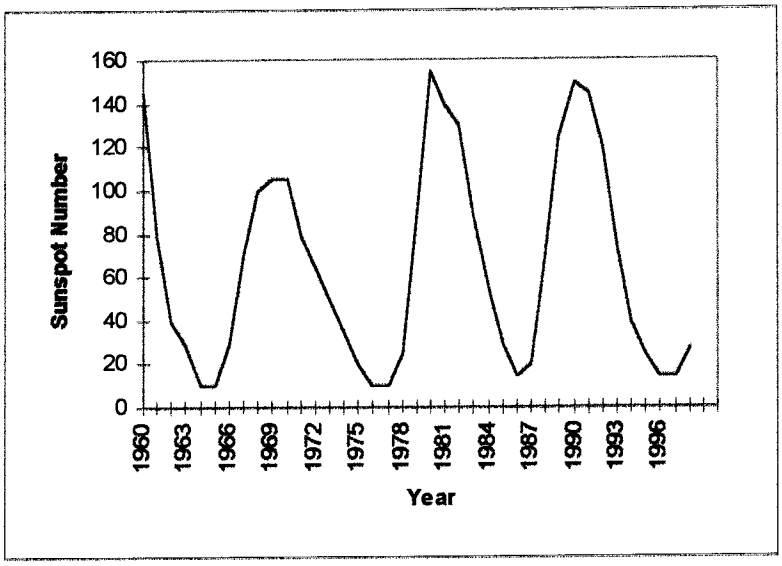

Figure 2.3: Sunspot Activity Over the Years (1960-2000)
(adapted from Klobuchar, 1991)

Handling Ionospheric Effects in the Case of Single Frequency Users

GPS observations on both the L1 and L2 carrier can overcome the ionospheric problem through the construction of a linear combination known as the ionosphere-free combination. For short baselines, the ionosphere-free combination may not be the best strategy as it is "noisier" than the single frequency measurements (Leick, 1995). However, in the case of single frequency users, the following options are available;

1. Differencing data between two receivers, assuming that the ionospheric delay at the two sites are, to some extent, spatially correlated (for baselines up to few tens of kilometres in length).

2. Predicting the delay using an ionospheric model, for example as transmitted in the navigation message. This model can generally compensate for 50% of the ionospheric effect at mid-latitudes (Klobuchar, 1987).

3. Use the C/A-code and the L1 divergence property to predict the ionospheric group delay. This however requires relatively precise C/A-code measurements free from multipath disturbance (Qiu, 1993).

4. Use a locally-derived ionosphere model, from the analysis of a network of permanent dual-frequency GPS receivers (Lin & Rizos, 1996).

For short to medium baseline lengths (less than 20-30 km), for mid-latitude regions during periods of minimum solar activity, the first option is believed to be adequate for medium accuracy applications. For this reason, the first option was used in this investigations.

2.3.2.3 Multipath Effects

Multipath is the phenomena whereby a signal arrives at a GPS receiver via multiple paths due to various reflectors in the vicinity of the antenna, such as the earth's surface, buildings and other objects (Figure 2.4). Multipath signal reception can cause errors in the ranging measurements because of delays introduced by reception of the reflected signals as well as causing the signal to become noisier. The influence of these reflections depends on their signal strength and delay, compared to that the line-of-sight signal, the attenuation of the receiver antenna, and the tracking electronics of the GPS receiver.

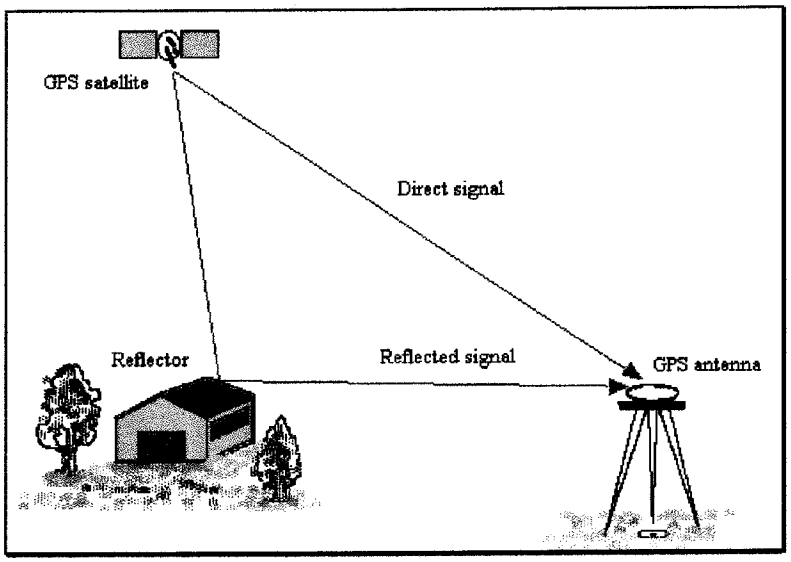

Figure 2.4: Multipath effect is a result of signals from a satellite reaching the antenna over more than one path.

The pseudo-range data, as well as the carrier-phases, are susceptible to multipath. The theoretical maximum effect of multipath on C/A-code measurements can reach 0.5 ms when the reflected/direct signal strength ratio is one, while on the carrier phase the effect is about two orders of magnitude smaller than for pseudorange data.

Multipath error in static and kinematic GPS is still inevitable in many cases, although various measures can be taken to reduce it. Since multipath is not spatially correlated

across multiple receiver sites, and hence cannot be eliminated through data differencing techniques, it remains the dominant source of error in differential GPS (Braasch, 1994-95). For a short baseline, multipath error can dominate the adjusted residuals and thus affect the site occupation time needed to resolve the ambiguities. Multipath can be reduced by carefully selecting the site, and through design improvements of the receiver antenna and tracking firmware. It can also be modelled to some extent (Braasch, 1995).

Some characteristics of multipath and its effect on the measurements are:

- It can cause 'jumps' in the signal of the order of its effective wavelength. For C/A-code this could mean tens or hundreds of metres, but of the order of only a decimetre for phase measurements of the carrier wave.

- Because multipath is receiver-satellite geometry dependent, and the causes of multipath tends to be permanent features, the multipath effects will generally to repeat on a daily basis at the same receiver site.

- As the satellite-receiver geometry changes (and hence the angle of incidence and reflection of the signal of the reflective surface), the multipath effect changes, and generally 'averages out' over a period ranging from several minutes to quarter of an hour. This makes static GPS positioning more accurate and reliable than positioning of a moving GPS receiver.

In practice, receiver noise and multipath cannot be separated and their combined effect becomes the prime disturbance in the resolution of the ambiguities, as well as in the final adjusted coordinates.

In these investigations, it is assumed that the practical way to minimise multipath effects is in selecting a multipath-free site. No investigations has been made of hardware (antenna) enhancements such as the choke ring, nor an attempt to model the multipath effect on the observations.

A 'normal' error budget in GPS observation for the C/A-code pseudo-range and the carrier phase measurements are as given in Table 2.4 (Wells et al., 1986; Erickson, 1995).

Table 2.4: Error Budget in GPS Observation

Error sources	C/A-code	L1 Carrier-phase
Measurement noise	2-3 m (0.2-0.3 m)	2-3 mm (0.2-0.3 mm)
Ionospheric*	50 m	50 m
Tropospheric*	2.3 m	2.3 m
Multipath	0.5-20 m	few cm

* Extreme values at zenith

2.3.3 Algorithms for Data Reduction

The algorithm used to process the data will determine the level of treatment of the biases in the data, and hence the computed position accuracy. The algorithm chosen on the other hand, depends on the type of observable available, for example if dual-frequency carrier-phase is available, then the ionospheric-free combination observable can be formed to eliminate the ionospheric delay. With only single-frequency data, the ionospheric delay has to be estimated, modelled or eliminated through the use of some technique. The other factor is the level of accuracy required. Geodetic type accuracy would require the tropospheric delay to be estimated together with the satellite orbit. However, for intermediate accuracy requirements the tropospheric biases are considered to be sufficiently well accounted for through data differencing. The GPS satellite orbits are treated as fixed. In these investigations, the choice of data processing algorithm has been limited to those that are applicable for single frequency users, and suitable for low-intermediate accuracy applications.

A hierarchy of possible data processing strategies is as given in Figure 2.5:

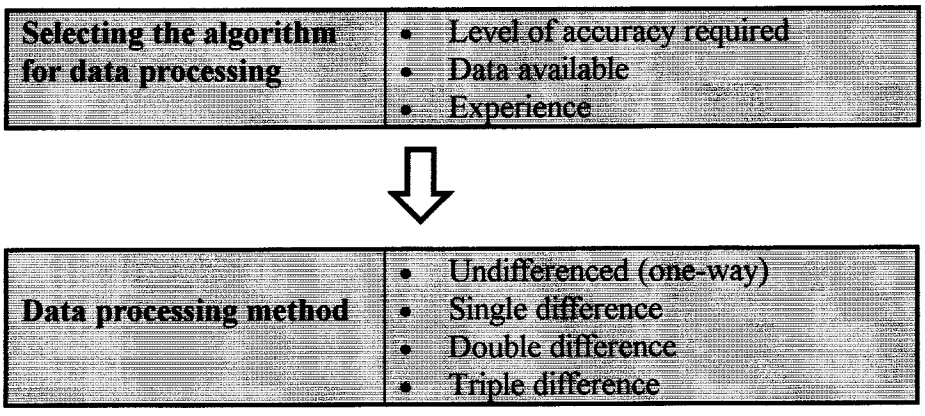

Figure 2.5: A Hierarchy of Data Processing Strategy

It is usual to employ the double-differencing techniques for data reduction (Wells et al., 1986; Leick, 1995; Hofmann-Wellenhof et al., 1994). As indicated in Table 2.5 this technique eliminates common, and highly correlated, biases between the stations. Also related to operational conditions, the double-differencing technique works well for short to medium length baselines, and hence is ideally suited for low-intermediate accuracy applications. The differencing technique will be discussed further in Chapter 5.

2.3.3.1 Treatment of Errors and Biases

Errors and biases in GPS solutions can be handled in several ways (Grant et al.,1990);

Table 2.5: Options for Handling GPS Biases and Errors for Single Frequency (adapted from Rizos, 1996)

Biases and errors	Estimated	Eliminated through differencing	Measured	Modelled	Ignored
Satellite clock		✓			
Satellite orbit		✓			
Receiver clock	✓	✓			
Fixed station coordinate					✓
Ionospheric delay		✓		✓	
Tropospheric delay		✓		✓	
Phase ambiguity	✓				
Cycle slips	✓	✓2			✓3
Antenna Phase centre					✓
Multipath					✓1
Receiver noise		*			✓
Selective Availability		✓			✓

Comments to Table 2.5:

1 - avoid multipath environment in station selection
2 - triple differencing
3 - minor cycle slips (a couple of cycles) may be hard to detect
* - differencing actually amplifies the noise!

1. They can be estimated as explicit parameters,
2. Those biases linearly correlated across different data sets can be eliminated by differencing,
3. The biases can be directly measured, for example using observations on a second frequency in the case of the ionospheric delay,
4. The biases can be modelled, as is sometimes attempted for the tropospheric delay,
5. They can be ignored (either because of their white noise characteristics as in the case of receiver noise, hoping the averaging process will minimises or eliminate its effects, or because there is nothing that can be done, as in the case of multipath) and assume that its effect will not be too damaging to the results.

2.3.4 Operational Conditions

The operational conditions or constraints include the receiver-satellite geometry, the length of the observation session, the mode of operation (whether the antenna was static or kinematic), the baseline length, etc. These limitations are in a sense "constraints" on the choice of the observables and the algorithms to be used. Some of these constraints are user influenced, others are not. Examples of user-influenced constraints are the hardware, baseline length, observation span, while the latter are receiver-satellite geometry, ionospheric, tropospheric and multipath effects.

2.3.4.1 GPS Satellite Constellation

The GPS satellite constellation consist of 21 operational + 3 active spare Block II satellites arranged in six nearly-circular orbits (denoted as the A, B, C, D, E and F) at about 20,200 km altitude in a 'cage-like' configuration (Figure 2.2). The GPS constellation is designed to enable the user in any part of the world to observe a minimum of four satellites at all times. For a low elevation cut-off angle, the number of visible satellites may increase to 8-10. The orbital period is one half day (sidereal time), ensuring repeated satellite ground-tracks every day (in reality every 23 hours 56 minutes, or sidereal day).

The U.S. Air Force Space Command (AFSC) formally declared the GPS satellite constellation as having met the requirement for full operational capability (FOC) on April 27, 1995. FOC means that the GPS constellation meets the requirements laid out in the System Operational Requirements Document and related performance documents, including the U.S government's Radio Navigation Plan (GPS World, 1995b). For all practical purposes however, the system has been effectively complete since initial

operational capability (IOC) was declared in late 1993 (based on 23 blocks IIs and a sole Block I satellite then in orbit).

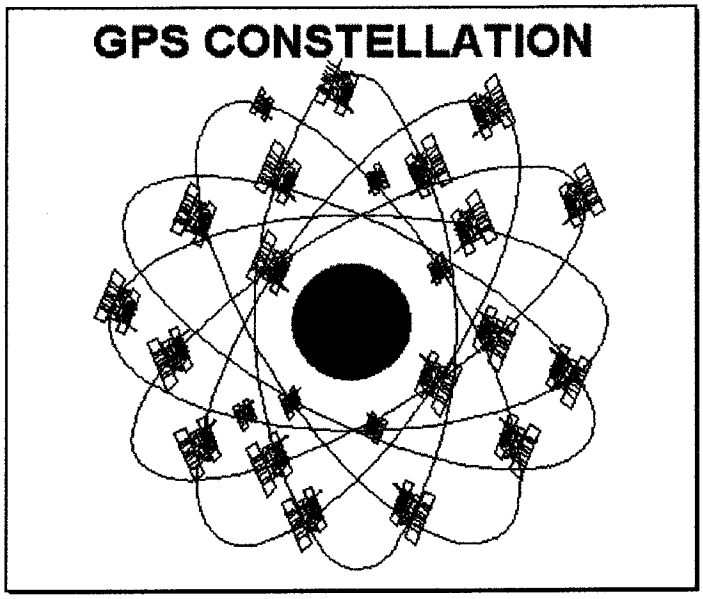

Figure 2.6: GPS Satellite Constellation (from Danna, 1996)

Geometric Indicators

Navigation accuracy is generally associated with the strength of the receiver-satellite geometry expressed, in terms of a Dilution Of Precision (*DOP*) factor, a unitless number which represent the ratio of the positioning accuracy to the measurement accuracy:

$$\sigma = \sigma_o . DOP \tag{2.8}$$

where σ_o and σ are the measurement accuracy and the position accuracy respectively.

A number of different definitions of *DOP* factors can be defined: *PDOP*, *HDOP*, *VDOP* and *TDOP*, depending on the coordinate component or combination of coordinate components considered (Rizos, 1996):

$$\begin{aligned} PDOP &= \sqrt{\sigma_E^2 + \sigma_N^2 + \sigma_H^2} = \sqrt{\sigma_X^2 + \sigma_Y^2 + \sigma_Z^2} \\ HDOP &= \sqrt{\sigma_E^2 + \sigma_N^2} \\ VDOP &= \sqrt{\sigma_H^2} \\ TDOP &= \sqrt{\sigma_T^2} \end{aligned} \tag{2.9}$$

where

σ_E^2, σ_N^2, and σ_H^2 are variances of the east, north and height components

σ_X^2, σ_Y^2, and σ_Z^2 are variances of the X, Y, and Z components

σ_T^2 is the variance of the estimated receiver clock error parameter

obtained from the VCV matrix of the least squares solution (scaled by the variance of the unit weight).

In the case of GPS point positioning, which requires the estimation of four parameters (3-D position and receiver clock error) the most appropriate *DOP* factor is the Geometric Dilution of Precision (*GDOP*):

$$GDOP = \sqrt{(PDOP)^2 + (TDOP)^2} \tag{2.10}$$

GDOP can be interpreted as the reciprocal of the volume V of a tetrahedron that is formed from the four satellites and the receiver position. The best geometric situation for point positioning is when the volume is a maximum, i.e., when one satellite is at the zenith and the other three are evenly spaced around the horizon.

Since position computation in GPS surveying essentially differs from the instantaneous fix in navigation (carrier-phase data over an observation span is used instead of single epoch code-range data) hence several different precision indicators has been suggested. Merminod (1990) and Merminod and Rizos (1994) introduced *BDOP* - Bias Dilution of Precision; and the Trimvec[tm] program refers to *RDOP* - Relative *DOP*. In this investigations, *BDOP* has been used and thus will be described further.

BDOP

The normal matrix of a batch Least Squares adjustment solution for position computation using carrier-phase observations can be partitioned as follows;

$$N_{\hat{X}} = \begin{bmatrix} N_{cc} & N_{cb} \\ N_{bc} & N_{bb} \end{bmatrix} \tag{2.11}$$

where the coordinate part is contained within the N_{cc}, and the ambiguity is within the N_{bb} sub-matrix. The Variance-Covariance (VCV) matrix is the inverse of the normal matrix;

$$Q_{\hat{X}} = \begin{bmatrix} Q_{cc} & Q_{cb} \\ Q_{bc} & Q_{bb} \end{bmatrix} = N_{\hat{X}}^{-1}. \tag{2.12}$$

Using these sub-matrices, several *BDOP* can be derived (Merminod, 1990);

$$\begin{aligned} BDOP1 &= \sqrt{trace(Q_{cc})} \\ BDOP2 &= \sqrt{trace(Q_{bb})} \\ BDOP3 &= \sqrt{trace(N_{cc}^{-1})} \end{aligned} \tag{2.11}$$

BDOP1 is the precision indicator for the coordinates in an ambiguity float solution, *BDOP2* is the precision indicator for the ambiguities determined in the float solution, and *BDOP3* is the precision indicator for the coordinate in an ambiguity fixed solution. Figure 2.7 gives the relation between the number of satellites used in the computation with the *BDOP1* value (unitless). It can be seen that for only four satellites, the geometric information is not strong enough (note the 'shoot-up' of the *BDOP1* value), although solution can still be achieved. Generally more than five satellites are needed to have a *BDOP1* values under 3.

Figure 2.7 gives an example of the relation between the number of observed satellites and the *BDOP1* factor.

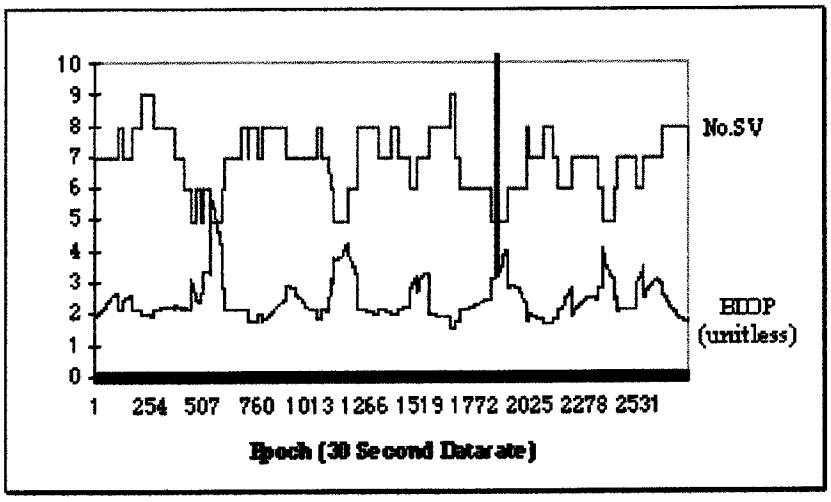

Figure 2.7: Relating Number of Satellites to *BDOP1* factor

Satellites Availability

The FOC of the GPS satellites constellation, provides more than 4 visible satellites at almost everywhere on the world, 99% of the time. For a higher cut-off angle normally

employed in surveying (e.g., 15 degrees mask), a percentage slightly less than that, e.g., 95%, may be obtained.

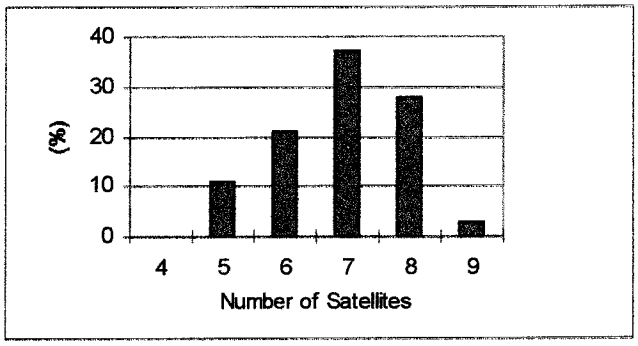

Figure 2.8: Satellite Availability in Bandung, Indonesia (in 24 Hours Percentage)

Satellite Outages

One thing that a user needs to be aware of is the occurrence of satellite outages. Satellite outages are defined as periods of poor satellite geometry (Johns and Conley, 1994). During outages, GPS navigation is not possible due to a less than favourable number of visible satellites or when the DOP exceeds some threshold value, e.g., 6. Sources of outages are satellite malfunctions, or the maintenance routine carried out by the Control Segment. GPS users are advised of these happenings through the Notice Advisory to NAVSTAR Users (NANU) issued by the United State Naval Observatory (USNO) (e.g., Table 2.6).

Table 2.6: Satellite Maintenance Schedule in NANU's for Day 233

UNITED STATES NAVAL OBSERVATORY (USNO)
AUTOMATED DATA SERVICE (ADS)

NOTICE ADVISORY TO NAVSTAR USERS (NANU) and
GENERAL MESSAGE (GENMSG) TO GPS USERS

170-95228	R 161542Z AUG 95	PRN12/SVN10 UNUSABLE DAY 228/1400-1447 UTC
171-95244	R 181618Z AUG 95	PRN27/SVN27 SKED UNUSABLE DAY 244/0100 UTC FOR UP TO 12 HOURS FOR REPOSITIONING MAINT.
172-95232	R 201524Z AUG 95	PRN12/SVN10 UNUSABLE DAY 232/1500-1515 UTC
173-95233	R 210831Z AUG 95	**PRN27/SVN27 UNUSABLE DAY 233/0314-0757 UTC FOR MAINTENANCE** REF: NANU 168-95233
174-95251	R 251515Z AUG 95	PRN24/SVN24 SKED UNUSABLE DAY 251/1100 UTC FOR UP TO 15 HOURS FOR MAINTENANCE

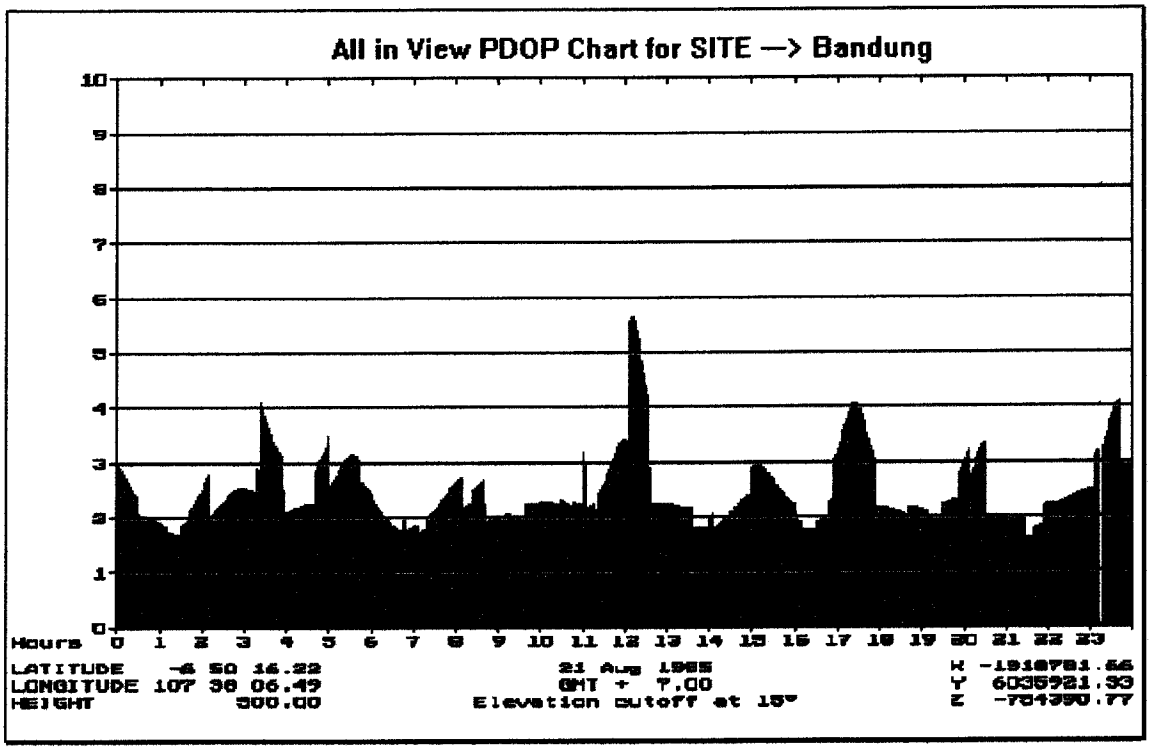

Figure 2.9: Plot of PDOP of Day 233 for All Satellites in Bandung, Indonesia

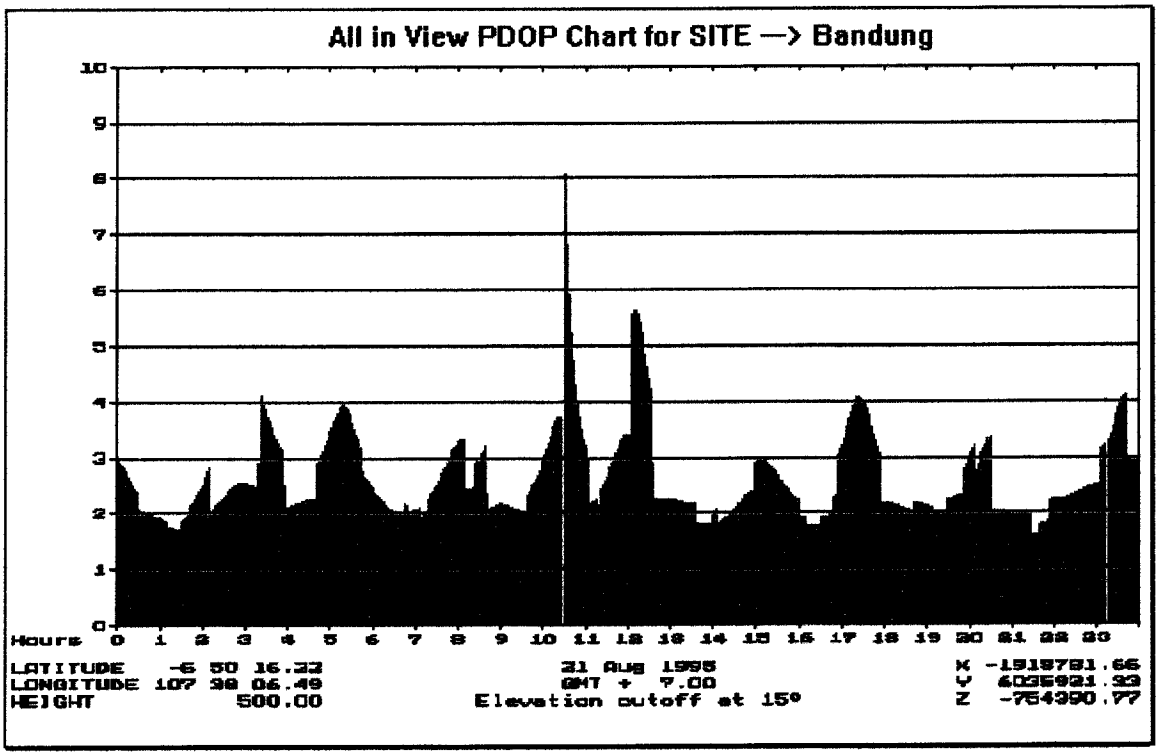

Figure 2.10: Corresponding plot of PDOP of Day 233 without SV27

An example of the effect of the withdrawal of one satellite (SVN27, for maintenance reason as in Table 2.6) on the value of *PDOP* on DAY233 for one site in Bandung, Indonesia, is given in Figure 2.9 and 2.10.

Johns and Conley (1994) also reported that satellite maintenance activity can cause the value of PDOP to exceed 6 for several minutes at a time. Conley et al. (1995) further reports that on a few days a year, PDOP values as high as 12 are possible for as long as 20 minutes, associated with satellite outages. But this only applies to specific areas in the world, while the removal of two satellites from service may have absolutely no effect at all in other areas.

Another kind of satellite outage was reported by Stanford University (ION Newsletter, 1995). During the October 1994 trials of DGPS assisted landings, they found that SV17 has gone invalid for some 6 seconds. Unable to determine the cause, they contacted the GPS Command Centre who then admitted that such glitches were not an uncommon design flaw in the Block II (only) satellites.

2.3.4.2 Length of Observation Span

Traditionally in static GPS surveying utilising the carrier-phase measurements, the norm for an observation span is of the order of half-an-hour to two hours, depending on the quality of data observed and the baseline length. Since carrier-phases are ambiguous measurements with unknown full-cycle ambiguities, this length of data span is necessary to ensure a significant change in satellite geometry so that the ambiguities can be reliably estimated, and then resolved to their integer values (Rizos, 1996). Shorter observation sessions will increase the risk of poor quality results - particularly when there are other factors that affect the quantity of the observations. Nowadays, innovations in hardware and software have led to significantly reduced observation spans, through the application of Rapid Static Positioning (RSP) method, which requires only about several minutes of data to solve for the carrier-phase ambiguities (Seeber, 1993). It may be just a matter of time before ambiguity resolution techniques are able to carry out reliable instantaneous (one-epoch) resolutions. Precise kinematic positioning and surveying will then be indistinguishable.

On the other hand, the navigation mode which utilises code measurements, can provide an instantaneous positioning capability since the code measurements are unambiguous range observations.

Techniques that utilise combinations of both carrier-phase and code measurements would logically fit between these two extremes, hence only a small number epochs of data may be sufficient in order to suppress the code measurement noise and to resolve for the carrier-phase ambiguities.

There are other factors known to have an affect on the length of the observation span, other than the requirement for reliable ambiguity resolution, including (Hofmann-Wellenhof et al., 1994):

- The relative geometry of the satellites and the change in the geometry. The number of satellites available also affects the geometry. Generally the more satellites observed, the better the geometry will be, hence the shorter the observation session length can be made.

- The degree of the ionospheric disturbances (for single-frequency user). The effect is worse during daylight in the early afternoon, particularly in higher latitude areas and in the tropics. Observation sessions may need to be longer compared to other times/locations.

- The length of the baseline. Generally short baselines require a shorter observation span than long baselines.

- Obstructions at the antenna site.

A useful method of determining the optimum observation session length for large project is to adopt longer than normal observation sessions on the first day. This data would yield the "ideal" results. Then shorter observation span could be processed to determine the point where good results can no longer be obtained at a certain probability. Table 2.7 gives typical observation session lengths with respect to baseline length (see, for example, Hofmann-Wellenhof et al., 1994).

Table 2.7: Session Length as Function of Baseline Length

Baseline length (km)	Observation session (minutes)
0.1 - 1.0	10 - 30
1.1 - 5.0	30 - 60
5.1 - 10.0	60 - 90
10.1 - 30.0	90 - 120

2.3.4.3 Baseline Length

Geometrically, the baseline length is constrained by the type of survey work being carried-out and the equipment being used. For example, first order control network would require station spacing to be between 30-50 km, while third order network stations can be as close as ten kilometres. As far as equipment is concerned, visibility with the theodolites and range measurement limit of the Electromagnetic Distance Meter (EDM) or total stations, is a factor to be considered. This could be quite short, perhaps only a kilometre or so. Theoretically, there is no fixed upper limit in distance, but practically speaking most survey project areas will be limited to few tens of kilometres in extent.

Physically, the baseline length determines the level of spatial correlation of many measurement biases between the two stations. But these physical correlations depend on many other factors as well, such as the geographical locality, the time of day or year or season, etc. A major concern is the ionospheric bias. The residual tropospheric effect (that which remains after a model for the delay has been applied) also starts to decorrelate at about 10-20 km.

So it is useful to define a short baseline, in the sense of normal surveying applications, as between 5 and 20 km. That is, most of the time surveyors will use GPS receivers to replace conventional angle and distance measuring equipment when it is cost effective to do so, but unlikely for baseline shorter than 5 km.

2.3.4.4 GPS Receiver Hardware

In the case of dual-frequency GPS receivers, given the above operational conditions, centimetre level accuracy can be expected with high reliability, as well as for short observations spans. Such hardware is, however, quite expensive. The data from single-frequency phase-tracking GPS receiver cannot match the ambiguity resolution reliability of dual-frequency receivers and hence the length of the observation span may be an important constraint. On the other hand, the use of GPS navigation-type receivers is a further constraint in that the standard phase processing algorithms cannot be used.

The hardware choice determines also the 'mechanisation' of which the measurement is being made. Some of the older 'mechanical' receivers may have receiver noise of a few metres for the C/A-code measurement and a few millimetres for the L1 carrier-phase,

while some of the recent digital receivers have improved noise levels to the decimetres level and fractions of millimetres respectively, about a tenth fold of improvement.

2.4.3 Selective Availability

Selective Availability

Selective Availability (SA) is a policy implemented by the U.S military on the GPS service as a matter of national security, since March 1990 on the Block II GPS satellites. It degrades the civilian signal (or the SPS) so that it limits the horizontal positioning accuracy to about 100m (at the 95% confidence level) and height determination to 150-170 m (at the 95% confident level). This is achieved through two strategies or components (Georgiadou & Doucet, 1990). Firstly the "epsilon" (ε) component which is accomplished by truncating the transmitted navigation message so that the coordinates of the satellites cannot be accurately computed, and secondly the "delta" (δ) component which is achieved by 'dithering' the satellite clock frequency in such a way that it introduces an additional unmodelled error in the timing used to derive the range measurement.

The activation of SA does not significantly affect GPS survey techniques using the differential method (Tolman et al., 1990), but instead targets real-time, single receiver-navigation users. In the case of orbital error, point positioning errors are of the same magnitude as the satellite (orbital) error, but in the case of relative positioning only relative baseline errors correspond to relative orbital errors. In geodetic applications, on the other hand, where post-processing of data is the norm, this bias can be overcome by using post processed ephemerides. The dithering of the satellite clock produces range noises that translate into point positioning errors. When two receivers are used to determine vector between them, the dithering can be negated by ensuring that the receiver measurement timetags are accurate to a few milliseconds of GPS time. By differencing the phases measurements between receivers, any dithering offsets will cancel.

Chapter 3

ADDRESSING THE INTERMEDIATE ACCURACY APPLICATIONS OF SURVEYING AND MAPPING

3.1 Intermediate Accuracy Range

GPS is able to address high accuracy surveying applications. These include high precision crustal movement monitoring for geodynamics and zero order control network for geodesy. Accuracies at the decimal ppm level has been reported for long baseline observations (e.g., Bock et al., 1985; Beutler et al., 1987b; Blewitt, 1989). However, such high precision applications only represent a small portion of the total GPS surveying and mapping applications. The largest group of applications are in the intermediate and low-order accuracy spectrum, such as establishing control networks for large scale mapping, engineering, gravity, photogrammetry, hydrographic surveys and for GIS data capture.

For the purposes of this research, the intermediate accuracy range will mostly encompass the decimeter to metre accuracy classification range, as proposed in Table 3.1, as well as up to the DGPS accuracy range which is between 2-5 m.

Table 3.1: Position Accuracy Standard Classifications (Leick, 1995)

Classification	Range of Position Accuracy
millimetre	< 5 mm
centimetre	5 mm - 5 cm
decimetre	5 cm - 20 cm
submetre	20 cm - 0.5 m
metre	0.5 m - 1.5 m
multimetre	1.5 m - 10 m
decametre	> 10 m

This chapter addresses some issues in this intended accuracy range.

3.2 Surveying and Mapping Applications in the Intermediate Accuracy Range

The general class of moderate accuracy surveying and mapping applications can be classified as follows;

1. Land Surveying and Mapping
2. Geographic Information System (GIS) applications
3. Hydro-Oceanographic Surveying

1. Land Surveying and Mapping

Applications in this area include providing control points for such activities as topographic mapping and gravity surveys for mining and geological studies, providing ground truth points for photogrammetric mapping and satellite images. Several other applications can also be identified in forest resource mapping. For control survey applications, some accuracy standards are available, such as the one given by the U.S. Federal Geodetic Control Committee (FGCC, 1990), as referred in Table 3.2, and also the Australian IGACSM (1994). For other applications, the required accuracy is often related to the mapping scale involved. One such accuracy statement is as quoted by Masters et al. (1994) that; "*90% of well defined points should be within 0.8 mm of their true position on the map*".

Table 3.2: Horizontal Control Survey Accuracy Standards
(e.g., for a 10 km baseline)

Order & Class	Relative Accuracy Requirement	Positional error
1st	1:100,000	0.1 m
2nd		
- Class I	1: 50,000	0.2 m
- Class II	1:20,000	0.5 m
3rd		
- Class I	1:10,000	1 m
- Class II	1: 5,000	2 m

Forest resource mapping applications might involve the establishment of forest boundary, forest area calculations or positioning sampling areas. In one reported case

(Green et al., 1992), mapping of forest roads to a scale of 1:25,000 only required the use of two simple single frequency GPS receivers, operated in differential mode. This particular project, which only required about 20 m horizontal positioning accuracy, can be easily satisfied with C/A-code positioning techniques.

2. Geographic Information System (GIS) applications

Data acquisition is generally regarded as the most expensive phase of setting up a GIS database. Estimates of 80-90 percent of the cost of a GIS project are often attributed to the data capture phase (Masters et al, 1994). Surveying activities include those providing coordinates of the ground control for the base map and also updating GIS information, verifying mapped features in the database, or entering new information into the database. A variety of accuracies are therefore required, which are often related to the mapping scale involved. One such example is illustrated in Table 3.3.

Table 3.3: Map Accuracy for GIS Databases
(Masters et al, 1994)

Scale of Mapping	Map Accuracy
100,000	50 m
20,000	10 m
10,000	5 m
5,000	2.5 m
1,000	0.5 m
500	0.5 m

3. Hydro-Oceanographic Surveying

Typical applications in this accuracy range are; hydrographic surveying, precise navigation in coastal waters, harbour approach, sea bottom mapping in the Exclusive Economic Zone or scientific purposes, precise gravimetric and seismic surveys, calibration of transponder systems, positioning of underwater sensors and samplers in marine prospecting for mineral resources (Seeber, 1993). An example of positional accuracy requirements for such activities are as given in Table 3.4.

Table 3.4: Hydrographic Activities Positional Accuracy Requirements (from Mourad & Fubara, 1974, as quoted by Thompson, et. al., 1983).

MARINE ACTIVITIES	Relative* Accuracy (m)			Absolute# Accuracy (m)		
	Lat.	Long.	Ht.	Lat.	Long.	Ht.
Geodetic Operations						
Control points	1	1	1	1	1	5
Geoid	-	-	0.1	-	-	0.5
Calibration test ranges	1	1	0.3	10	10	5
Gravity base stations	10	10	1	10	10	5
Ocean Physics & Oceanography						
Mean Sea Level / tides	-	-	-	50-100	50-100	0.1
Ice sheet motion	1-5	1-5	-	?	?	0.1
Stationary buoy locations	10	10	-	10	10	-
Drifting buoy locations	50-100	50-100	-	50-100	50-100	-
Ocean Tracking Stations	-	-	-	10	10	5
Search, Rescue and Salvage	1-10	1-10	-	20-100	20-100	-
Ocean Resources						
Geophysical surveys	10-100	10-100	5	V	V	V
Drilling	1-5	1-5	1-5	V	V	V
Pipelines / cables lying	1-10	1-10	-	V	V	V
Dredging	2-10	2-10	-	V	V	V

* Relative - repeatability, #Absolute - Referred to known geodetic system, V - variable

The other point of issue in relation to moderate accuracy applications is the extent of the area involved in a particular project. It has been pointed out in Rizos et al. (1994) that the extent of the working area (or baseline length), is a constraint contributing to the limit of the accuracy achievable in such a work. Hence, for the purpose of benchmarking the low-cost GPS systems, the extent of the working area must be defined.

3.3 Defining Baseline Lengths for Intermediate Accuracy Range Applications

In surveying and mapping applications, for each accuracy band, a typical working area is defined in terms of baseline length, which in a way limits the effectiveness of the system employed. For example, in the case of first order geodetic control, figures of about 20-60 km are often quoted (e.g., Clark, 1963; Torge, 1980). Traditionally, in the case of moderate surveying accuracy applications, two factors limit the size of the working area. The first one is the range of the equipment being used, such as the medium and lower-range EDMs, and line of sight of the optical theodolites. Secondly, by the type of project that they are concerned with. In practice, most project areas will be limited to a few tens of kilometres, unless such projects involve the mapping of roadways, aqueduct systems, etc.

When considering the use of a GPS system in place of traditional surveying technologies, for which the line of sight nor the equipment range limitations are irrelevant, the main consideration would be the atmospheric conditions over the area, specifically, the ionospheric and tropospheric delay. Hence, the areal extent to which the double-differencing technique employed in the data processing effectively eliminates these biases, will limit the size of the working area.

The activity of the ionosphere is partly a function of the eleven-year cycle of sunspot activity. When the sunspot activity is low, the ionosphere is less active, hence the effect on microwave signals from GPS satellites is similar over a wider area then when the sunspot activity is high. In 1983 when the sunspot activity was low, single-frequency phase-measuring receivers provided phase measurements which allowed for the integer ambiguity to be resolved up to distances of 60 km. At the maximum of the most recent sunspot activity in 1990-1991, integer ambiguities were difficult to identify, at times, even over 10 km distances (Goad, 1995).

Hofmann-Wellenhof et al. (1994) claimed in this period, single frequency receivers can be used up to distances of 30 km, because the influence of the ionospheric refraction cancels during observation differencing between the sites, with the caution that baseline distances should be reduced during periods of high sunspot activities. The residual troposphere (i.e., that which left after a model has been applied) on the other hand, starts to decorrelate at about 15 km (Ibid, 1994).

Hence in this research it will be assumed that baseline lengths will follow the normal surveying applications, that is, ranging up to a few tens of kilometres. Hence surveyors

will use GPS receivers in place of conventional angle and distance measuring equipment when the GPS technology is cost effective.

Another important point of discussion is on the issue of standards and specifications for using GPS systems for moderate accuracy applications. For some applications, GIS mapping for example, where the ease of using GPS makes the technology very attractive for almost all applications, the issue has not been clearly addressed (Subari & Rizos, 1995b), partly because of the relatively rapid developments in GPS. One of the issues concerns the applications of the homogeneous nature of GPS positioning, to the non-homogeneous physical identification of the features. The second issue is concerned with the 'required positioning accuracy' of features for the database, in relation to the accuracy of the GPS system being used. This investigation will make some proposals concerning these issues, particularly in relation to the use of low-cost GPS systems.

3.4 Issues Concerning Accuracy Standards and Requirements

For high accuracy applications (geodesy and surveying) and low accuracy (navigation) applications, the appropriate GPS system is clearly defined, both in terms of the instrumentation (hardware & software) and the field procedures to be used (e.g., FGCC, 1989; IGACSM, 1994). It has become standard practice to use dual-frequency receivers for applications in geodesy and modern GPS surveying due to the critical ionospheric influences and the advantages that dual-frequency instrumentation has in rapid ambiguity resolution. On the other hand, for most navigation purposes, using single frequency C/A-code receivers is sufficient to satisfy accuracy requirements at the 50-100 m level. A differential option (DGPS) can address accuracy requirements at the 2-5 m level.

However, for intermediate accuracy static positioning applications, say in the range of a few decimetre up to the few metre accuracy, the system definitions are comparatively vague, both in terms of the hardware & software and the field procedures. Issues that need to be addressed include: what observations to use (pseudo-range or carrier-phase)? Single- or dual-frequency instrumentation? Limit of the baseline length? Length of observation span? The answers to such questions will largely influence the GPS economics for moderate accuracy applications: both the capital costs and project survey costs. Currently various system configurations and operational procedures are possible, resulting in various level of accuracy and reliability. However there is no clear objective analysis of the performance of such systems.

One reason for this is the growing diversity of moderate accuracy GPS applications. In addition to lower order control surveys, there are now many GIS mapping applications. However, GPS for GIS applications is a relatively new but rapidly expanding area, hence there are no 'standards' or 'guidelines' available. Efforts to establish this standard are still in their infancy, as reported in Ostensen (1994).

Furthermore, for many GIS applications GPS is being used for a number of different purposes, for example: for locating point features in the field, for updating an existing database, and for verifying mapped features in the databases. The accuracies of each determinations are generally unspecified, thus the appropriate GPS system and procedures, as well as data processing modes to be used, cannot be specified. An attempt to specify this, based on the scale of the database map, has been made by Masters et al. (1994), as illustrated in Table 3.5.

Table 3.5: Matching GPS to GIS Databases (Masters et al., 1994).

Scale of Mapping	Map Accuracy	GPS Processing Mode
100,000	50 m	Navigation
20,000	10 m	DGPS*
10,000	5 m	DGPS*
5,000	2.5 m	Phase Smoothing
1,000	0.5 m	Phase Smoothing
500	0.5 m	Kinematic, Rapid Static

*Differential GPS

Another point worth noting here is that, for GIS database mapping, the definition of the accuracy requirement itself is uncertain. Many have discussed this problem of GPS/GIS integration with respect to its accuracy compatibility, e.g., Mekenkamp (1994) and Goodchild (1993). Consider the problem of locating some well-defined point features, and their positional accuracy, as illustrated in Table 3.6. Clearly the accuracy with which these points can be physically defined (and not just surveyed) varies considerably. However, when using one GPS system to locate these features for the purpose of data capture for a GIS database, the level of accuracy for all of these points must be consistent.

Hence it is important that, when establishing standards and specifications for using GPS for GIS, one should take into account the accuracy with which features can be defined physically on the ground, and not merely some 'specified' mapping accuracy.

Table 3.6: Accuracy of some point features in GIS databases
(Subari & Rizos, 1995b)

Point feature	Positional accuracy
Survey mark	1 cm
Corner of a building	10 cm
Street intersection	1 m
Waterways boundary (e.g., river)	2-5 m
Forest boundary	10 m
Soil type demarcation boundary	50 m

3.5 Low-Cost GPS Systems for the Intermediate Accuracy Applications

Clearly, most of the moderate accuracy requirements in Table 3.6 can be addressed by low-cost GPS systems, based on single frequency GPS receiver measurements. An example of some proposed matching are indicated in Table 3.7 (Subari & Rizos, 1995b).

Table 3.7: Matching GPS Systems to GIS Database Accuracy Requirements

Scale of Mapping	Map Accuracy	GPS System
100,000	50 m	C/A-Code Point Positioning
20,000	10 m	C/A-Code Double-Difference - Single Epoch
10,000	5 m	C/A-Code Double-Difference
5,000	2.5 m	Mixed C/A-Code and L1 Phase
1,000	0.5 m	L1 Triple-Difference Doppler-Created-Phase Double-Difference
500	0.5 m	L1 Double-Difference (ambiguity-float)

Note that the first three classes of accuracy requirements can be addressed by navigation-type GPS receivers (utilising only the C/A-code measurement), while the other three classes of accuracy requirements can be serviced using single-frequency phase tracking receivers. Of course there need not be a one-to-one correlation between accuracy and the GPS technique used. A higher accuracy technique could be used than that indicated appropriate for the scale of map. From the point of view of accuracy therefore, there is no need for expensive dual-frequency instrumentation for the intermediate accuracy applications.

Chapter 4

LOW-COST GPS SYSTEM

4.1 Introduction

GPS surveying has generally been considered an expensive exercise, with GPS hardware and software costs for a pair of receivers often being considerable more than AUD$50,000. This is one of the relatively few reasons why surveyors may be reluctant to use the technology (Subari and Rizos, 1995c). But these high cost systems are intended for the highest accuracy applications, where much R&D has been invested to support only a very small 'niche' market. Nevertheless, GPS technology on the other hand, has been progressively refined and developed over the last decade, resulting in cheaper GPS tracking sensors or 'engines', with varying capabilities, being now available for system developers.

Table 4.1: GPS Accuracies, Receiver Cost and Measurement Capabilities

GPS APPROACH	ACCURACY ESTIMATE	RECEIVER COST ESTIMATE*	GPS SIGNALS				
			L1 C/A CODE	L1 P-CODE	L1 CARRIER	L2 P-CODE	L2 Y-CODE
SPS NAVIGATION	100 M	$1,000	X				
SPS DIFFERENTIAL >30KM	10 M	$5,000	X				
SPS DIFFERENTIAL <30KM	1 M	$5,000	X				
PPS NAVIGATION	10 M	$10,000	X	X		X	
ANTI-SPOOFING NAVIGATION	10 M	$20,000?	X	X	X	X	X
L1 CARRIER PHASE SURVEY	0.1 M	$10,000	X		X		
L1 L2 CARRIER PHASE SURVEY	0.01 M	$15,000	X	X	X	X	

* in U.S Dollars

Peter H. Dana 8/28/94

The varying capabilities of these GPS sensors thus provides flexibility, enabling the technology to be used for different surveying applications (e.g., different accuracy requirements), by allowing for varying hardware configurations and processing strategies. As a rule of thumb, however, the higher accuracy requirement, the more expensive the hardware and the more complex the data processing that is required (though this complexity may be "shielded" from the user). One example of a classification of GPS usage and costing, is given in Table 4.1 (Danna, 1996).

It must be emphasised however, that this research focuses on low-cost GPS system configurations that can address the moderate surveying and mapping accuracy range.

4.2 Low-Cost GPS Surveying System

A low-cost GPS surveying system is defined here as relatively 'inexpensive' GPS hardware (at least in comparison to the survey grade GPS systems), with an appropriate processing software package, that can deliver positioning accuracy acceptable for the intermediate accuracy applications for which it is intended. The hardware should cost around (preferably less) AUD$5,000, and hence will be of the single frequency variety, preferably capable of measuring phase or phase-related data (note that phase processing is the key to high surveying accuracy), in addition to the standard C/A-code pseudo-range measurements. The software on the other hand must be capable of processing C/A-code data and phase or phase-related data, individually or in combination as well as having the normal 'user friendly' features that surveyors have grown accustomed to. For the complete system, including a host computer for the receiver (if necessary) as well as for data processing, a cost of less than AUD$10,000 is considered realistic.

It should be noted that although GPS surveying receivers, which may be priced around AUD$25,000 each, can record data internally in the field, a computer is still required in order to post-process the raw data ("real-time" systems are even more expensive).

4.2.1 Commercial Low-Cost GPS Surveying System

Commercial low-cost packages are available, such as the Magellan Series, the Magnavox receivers, the NovAtel GPSCard Series, Canadian Marconi and others. They are priced around (1996) AUD$6,500 - AUD$25,000, depending on the Input/Output (I/O) options given. The least expensive ones only give position output and hence are not significantly different from GPS navigation type receivers, while the ones which can output raw measurement data, will cost more. These systems, are normally offered

without software, or at best a very rudimentary package, with little built-in functionality for flexible data post-processing to be carried out (Subari & Rizos, 1995b). To cite one example, it may not be possible to decode and convert GPS data to a standard RINEX format without developing your own software. RINEX data output can be considered a pre-requisite in order to process data using most commercial software packages (Gurtner et al., 1989a). These packages are an additional expenses. The accuracy also varies, ranging from several metres for real-time DGPS systems, to several decimetres for post-processed results, but the flexibility to vary the processing strategy is generally absent. Many of these systems however, also cannot be used with other brands of GPS receivers.

4.3 Options for Low-Cost GPS Surveying System

Some options for implementing low cost GPS systems, utilising appropriate inexpensive GPS receivers have been previously identified (Rizos, et al., 1995). Ideally the system should be flexible enough to be used either on its own, as well as mixed with standard GPS surveying systems or other low-cost receivers.

Option 1: Standard GPS surveying receiver and roving low-cost phase tracking receivers, using commercial software
This is an optimal solution, with advantages such as; • No data processing software development is required (use the already available commercial software) • The base receiver (standard GPS surveying receiver) can serve many low-cost roving receivers - low-cost hardware expansion • Takes advantage of the existing hardware/software in the organisation • The base receiver, as well as the data reduction software, can be any of the standard GPS surveying products
The problems may be; • Data compatibility (to the low-cost receiver), such as; - Can the commercial software readily accept the low-cost receiver's data? - Can the software algorithm accommodate the data type?
Level of positioning accuracy expected: **centimetres to decimetres**

Option 2: Two low-cost phase tracking receivers, using commercial or 3rd party software
This option is the ideal alternative, with advantages such as; • No data processing software development is required (use readily available commercial or 3rd party software), • Low-cost capital expense for hardware
The problems that need to be addressed may include; • Conversion of data into proprietary format for use with the commercial software, or RINEX format in the case of 3rd party processing software, • Relatively high cost software (around US$5,000-$15,000), • Limited range of 3rd party software packages, • Many commercial software packages do not accommodate data from "foreign" receivers • Data compatibility: - Can the commercial software readily accept the low-cost receiver's data? - Can the software algorithm accommodate the data type?
Level of positioning accuracy expected: **centimetres to decimetres**

Option 3: Two high quality C/A-code pseudo range receivers using 3rd party software
This is a trade-off option with the advantage of; • A robust system suitable for rapid positioning.
The problem is generally that; • Code processing software is required - and generally commercially available surveying software is very expensive if used only to support code processing
Level of positioning accuracy expected: **decimetres to submetre**

Option 4: One low-cost phase tracking receiver and an 'ultra' low-cost roving navigation receiver, using optimised software.
This is the cheapest hardware option
Problems that need to be investigated include; • Development of optimised software, e.g., to support Doppler-created-phase data processing, which is not generally available
Level of positioning accuracy expected: **submetre**

Some investigations of these options have been reported, e.g., Cannon et al. (1992), Rizos et al. (1994). What is, in addition, required are 'bench-marking' tests to determine the overall performance characteristics of such systems, and in particular to study the level of repeatability (or what we will refer to as 'reliability') of the accuracy achievable under varying operational conditions.

4.3.1 Hardware for Low-Cost GPS Systems

Two most important hardware components of a GPS system are the GPS receiver and the antenna.

GPS receiver

The receiver suitable to use for the low-cost GPS system should cost around (preferably less) AUD$5,000, and hence will be of the single frequency variety (Figure 4.1), preferably capable of measuring phase or phase-related data (note that phase processing is the key to high surveying accuracy), in addition to the standard C/A-code pseudo-range measurements. Generally, these type of GPS receivers, belong to the 'navigation type' category.

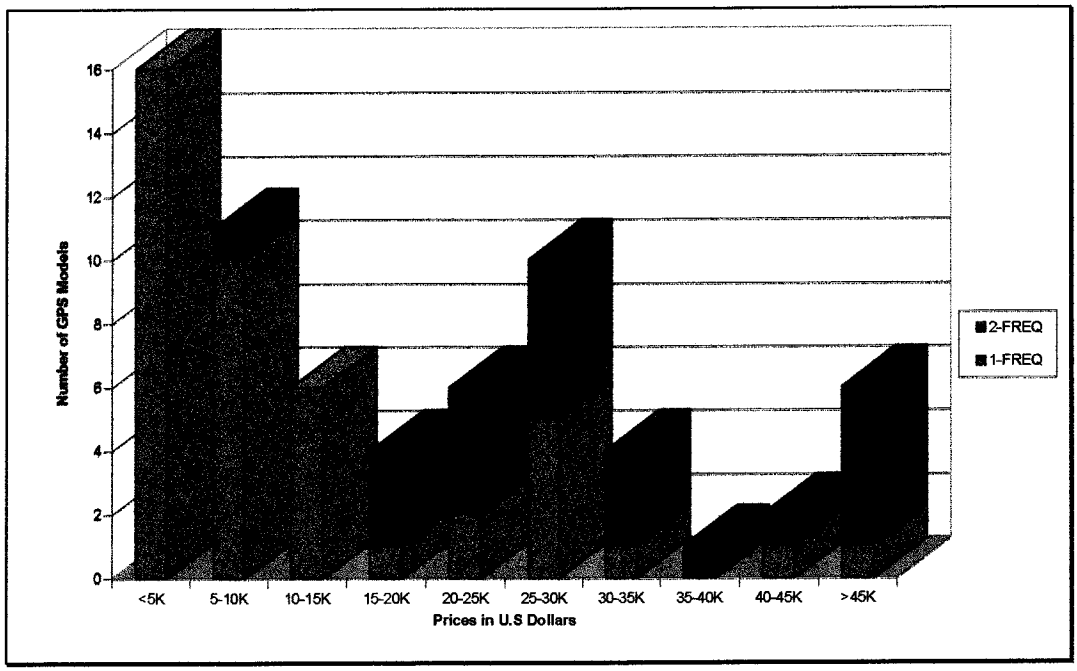

Figure 4.1: GPS Receivers cost (after Rizos et al, 1994)
(Source: GPS World Jan 1995)

In the last few years, the production of GPS "engines" or "sensors" in the form of OEM (Original Equipment Manufacture) and PCMCIA (Personal Computer Memory Card International Association), has expanded to support third party GPS receiver development. These receivers, most of which are simply the "engine" of navigation type GPS receivers, are comparatively inexpensive. One thing to note about these types of receivers is that they require a host computer (Fenton et al, 1991; Cannon et al, 1992; Cannon & Lachapelle, 1992).

The actual physical configuration of the hardware is usually immaterial as most receivers are capable of measuring the raw C/A-code and the L1 data to a similar accuracy (Rizos, 1996). On the other hand, the measurement of L2 phase is more problematic as it depends on "various" codeless tracking technology. L2 measuring receivers were not considered in this study. With the implementation of several receiver firmware innovations such as the "narrow-correlator technology" and "multipath-elimination technology", the accuracy of the C/A-code data has improved tenfold. However, these technologies have not been available to most low-cost GPS receivers.

Since high precision positioning requires phase data processing and some of these low-cost GPS receivers have the capability of tracking phase or phase-like data, it is possible to consider them for surveying use. Rizos et al. (1994) has identified and grouped these receivers into several classes:

Class 1;

- Instruments giving the same performance characteristics as "standard surveying" receivers, such as selectable data rate, steered time-tags, etc., such as the NovAtel GPSCard Series,

Class 2;

- Instruments capable of outputting phase data at a fixed rate, with little further utility, such as the Magellan receivers,

Class 3;

- Instruments that measure phase-rate (or Doppler), which could be used to construct a triple-difference-type observable, or integrated to construct a phase-like observation, such as the Trimble SVeeSix receiver.

Commercial data sheets describing measurement accuracy of a GPS receiver can sometimes be misleading. This is because the operational conditions under which the accuracies were obtained are not generally described. In general, the quoted measurement accuracies are for the best conditions of very high signal-to-noise values.

The antenna

The are several different types of GPS antennas - monopole or dipole configurations, quadrifilar or spiral helices, and microstrips. The microstrip, or patch, antenna are the most common antenna (Langley, 1991) because of its ruggedness and ease of construction. Most navigation-type GPS receivers use microstrip antennas.

An important characteristic of a GPS antenna is its gain pattern, which describes the sensitivity over a range of elevation angles, and its ability to discriminate multipath signals. Another significant factor is the stability of the antenna phase centre, the electrical centre to which position information actually refers (Ibid, 1991).

Antennas meant for static land use are normally design to have a low gain at low elevation (< 15 degrees) (Cannon et al., 1992), with a cut off angle of 15 degrees generally applied to minimise residual atmospheric and the multipath effect. Some mechanical devices, such as ground planes, or choke rings, can be used to suppress multipath signals. For high accuracy surveying applications, the antenna phase centre variation, which can amount to several millimetres, becomes an important error sources that needs to be accounted for, especially if mixing different types of antennas. However, for intermediate accuracy applications, this error can be ignored.

4.3.2 Software

Software is obviously an important component of a GPS system. A standard GPS surveying system comprises a tightly bundled hardware and software package. Inexpensive GPS receivers, on the other hand, generally are not offered with a complete software. (Indeed, if there is one, it is some sort of data logging software only).

Non-vendor software is therefore necessary for the configuration of any low-cost GPS system. Three classes of software are needed, namely, the data logging/receiver control software, the data pre-processing software and the data reduction software (Figure 4.2).

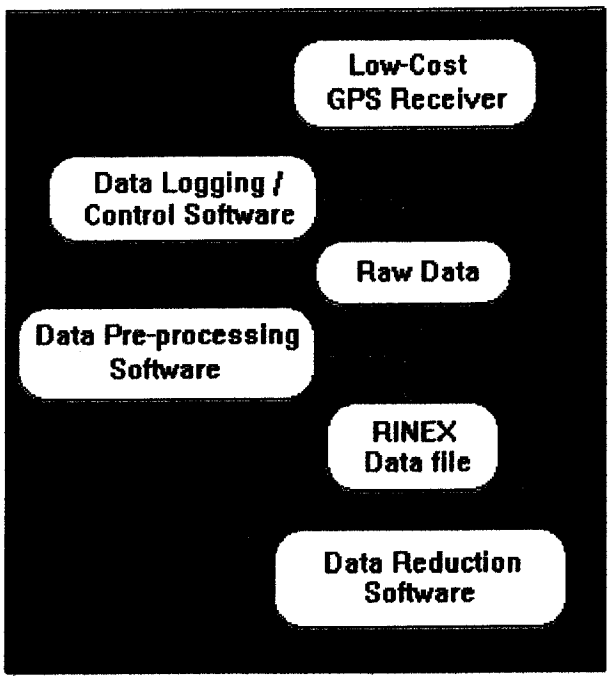

Figure 4.2: Software Modules within a Low-Cost GPS System

Data Logging Software

This software manages the interaction with the hardware, performs such functions as decoding the measurements records and recording them to a hard disk. Generally this software is supplied by the GPS manufacturer, together with 'manuals' describing the data formats, data corrections, etc., for the specific receiver.

Data Pre-Processing Software

To be able to use data collected by a low-cost GPS receiver, it is vital to understand the nature of the raw data collected by a specific receiver. Receiver mechanisms and technical details concerning the data collection and other in-hardware data "treatment" must be known. For example the issue of data time tagging - does the time tag correspond to the received time tag, or the transmitted one? has any data correction been applied, such as receiver clock error? has the data internally processed by the receiver?

Software in this class will apply the necessary data 'treatment' or correction, such as computing the receiver clock's error (obtained from a pseudo-range navigation solution) and apply it to the measurement time tag, and sometimes to the data. Cycle-slip detection and repair can also be carried out at this stage. Finally the data file needs to be converted to the RINEX format. Up to this level, generally the user has to develop their own software.

In this research, all the software has been developed in-house by Mr Hirsch, our laboratory manager and software specialist.

Cycle Slip Detection and Repair

For single frequency users, the only reliable way of detecting cycle slips is through a scan of the double-difference observations (Heroux & Kluesberg, 1989). Double-differencing eliminates the receiver and satellite clock biases, as well as the common biases effects due to the atmospheric refraction and satellite orbit errors. By computing the rate of change of phase over two observation epochs (i.e., forming the triple-differenced observable), cycle slip will show up as 'jump' in the data series. Note that uncorrelated short term ionospheric variations may still contaminate the data, hence this method may not detect small slips < 5 cycles. The second step may involve the fitting of piecewise polynomials to the double-difference observations to enhance the sensitivity to small cycle slips.

Data Reduction Software

In an ideal world, the commercially available (vendor specific) data reduction software would be used to process data collected from low-cost GPS systems, as in the first and second options discussed earlier. Hence, the laborious work of developing data reduction software is not necessary.

Some 'real-world' technical problems to this approach have been identified (Subari & Rizos, 1995b) including;

1. Such software generally inputs data in certain proprietary formats, though some can accept data files in the RINEX format. However, the 'treatment' of the data must be known as there are several ambiguities within the RINEX format specifications.

2. Such software are intended for high accuracy surveying applications, hence they typically only accept carrier-phase data for the processing,

3. Such software generally does not accommodate C/A-code solutions, or combined C/A-code and L1 carrier-phase solutions.

Third party software for surveying purposes are being marketed for about AUD$6,500 (1996). An example is the SEMIKIN^{tm} package. Third party GPS software generally accept RINEX data files as input. Many of these third party software packages are intended for high accuracy surveying applications, and does not accommodate data processing using C/A-codes, nor the combined C/A-code and the L1 carrier-phase measurements.

Hence it is advantageous that purpose-written software, intended for use with low-cost GPS systems, be developed.

Some data reduction algorithms suitable for use with low-cost GPS systems have been proposed in Rizos et al. (1994), and test results have been reported in Rizos et al. (1995). This research considers seven types of GPS data processing algorithms:

1. C/A-code pseudo-range double-difference solution
2. Precise C/A-code pseudo-range double-difference solution
3. Combined C/A-code and L1 carrier-phase double-difference solution
4. Combined Precise C/A-code and L1 carrier-phase double-difference solution
5. Ambiguity-free (float) L1 carrier-phase double-difference solution
6. L1 carrier-phase triple-difference solution
7. Rapid Static Positioning using L1 carrier-phase (RSP-L1)

All of the above mentioned algorithms have been implemented in the software developed for this research, within a package known as BASEPACK. The input for this software is a database file created from the individual instrument RINEX data files.

4.3.3 BASEPACK

A data reduction software package for BASEline computation PACKage (BASEPACK) intended for use with a low-cost GPS surveying system has been developed by the author. The characteristics of the software, and the nature of the data reduction that can be handled are summarised below;

1. BASEPR

- C/A-code pseudo-range double-difference solution

2. BASEPH

- Ambiguity-free (float) L1 carrier-phase double-difference solution

3. BASEPRPH

- Combined C/A-code and L1 carrier-phase double-difference solution

4. BASETRP

- L1 carrier-phase triple-difference solution

5. BASERSP

- Rapid Static Positioning using L1 carrier-phase (RSP-L1)

This software has been extensively used in this research. Further discussion concerning the algorithms employed within each software module is given in the next chapter.

4.4 Mixing a Low-Cost GPS Receiver with Standard GPS Surveying Receivers

As described in the first option, a low-cost GPS receivers could be used in combination with existing standard surveying receivers. Subari & Rizos (1995a) have studied the feasibility of mixing two types of GPS receivers. Results on identical baselines, have shown that comparable results can be obtained with using standard GPS surveying receivers. Several technical problems have also been identified, among which the important ones are with regards to data availability and compatibility.

4.4.1 Data Availability and Compatibility

When mixing a low-cost GPS receiver with a survey grade receiver, data available for the processing is restricted to those data types measured on the low-cost receiver, which at the most are the C/A-code, the L1 Doppler and the L1 carrier-phase measurements. On the other hand, if the standard receiver has precise code measurements, e.g., P1 or P2, then these codes can be use with the C/A-code from the low-cost receiver.

Different receivers have their own distinctive way of storing collected data, thus the data normally would not be readily compatible with each other (for more than one different brand of receivers), as well as for the data reduction software. A program is thus needed to 'convert' these various data formats into a common format, the Receiver INdependent EXchange (RINEX) format (Gurtner et al., 1989a). The BASEPACK Software developed in this research uses RINEX files for data input.

4.4.2 Some Technical Issues Concerning the Mixing of Data from Different Receiver Types

Some technical issues regarding data compatibility in mixing different GPS receivers (which applies more seriously with low-cost receivers) have been identified (Subari, 1996), including;

Receiver clock error and time tags

With regard to receiver clock error and time tagging of the observation data, Rizos (1996) points out that three requirements must be met in order to effectively use the data differencing technique in the processing algorithm. These are;

1. All receivers should make observations to common-view satellites at epochs which are within 30 milliseconds of each other, to ensure that satellite errors cancel in between-receiver differencing.

2. Receivers should be synchronised with each other at the microsecond level to ensure that all observation time tags are consistent with each other.

3. All receivers should be "externally" synchronised to the satellite ephemeris (in general GPS time) at the millisecond level.

Point 2 and 3 can be easily met if the navigation solution (in which the receiver clock error is estimated for) is used to individually synchronise the receiver's clock to GPS time (better than 1 microseconds level can be achieved). On the other hand, it is point 1 that is lacking in most low-cost receivers. Some receiver, for example, do not even conform to this requirement when 'observing' different satellites within each 'epoch', i.e., each satellite is observed at slightly different times (e.g., see Table 4.2 for the SVeeSix GPS receiver).

Table 4.2: Example of one epoch observation for SVeeSix Receiver

SV No.	GPS WEEK	SECONDS	No. of Obsn.	Obs #	Observations: C/A (ms frac.) D1
19	814	515459.750324	2	1	97184.08045946537
				6	2339.89501953125
18	814	515459.751970	2	1	290707.8738335865
				6	-10.4491605758667
27	814	515459.754591	2	1	177283.289511007
				6	3974.75927734375
15	814	515459.752505	2	1	151245.7289157073
				6	-1762.259887695312
14	814	515459.752531	2	1	159100.312807714
				6	1419.073486328125
29	814	515459.753831	2	1	248981.2677557947
				6	-574.0400390625

Hence, a pre-requisite to using data observed by such receivers is to 'move' the data to a common time tag, for example a nominal second value, before outputting it to a data file. In the case of the SVeeSix which also record the Doppler measurement, this can be done by a straight forward interpolation, taking the Doppler measurement as the best estimate for the rate of change of the range, with the opposite sign. This is done as the following;

$$C_{t_o} = C_{t_1} + \Delta C_{t_1 - t_o} \tag{4.1}$$

with

$$\Delta C_{t_1 - t_o} = -D_{t_1}(t_1 - t_0) \tag{4.2}$$

where

t_1 is the observed time tag

t_0 is the nominal time tag

C_{t_1} is the measured C/A-code at t_1

D_{t_1} is the measured Doppler at t_1

C_{t_o} is the measurement at nominal time tag t_0

4.5 System's Performance Characteristics

For the purpose of quantifying the performance characteristics of low-cost GPS systems, two parameters need to be defined, namely, the ***accuracy*** and ***reliability*** of the system (Rizos et al., 1995).

4.5.1 Accuracy

System's accuracy is defined in term of its ***positional error*** i.e., the ***level of "closeness"*** of the results given by the system ***to the "true" value*** (Rizos, 1996). Understandably, there are several factors influencing the accuracy of the results. These can be divided into; the observation type, the signal disturbances present, the algorithm used and the operational conditions (Rizos et al., 1995).

The observation type may be the C/A and/or Precise pseudo-range, the carrier phase, and the Doppler. The standard C/A-code measurement precision is at the few metre level, while the P-code measurement accuracy is at several decimetre level. Some new GPS receivers, utilising the so-called the 'narrow-correlator' technology, can make C/A-code measurements to about the same level of precision as the P-code measurements (Lachapelle et al., 1992). The signal disturbances introduce systematic biases in the observations, but most of them are beyond the control of the users. The algorithm used to process the data will determine the level of the treatment of the biases in the data, and thus the computed position accuracy. The operational issues include the satellite geometry, the length of the observation session, the mode of operation (such as whether the positioning mode is static or kinematic), the separation of the antennas (i.e., the baseline length), etc.

Assuming a certain measurement precision, and the presence of an 'acceptable' level of residual biases (remaining after the application of processing algorithm based on the double-differencing of simultaneously observed GPS data), it is the operational issues that influence accuracy the most. The operational issues will impact the quality of the positioning results in several ways, for example: (a) the baseline length will affect the magnitude of the residual biases (the longer the baseline, the larger the residual biases, and hence a reduction in accuracy), and (b) the length of the observation session affects the sensitivity of the solution to residual biases, satellite geometry, etc.

However, in considering a GPS system it is not only the achievable accuracy which is important, but also the factors influencing the accuracy, so as to provide a measure of reliability under a range of operational conditions.

4.5.2 Reliability

Reliability is defined in this context as a measure of the ***degree of repeatability*** of the accuracy of the results given by the system, measured in the form of a percentage. If the obtainable positioning accuracy is stable, it suggested that the reliability of the system is high, while if the obtainable positioning is highly variable, then the reliability of the system is considered to be low.

Given a certain level of reliability, say 95%, two things remain to be specified: (1) the level of accuracy which this corresponds to, and (2) the operational constraints that must be specified to ensure this accuracy and reliability (Rizos et al., 1995).

If accuracy under certain operational conditions is not influenced greatly by factors beyond the surveyor's control, then the level of accuracy may be set with certainty. If, however, accuracy is quite unpredictable, sometimes being high and sometimes inexplicably low, then the accuracy threshold corresponding to the required reliability may have to be set quite low.

4.6 Optimisation in Designing a Low-Cost System

'Targets' in developing a low-cost GPS surveying system can thus be identified as;

- High accuracy
- High reliability
- Low-cost

The objective in developing the 'best' low-cost GPS system is to achieve maximum accuracy, and reliability at minimum cost. The objective function in this case would be as follows:

$$F = a.P + b.R + c.C^{-1} \qquad (4.3)$$

with F as the *objective function*, a as the coefficient for the accuracy, P, b as the coefficient for the reliability, R, and c as the coefficient for the cost, C. Hence, the objective is to make F = *maximum* with suitable coefficients of a, b and c.

The GPS system consists of the hardware and software components, plus certain field observation constraints. In developing a low-cost GPS system for surveying, the hardware is restricted to the C/A-code system or single frequency carrier-phase type, costing less than about AUD$6,500. The software should be able to process and manipulate data collected from such hardware, and satisfy the intended intermediate accuracy requirements. The field procedures will be limited by the constraints imposed to achieve the highest level of reliability, such as short baseline separations, low multipath environment, etc.

Chapter 5

DATA REDUCTION ALGORITHMS

In this chapter the mathematical models associated with the data reduction algorithms implemented in the BASEPACK Software are described, along with the differencing techniques and other related topics. The least squares estimation procedure which serves as the basis for all the data processing algorithms is first reviewed.

5.1 Least Squares Estimation

The observation equations in (2.2) and (2.3) can be expressed in their parametric form (Uotila, 1985; Harvey, 1994):

$$L = F(X) \tag{5.1}$$

where L is the vector of observations and X is vector of the solve-for parameters, which in the case of GPS may include the station coordinates, the carrier-phase ambiguities and other nuisance parameters. The linearised form of the observations is

$$V = AX - L \tag{5.2}$$

where V is the vector of residuals of the observations and A is the design matrix of the system. The least squares criteria for solving the linearised system (5.2) is the minimisation of the quadratic form of the residuals:

$$V^T PV = \Omega = minimum \tag{5.3}$$

with P is the weight matrix for the observations, also obtained as the inverse of the variance-covariance matrix of the observations, $P = C_l^{-1}$. In many cases, where each observation is treated as being independent of other observations, C is a diagonal matrix whose elements are the variance of the observations σ_i^2, thus, $C = \sigma_i^2 I$, with I being the

identity matrix with dimension n x n, where n is the number of observations in the system.

The corrections to the solve-for parameters $\hat{X}$ is then obtained as follows:

$$\hat{X} = (A^T PA)^{-1} A^T Pl \tag{5.4}$$

where $l = L_b - L_c$, with L_b is the vector of actual observations and L_c is the vector of computed values based on apriori values of the parameters X_o .

Then

$$X = X_o + \hat{X}. \tag{5.5}$$

The variance-covariance (VCV) matrix of the parameters $Q_{\hat{X}}$ is given by:

$$Q_{\hat{X}} = (A^T PA)^{-1} \tag{5.6}$$

and the aposteriori variance of unit weight is computed as

$$\hat{\sigma}_o^2 = \frac{V^T PV}{DF} \tag{5.7}$$

where $DF = n - u$ is the degree of freedom for the solution, with n and u being the number of observations and unknowns, respectively.

The solution may be iterated, replacing X with X_o and equation (5.4) solved again, until the $\hat{X}$ does not undergo significant change, or its values are below a preset tolerance.

5.1.1 Scaling the VCV matrix

It is generally known that the estimated matrix for an estimated GPS baseline vector in equation (5.6) utilising carrier phase measurements is over-optimistic by a factor of between three to ten times (Hofmann-Wellenhof et al., 1994), especially for short observation sessions (such as the Rapid Static Positioning mode), due to the neglect of between-epoch correlations. A procedure to standardise the VCV matrix has been suggested by Han & Rizos (1995a) based on :

$$sQ_{\hat{X}} = \alpha Q_{\hat{X}} \tag{5.8}$$

with $sQ_{\hat{x}}$ being the standardised VCV matrix and α, the *standardisation factor* given as;

$$\alpha = \frac{n(1+f)}{n(1-f)+2f} \tag{5.9}$$

where

n is number of observations

f is the correlation coefficient of the measurements, computed as

$$f = exp\left(-\frac{|\tau_i|}{T}\right) \tag{5.10}$$

a function of the time lag $|\tau_i|$ (or data rate in this case) and the correlation period T (in seconds). El-Rabbany (1994) gives typical values of T between 250-350 seconds. Table 5.1 below gives the value of the correlation coefficient f, for the carrier-phase measurements, for different data rates and for T=260 seconds.

Table 5.1: Correlation Coefficient for Different Data rates

Correlation coefficient	**Data rate (in seconds)**						
	1	5	10	15	20	30	60
f	0.996	0.981	0.962	0.944	0.926	0.891	0.794

The 'standardised' a posteriori variance of unit weight is then computed as follows (Han and Rizos, 1995a);

$$s\hat{\sigma}_o^2 = \frac{1}{DF(1-f^2)}\sum_{i=1}^{n-1}\left[(v_i - f.v_{i+1})^T C_l^{-1}(v_i - f.v_{i+1})\right] \tag{5.11}$$

with

v_i, v_{i+1} are the residuals of the i'th and the $i+1$'th observations respectively,

C_l is the VCV matrix of the observations,

while the other parameters are as defined earlier.

5.1.2 Testing the A Posteriori Variance of Unit Weight

For quality control purposes, a statistical test is normally applied to the aposteriori variance factor to check the fidelity of the stochastic and functional models. The null hypothesis H_o and the alternative hypothesis H_1 are (Ibid, 1995);

$$H_o: \quad \hat{\sigma}_o^2 = \sigma_o^2$$
$$H_1: \quad \hat{\sigma}_o^2 \neq \sigma_o^2 \tag{5.12}$$

and the corresponding test statistic is:

$$(n-u)\frac{\hat{\sigma}_o^2}{\sigma_o^2} > \chi^2_{n-u} \tag{5.13}$$

The rejection region of H_o utilising a two-tail test would then be:

$$(n-u)\frac{\hat{\sigma}_o^2}{\sigma_o^2} > \xi_{\chi^2_{n-u,1-\alpha/2}} \tag{5.14}$$

$$(n-u)\frac{\hat{\sigma}_o^2}{\sigma_o^2} < \xi_{\chi^2_{n-u,\alpha/2}} \tag{5.15}$$

where $\xi_{\chi^2_{n-u,\alpha/2}}$ and $\xi_{\chi^2_{n-u,1-\alpha/2}}$ are the lower and the upper limit of the $1-\alpha$, confidence interval for the χ^2 distribution statistic, with *n-u* degrees of freedom.

If the aposteriori variance $\hat{\sigma}_o^2$is rejected by the upper limit, biases in the observation such as cycle slips, multipath, larger residuals caused by the ionosphere and troposphere may be present in the data, or simply indicate that the specified variances of the observations are too high. If the a posteriori variance $\hat{\sigma}_o^2$is rejected by the lower limit, the mathematical model $L = F(X)$ may contain too many parameters e.g., ionospheric or tropospheric scale parameters are included even though their affect is not significant, or simply indicate that the specified variances of the observation are too low.

5.1.3 Observation Accuracy Dependency with Satellite Elevation

Common procedures in GPS data processing (e.g., in the batch least squares solution) is to assign the same accuracy to all observations of the same type, thus assigning the same weight, irrespective of the elevation of the satellite, hence resulting in an over-optimistic solution accuracy. Jin (1995) suggests that the accuracy of GPS observations (especially the pseudo-ranges) decreases with decreasing elevation angle above the horizon, and that this relationship can be quite well modelled by an exponential function. A simple mapping function for the observation accuracy has been adopted in this investigations:

$$\sigma_P = \frac{1}{\sin \alpha} \sigma_o \tag{5.16}$$

where σ_P is the accuracy of the observation (in terms of it's standard deviation) taking into account the elevation of the satellite α, while σ_o is the 'nominal' accuracy of the measurement.

5.2 Relative Positioning Using the Data Differencing Technique

Relative positioning based on the data differencing technique requires simultaneous observations to be made at both the reference receiver and the unknown receiver(s). Simultaneity means that the two (or more) sites observe the same satellites, with observation time tags being recorded to within a few milliseconds of each other (Rizos, 1996). Assuming such simultaneity exists between the two sites defining a baseline, linear combinations of the observations can be formed to generate various single, double or triple-differenced observables.

The objective of relative positioning is to determine the position (or coordinate) of an unknown point with respect to the reference point. For most surveying applications, both of the points can be considered as being stationary. Relative positioning aims to determine the baseline vector between the two points. Introducing the corresponding position vectors for sites A and B, X_A, X_B, the relation (Hofmann-Wellenhof et al., 1994):

$$X_B = X_A + b_{AB} \tag{5.17}$$

may be formulated and the components of the baseline vector b_{AB} are given by:

$$b_{AB} = \begin{bmatrix} X_B - X_A \\ Y_B - Y_A \\ Z_B - Z_A \end{bmatrix} = \begin{bmatrix} \Delta X_{AB} \\ \Delta Y_{AB} \\ \Delta Z_{AB} \end{bmatrix}. \tag{5.18}$$

5.2.1 Double-Differencing Implementation

Two data differencing strategies can be used, namely the "fixed-base differencing" method and the "sequential differencing" method (Rizos, 1996). The fixed-base differencing is carried out by differencing all the data to satellites from the same base satellite, while in the sequential mode the data differencing is performed between

adjacent satellites. The two technique are technically the same and while giving different observation correlations, they will produce identical results, if the mathematical correlations are considered in the data processing, as discussed below. In these investigations, the former differencing strategy has been employed.

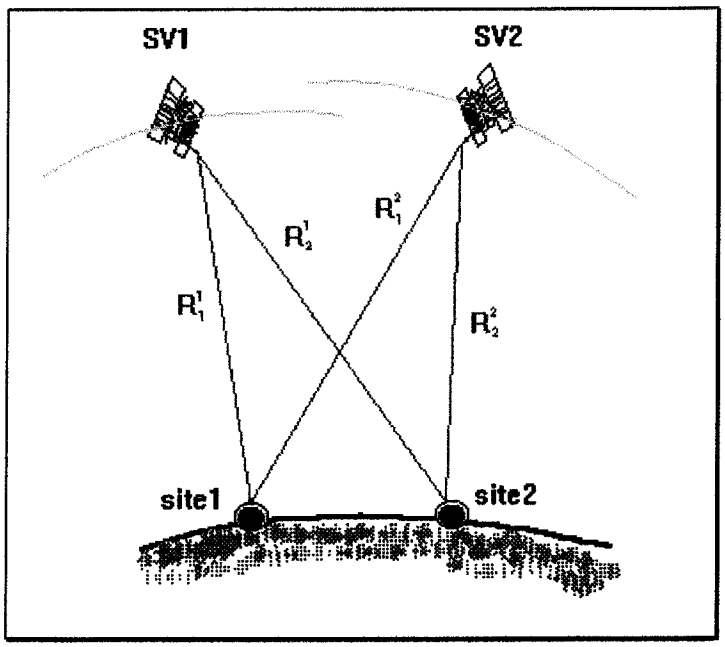

Figure 5.1: Relative Positioning with GPS: Two Receivers Simultaneously Observing Two Satellites

Consider the case of two receivers observing two satellites, as in Figure 5.1.

In the following discussions, although illustrated using the carrier phase algorithm, the techniques apply equally to the pseudo-range measurements.

In principle there are two ways to implement the double-differencing algorithm. The first one is by directly applying the double-differencing on the undifferenced, or one-way, observations $\Phi_1^1, \Phi_1^2, \Phi_2^1$ *and* Φ_2^2, as follows;

$$\Delta\nabla\Phi_{12}^{12} = \left(\Phi_1^1 - \Phi_1^2\right) - \left(\Phi_2^1 - \Phi_2^2\right). \tag{5.19}$$

with $\Delta\nabla$ as symbol for the double-differenced observation.

A second approach employs a differencing operator D, which is applied to the undifferenced observations:

$$\Delta\nabla\Phi_{12}^{12} = \begin{bmatrix} 1 & -1 & -1 & 1 \end{bmatrix} \begin{bmatrix} \Phi_1^1 \\ \Phi_1^2 \\ \Phi_2^1 \\ \Phi_2^2 \end{bmatrix} \tag{5.20}$$

and the double-differenced would be:

$$\Delta\nabla\Phi_{12}^{12} = D. \begin{bmatrix} \Phi_1^1 \\ \Phi_1^2 \\ \Phi_2^1 \\ \Phi_2^2 \end{bmatrix} \tag{5.21}$$

In this case, D = [1 -1 -1 1]. The dimension of matrix D is *n-1 x 2n*, where n is the number of observations in the epoch.

Both approaches are technically the same, and the difference is basically ease of programming the algorithm (Subsuantaeng, 1990). In these investigations, the second approach is employed.

When the number of satellites is greater than two, say four in this case, the double-differencing operator D would be;

$$D = \begin{bmatrix} 1 & -1 & 0 & 0 & -1 & 1 & 0 & 0 \\ 1 & 0 & -1 & 0 & -1 & 0 & 1 & 0 \\ 1 & 0 & 0 & -1 & -1 & 0 & 0 & 1 \end{bmatrix}.$$

5.2.2 Correlations in the Differencing Algorithm

The apparent simplicity of the data differencing algorithm is shattered because the resulting differenced observations are correlated. Only if this correlation is properly taken into account, will the baseline results be identical to the undifferenced results. For single baseline data processing this correlation fortunately is relatively easy to handle (Beutler et al., 1987a). One way is to use the Gram-Schmidt scheme as suggested by Remondi (1984), or to compute the weight matrices of all the simultaneous double-difference as the inverse of the corresponding VCV matrix. This weight matrix may be computed once only for a certain visible satellite constellation. Details of how the correlated weight matrix is computed is explained below.

In general, there are two types of data correlations; (1) *physical correlations*, and (2) *mathematical correlations* (Hofmann-Wellenhof et al., 1994). The signals from one satellite received at two points are physically correlated since they refer to the same satellite. Usually the physical correlation is not taken into account as it is assumed to be removed during data differencing. Therefore, the main interest are the mathematical correlations introduced by data differencing process.

If it is assumed that the carrier phase errors have a random behaviour represented by a normal distribution with expectation value zero and variance σ^2, then the measured (or raw) phase data can be therefore assumed to be linearly independent, or uncorrelated. Introducing the vector L of observations, then

$$Q_L = \sigma^2 . I \tag{5.22}$$

is the VCV matrix for the observables, where I is the identity matrix with dimension n x n, and n is the number of observations in the epoch.

The VCV matrix of the double-differenced observables can be derived utilising the variance propagation law as follows;

$$Q_{DD} = D.Q_L.D^t \tag{5.23}$$

where D is the double-difference operator matrix. Applying equation (5.22):

$$\begin{aligned} Q_{DD} &= D.\sigma^2 I.D^t \\ &= \sigma^2 .DD^t \end{aligned} \tag{5.24}$$

In the example of observation to four satellites mentioned earlier, the VCV matrix of the double-differenced data would be;

$$Q_{DD} = \sigma^2 \begin{bmatrix} 4 & 2 & 2 \\ 2 & 4 & 2 \\ 2 & 2 & 4 \end{bmatrix} \tag{5.25}$$

clearly, the DD observables are correlated.

5.3 C/A-Code Relative Positioning

The mathematical model in equation (2.1) can be written in the general form:

$$P_j^i = \rho_j^i + c.(dT_j - dt^i) + I_j^i + T_j^i + M_{P_j^i} + \varepsilon_{P_j^i} \tag{5.26}$$

for site *j* and satellite *i*. For example, two sites, *1* and *2*, observing two satellites, *1* and *2*, then equation (5.26) can be written for the series of observations;

$$P_1^1 = \rho_1^1 + c.(dT_1 - dt^1) + I_1^1 + T_1^1 + M_{P_1^1} + \varepsilon_{P_1^1} \tag{5.27a}$$
$$P_1^2 = \rho_1^2 + c.(dT_1 - dt^2) + I_1^2 + T_1^2 + M_{P_1^2} + \varepsilon_{P_1^2} \tag{5.27b}$$
$$P_2^1 = \rho_2^1 + c.(dT_2 - dt^1) + I_2^1 + T_2^1 + M_{P_2^1} + \varepsilon_{P_2^1} \tag{5.27c}$$
$$P_2^2 = \rho_2^2 + c.(dT_2 - dt^2) + I_2^2 + T_2^2 + M_{P_2^2} + \varepsilon_{P_2^2} \tag{5.27d}$$

Taking the difference between the sites for satellite *1*, (5.27a - 5.27c) the between-station single-differenced observable is obtained;

$$\Delta P_{12}^1 = \Delta\rho_{12}^1 + c.dT_1 - c.dT_2 + M_{P_1^1} - M_{P_2^1} + \varepsilon_{P_1^1} - \varepsilon_{P_2^1}. \tag{5.28}$$

Applying the same process for satellite *2*, the between-station single-difference observable is:

$$\Delta P_{12}^2 = \Delta\rho_{12}^2 + c.dT_1 - c.dT_2 + M_{P_1^2} - M_{P_2^2} + \varepsilon_{P_1^2} - \varepsilon_{P_2^2} \tag{5.29}$$

Note that in both equation (5.28) and (5.29), the ionospheric and the tropospheric bias has been eliminated, as has the satellite clock errors. This assumption is often made in the differencing technique, i.e., the commonness effect of both atmospheric delays for the two stations, if their separation is not great.

Forming the difference between equation (5.28) and (5.29) would result in what is known as the double-differenced observable, between site *1* and *2* and satellite *1* and *2*:

$$\Delta\nabla P_{12}^{12} = \Delta\nabla\rho_{12}^{12} + M_{P_2^2} - M_{P_1^2} - M_{P_2^1} + M_{P_1^1} + \varepsilon_{P_2^2} - \varepsilon_{P_1^2} - \varepsilon_{P_2^1} + \varepsilon_{P_1^1} \tag{5.30}$$

Note that one of the terms has been eliminated from the previous equations, namely the receiver clock errors of both sites. The double-differenced observable can also be formed

using the between-satellite single-difference, instead of equation (5.28) and (5.29), and the resulting double-difference will be the same as in equation (5.30).

The multipath and observation errors in equation (5.30) can be lumped together, resulting in:

$$\Delta\nabla P_{12}^{12} = \Delta\nabla\rho_{12}^{12} + \Delta\nabla M_{P_{12}^{12}} + \Delta\nabla\varepsilon_{P_{12}^{12}} . \tag{5.31}$$

In the standard data processing algorithm, measurement noises are treated as white noise, and hence are not modelled. Multipath on the other hand is in reality, more complicated. A satisfactory model does not exist, thus, the practical approach is to minimise it during data collection and to leave it out from the observation model, hoping that it will not degrade the solution accuracy much. The observation equation for the double-differenced pseudo-range observations therefore is:

$$\Delta\nabla P_{12}^{12} = \Delta\nabla\rho_{12}^{12} \tag{5.32}$$

with the design matrix A only containing terms related to the station coordinate parameters.

5.4 Carrier-Phase Relative Positioning

The mathematical model in equation (2.2) can be written in the general form:

$$\Phi_j^i = \rho_j^i + c.(dT_j - dt^i) - I_j^i + T_j^i + M_{\Phi_j^i} + N_j^i + \varepsilon_{\Phi_j^i} \tag{5.33}$$

for all sites j and satellite i.

As in the case of the code data, the observation model for the carrier phase data is the same except that there are additional parameters appearing in the model, the cycle ambiguity N, as indicated in equation (5.33).

Taking the difference between data from both sites to satellite *1*, the between-station single-differenced observable is obtained:

$$\Delta\Phi_{12}^1 = \Delta\rho_{12}^1 + c.dT_1 - c.dT_2 + M_{\Phi_1^1} - M_{\Phi_2^1} + N_1^1 - N_2^1 + \varepsilon_{\Phi_1^1} - \varepsilon_{\Phi_2^1} \tag{5.34}$$

The ambiguity terms can be lump together to give the single-differenced ambiguity term, thus equation (5.34) can be written as;

$$\Delta\Phi_{12}^{1} = \Delta\rho_{12}^{1} + c.dT_1 - c.dT_2 + M_{\Phi_1^1} - M_{\Phi_2^1} + \Delta N_{12}^{1} + \varepsilon_{\Phi_1^1} - \varepsilon_{\Phi_2^1}. \qquad (5.35)$$

Applying the same process to satellite *2*, a similar expression is obtained:

$$\Delta\Phi_{12}^{2} = \Delta\rho_{12}^{2} + c.dT_1 - c.dT_2 + M_{\Phi_1^2} - M_{\Phi_2^2} + \Delta N_{12}^{2} + \varepsilon_{\Phi_1^2} - \varepsilon_{\Phi_2^2} \qquad (5.36)$$

Note, as before, the ionospheric and tropospheric biases, assumed to be common at both sites are eliminated, as well as the satellite clock error term.

Forming the difference between equation (5.35) and (5.36) results in what is known as the double-differenced observable between site *1* and *2* and satellite *1* and *2*:

$$\Delta\nabla\Phi_{12}^{12} = \Delta\nabla\rho_{12}^{12} + M_{\Phi_1^1} - M_{\Phi_2^1} - M_{\Phi_1^2} + M_{\Phi_2^2} + \Delta N_{12}^{1} - \Delta N_{12}^{2} + \varepsilon_{\Phi_1^1} - \varepsilon_{\Phi_2^1} - \varepsilon_{\Phi_1^2} - \varepsilon_{\Phi_2^2} \qquad (5.37)$$

Note again that the receiver clock errors have been eliminated.

In theory, the ambiguity terms can be solved in the one-way form (for individual site-satellite), as in equation (5.33) or in the single-differenced form, as in equations (5.35) and (5.36), but the common trend is to lump it together as a double-differenced ambiguity. This ambiguity parameter still should have an integer value. Lumping further the multipath and noise terms, results in:

$$\Delta\nabla\Phi_{12}^{12} = \Delta\nabla\rho_{12}^{12} + \Delta\nabla M_{\Phi_{12}^{12}} + \Delta\nabla N_{12}^{12} + \Delta\nabla\varepsilon_{\Phi_{12}^{12}} \qquad (5.38)$$

Note that one could also form the double-differenced observable via the between-satellite single-difference, instead of equation (5.35) and (5.36).

In the standard data processing algorithm, the measurement noises are treated as white noise. Multipath on the other hand is more complicated, and there is no satisfactory model, thus, the general approach is to minimise it during the data collection period, and to remove it from the observation model. This will in turn have a direct effect on the position computation result and its accuracy. The final observation equation for the double-difference will thus be,

$$\Delta\nabla\Phi_{12}^{12} = \Delta\nabla\rho_{12}^{12} + \Delta\nabla N_{12}^{12} \tag{5.39}$$

with the design matrix A only containing the station coordinate and the double-differenced ambiguity terms.

The linearised system of equation would then be as in equation (5.2);

$$V = AX + L \tag{5.40}$$

with

$$A = [A_C \; A_N] \tag{5.41}$$

$$X = \begin{bmatrix} X_C \\ X_N \end{bmatrix} \tag{5.42}$$

with

$$X_C \in R^t$$

$$X_N \in Z^m$$

where X_C is the t x 1 real-valued parameter vector which includes the coordinate parameter, X_N is the m x 1 integer-valued parameter vector. R^t refers to the t-dimensional real space, while Z^m refers to the m-dimensional integer space. Normally the above least squares problem is first solved by replacing the Z^m with R^m, thus obtaining X_N as a real value in what is known as a bias "float solution" or "real-value ambiguity solution". Then the X_N are fixed to their likely integer values utilising an ambiguity-resolution-technique, and the solution is iterated holding these values fixed in a bias "fixed solution", as described below.

By substituting X_N , the real-valued double-differenced ambiguities for its integer-valued parameter:

$$X_N = N_k \tag{5.43}$$

The new value of the coordinate parameters is computed as follows (Han, 1995);

$$\tilde{X}_{C,k} = \hat{X}_C - Q_{\hat{X}_C\hat{X}_N} Q_{\hat{X}_N}^{-1} (\hat{X}_N - N_k) \tag{5.44}$$

with the corresponding VCV matrix:

$$Q_{\tilde{X}_{C,k}} = Q_{\hat{X}_C} - Q_{\hat{X}_C\hat{X}_N} Q_{\hat{X}_N}^{-1} Q_{\hat{X}_C\hat{X}_N}^T \tag{5.45}$$

and the new quadratic form of the residuals:

$$V_k^T PV_k = \Omega + R_k \tag{5.46}$$

with

$$R_k = \left(\hat{X}_N - N_k\right)^T Q_{\hat{X}_N}^{-1} \left(\hat{X}_N - N_k\right). \tag{5.47}$$

The standard deviation of unit weight m_k, is computed as:

$$m_k = \sqrt{\frac{V_k^T PV_k}{n-t}} \tag{5.48}$$

5.5 Triple-Difference Relative Positioning

In GPS surveying, triple-differenced (TD) carrier-phase data processing is resorted to for several reasons; firstly, uncorrelated TD observables are used to determine the initial values of the solve-for parameters; secondly, TD observables are also used to detect cycle-slips in the double-differenced data; thirdly, for long baselines (>100 km), when between-station common errors cannot be assumed to have been eliminated, hence the use of the TD is the most reliable means to perform the baseline computation (Rizos, 1996). Therefore, triple-differenced observables are used because (Ibid, 1996);

1. Relatively simple carrier-phase processing algorithm which can easily handle a changing satellite constellation,
2. Robust solution which is relatively immune to cycle slips in the carrier-phase data.

One problem in using TDs however, is that the observations are correlated with each other, within the same epoch (as the DDs), as well as between epochs (when forming the TDs). By not taking these correlations the accuracy of the results will be degraded. This is the reason why TD data are not used for high accuracy applications.

5.5.1 Mathematical Model

From the model for the double-differenced observable in equation (5.39), the TD can be formed by taking the between-epoch difference. If the nominal reception times, in receiver clock time are *t-1* and *t*, then the triple difference can be formed as;

$$\delta\Delta\nabla\Phi_{12}^{12}(t) = \Delta\nabla\rho_{12}^{12}(t) - \Delta\nabla\rho_{12}^{12}(t-1) + \Delta\nabla N_{12}^{12}(t) - \Delta\nabla N_{12}^{12}(t-1) \tag{5.49}$$

with the double-differenced ambiguity terms being eliminated as they are constant over time (assuming the same satellite constellation at time *t-1* and *t*), the triple-differenced observable can therefore be expressed as;

$$\delta\Delta\nabla\Phi_{12}^{12}(t) = \delta\Delta\nabla\rho_{12}^{12}(t) \tag{5.50}$$

If the assumption that the integer ambiguities are constant is false, then an extra term will be required to account for the cycle slip. This is why this observable is especially useful for cycle slip detection.

5.5.2 Implementing the Triple-Differencing Procedure

Starting with two double-differenced observables, at epochs *t-1* and *t*, the triple-differenced observable for epoch *t* can be constructed as follows;

$$\delta\Delta\nabla\Phi_{12}^{12}(t) = \Delta\nabla\Phi_{12}^{12}(t) - \Delta\nabla\Phi_{12}^{12}(t-1) \tag{5.51}$$

or, by using a between-epoch difference operator *C*, the above equation can be formulated as;

$$\delta\Delta\nabla\Phi_{12}^{12}(t) = \begin{bmatrix} 1 & -1 \end{bmatrix} \begin{bmatrix} \Delta\nabla\Phi_{12}^{12}(t) \\ \Delta\nabla\Phi_{12}^{12}(t-1) \end{bmatrix} \tag{5.52}$$

and the TDs would be:

$$\delta\Delta\nabla\Phi_{12}^{12} = C. \begin{bmatrix} \Delta\nabla\Phi_{12}^{12}(t) \\ \Delta\nabla\Phi_{12}^{12}(t-1) \end{bmatrix} \tag{5.53}$$

in this case *C* is the vector [1 -1]. In the case of four observed satellites, and hence three double-differenced observable at each epoch, the *C* operator would become the matrix;

$$C = \begin{bmatrix} 1 & 0 & 0 & -1 & 0 & 0 \\ 0 & 1 & 0 & 0 & -1 & 0 \\ 0 & 0 & 1 & 0 & 0 & -1 \end{bmatrix}.$$

5.5.3 Correlations of Triple-Differenced Observables

In the case of the triple-difference, the correlation matrix is slightly more complicated because it involves two DDs at two consecutive epochs. For a straightforward case (no satellites rise or set between the two consecutive epochs), the covariance matrix of the triple-differenced observable, Q_{TD} for a single epoch can be written as (Hofmann-Wellenhof et al., 1994);

$$Q_{TD} = C.Q_{DD}.C^t \tag{5.54}$$

with C and Q_{DD} as previously defined. Using the example of four satellite measurements from two sites, and the Q_{DD} from equation (5.25), the covariance matrix for the TDs would be;

$$Q_{TD} = \sigma^2 \begin{bmatrix} 8 & 4 & 4 \\ 4 & 8 & 4 \\ 4 & 4 & 8 \end{bmatrix} \tag{5.55}$$

which can further be simplified as;

$$Q_{TD} = 2\sigma^2 \begin{bmatrix} 4 & 2 & 2 \\ 2 & 4 & 2 \\ 2 & 2 & 4 \end{bmatrix} \tag{5.56}$$

which is in fact;

$$Q_{TD} = 2.Q_{DD} \tag{5.57}$$

Implementation of the TD correlation in the data processing software is not easy, especially when one has to consider satellite constellation changes. It is worth the effort considering that the noise of the triple-difference on the other hand, prevents a refined solution (Ibid, 1994). In these investigations, the *between-epoch correlation is not accounted for*, thus the results are expected to be inferior to those obtained using double-differenced data.

5.6 Combined C/A-Code and L1 Carrier Phase Relative Positioning

Code measurements are unambiguous but less precise, on the other hand carrier phase measurements are more precise but ambiguous. Other advantage is that in wooded areas, code measurements are less affected by foliage than carrier phase.

One option of utilising these measurements in order to exploit their respective advantages is by combining them together, taking into account their respective noises.

The combination of C/A-code with L1 carrier phase was first used in a code smoothing process by Hatch (1982) for kinematic positioning and for rapid static ambiguity initialisation, however, only the relative geometrical information contained in the carrier-phase is utilised. A limited study by Erickson (1992b) did not establish any differences between the carrier phase float solution and the combined code-carrier solutions. Sometimes the former gave a better solution and at other times the latter. A study has therefore been carried out in this research, implementing several weighting schemes and data intervals, in order to establish the performance of the combined measurements.

5.6.1 Mathematical Model

The following mathematical model for the combined code and carrier-phase measurements is used for the static batch least squares procedure.

Using the double-differenced model for both the code pseudo-range and the carrier phase, as given in equation (5.32) and (5.39);

$$\begin{aligned} \Delta\nabla P_{12}^{12} &= \Delta\nabla\rho_{12}^{12} \\ \Delta\nabla\Phi_{12}^{12} &= \Delta\nabla\rho_{12}^{12} + \Delta\nabla N_{12}^{12} \end{aligned} \tag{5.58}$$

the design matrix and the RHS vector for the combined algorithm would contain;

$$A = \begin{bmatrix} A_P \\ A_\Phi \end{bmatrix} \tag{5.59}$$

$$RHS = \begin{bmatrix} l_P \\ l_\Phi \end{bmatrix} \tag{5.60}$$

where A_P, l_P and A_Φ, l_Φ are the design matrix and the misclosure vector for the code and carrier phase measurements respectively. The A matrix will have n x m dimension, where n is the total number of code and carrier phase measurements, and m is the number of parameters to be estimated, including the unknown integer ambiguities of the carrier phases.

Chapter 6

SINGLE-FREQUENCY RAPID STATIC POSITIONING

6.1 Single-frequency Rapid Static Positioning (RSP-L1)

The most accurate GPS relative positioning requires that the initial phase ambiguities are resolved, and then constrained to their correct integer values in the subsequent "bias-fixed" solution. In traditional GPS surveying, site observation periods of the order of one hour or more are typically recommended for short baselines (< 30 km) to ensure sufficient change in satellite-receiver geometry for ambiguity resolution, with the longer observation periods necessary for longer baselines (Rizos, 1996). The resolution of these ambiguities to their integer values has become itself a field of study. In the most rudimentary procedures, the "float" or "real-valued" ambiguities from a least squares adjustment of double-differenced phase data are rounded up or down to their nearest integer value. In more sophisticated routines, candidate sets of integer ambiguities are constructed around the initial ambiguities and then tested by carrying out several "bias-fixed" solutions to select the likeliest set. These sophisticated routines require significantly less data than the conventional procedures, thus enabling "rapid static" positioning. Procedures which allow a shortening of the observation span have become the focus of study over the past five years.

The heart of any RSP algorithm is the Ambiguity Resolution Technique (ART). Over the past few years, a number of ART have been proposed, tested and implemented. These include the Ambiguity Function Method (AFM) (Mader, 1990); the Fast Ambiguity Resolution Approach (FARA) (Frei and Beutler, 1990); the Least Squares Ambiguity Search Techniques (LSAST) (Hatch, 1990); Spectral Decomposition method (Spectral) (Abidin, 1993); Fast Ambiguity Search Filter (FASF) (Chen, 1993); and the Least Squares Ambiguity Decorrelation Approach (LAMBDA) (Teunissen, 1994). The successful implementation of an ART will resolve the correct integer value of the ambiguities, thus enabling the bias-fixed solution to be obtained, and giving an estimated position that is of high accuracy. However, when the ambiguities are resolved to wrong

values, the bias-fixed solution will give a wrong position, generally worse than the initial bias-float solution! In the latter case, the bias-float solution results should be used instead. The general process of RSP procedure is depicted in Figure 6.1.

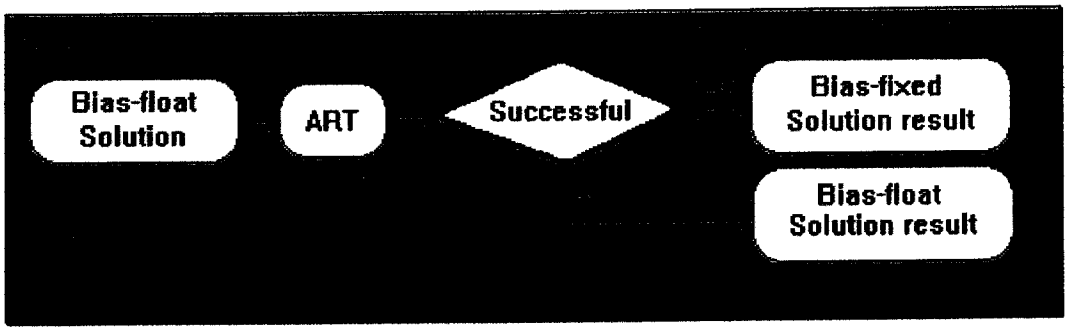

Figure 6.1: Flow Chart of the RSP Process

RSP algorithms implemented within commercial systems utilise the state-of-the-art hardware such as the Ashtech Z-Tracking System (Nolan et al, 1992), the Trimble Surveyors[tm] System, or Leica's System 200 (or 300). These systems are based on dual-frequency carrier phase measuring GPS receivers. Some of them also require the precise P-code measurements. In the case of RSP-L1 systems, only a few examples are available, such as SERCEL's Kinematic Application in Real Time (KART) system (Barboux, 1995), and Trimble's DS500. Most of these (RSP-L1) systems, although relatively inexpensive, are not as popular as the dual-frequency systems possibly due to the poorer reliability of the ambiguity resolution algorithm implemented within them. This research has investigated the reliability of RSP-L1 based on data obtained from low-cost single-frequency GPS receivers. Although not expected to be as reliable as the dual-frequency RSP systems, it still warrants testing as a candidate for a mapping system.

6.2 Ambiguity Resolution Techniques for RSP-L1

In principle, all ART mentioned above can be implemented for use in single-frequency GPS systems. The major disadvantage would be that the effective signal wavelength is about 19cm, while the dual-frequency system can use the "widelane" wavelength (a combination of the L1 and L2 which gives a wavelength of about 84 cm). The feasibility of resolving the ambiguities with a single-frequency system has been demonstrated for a variety of applications on land, at sea and in the air (e.g., Erickson, 1992a; Lachapelle et al., 1992, 1993). Assuming a relatively short baseline (say < 25 km), and the availability of at least six satellites with a PDOP < 3, the time to resolution was found to vary between a few tens to over a thousand seconds, depending on whether a choke-ring antenna were used or not (Lachapelle et al., 1993).

The procedure used for ambiguity resolution in RSP generally involves several steps. Firstly, a bias-float solution is obtained for the initial baseline estimate and the real-valued estimates of the ambiguities. Secondly, a search algorithm, employing one or more validation and rejection criteria is employed to identify the correct ambiguity combination, from the many candidate ambiguity sets contained within the search volume constructed around the initial position. Thirdly, assurance criteria is applied, normally utilising the contrast test between the minimum quadratic form of the residuals and the second minimum one, so that the ambiguity will be fixed if the "contrast" is sufficient, otherwise ambiguity resolution is considered to have failed. The process is depicted in the Figure 6.2.

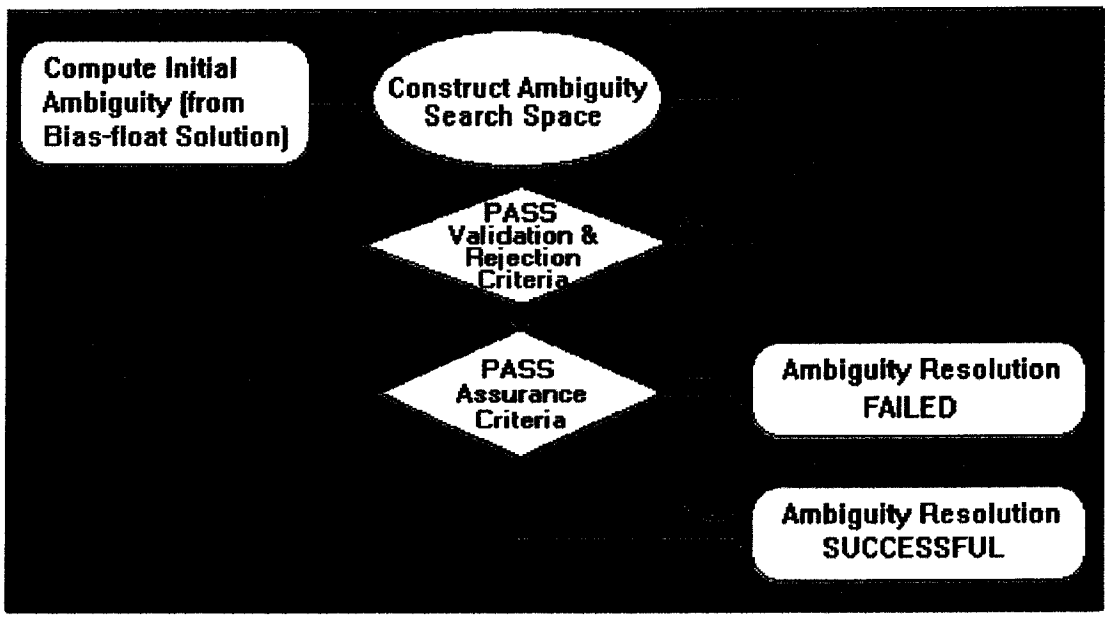

Figure 6.2: General ART Procedures

6.2.1 LAMBDA ART

Many of the earlier mentioned ARTs perform the search in the "ambiguity domain". In the case of short observation spans (as in RSP), one of the problems encountered is that the confidence ellipsoid of the ambiguities is usually rotated with respect to the coordinate axes and is extremely elongated, making ambiguity resolution difficult to perform. The LAMBDA method suggested by Teunissen (1994) uses an approach which transforms the original double-differenced ambiguities to a new set of transformed ambiguities. The confidence ellipsoid of the transformed ambiguities is more sphere-like in shape (and the ambiguities are fully decorrelated), thus permitting the ambiguities to

be solved in an efficient manner. Test carried out by Han (1995) have demonstrated that the LAMBDA method is superior in comparison to the other ARTs (Table 6.1).

Table 6.1: Comparing LAMBDA method with other ARTs (Han, 1995)

ART	Number of Initial Candidates	Number of the Candidates for the Final Decision	Computation Time (seconds)
FARA	2904739	176486	19.61
Cholesky	2904739	2904739	65.36
Spectral	2904739	84908	277.53
LSAST	7429	7429	0.83
FASF	4175	4175	0.55
LAMBDA	686	686	0.06

As this is the method used in this research, the LAMBDA algorithm is described below in detail.

The double-differenced phase solution parameters are (equation 5.42);

$$\hat{X} = \begin{bmatrix} \hat{X}_C \\ \hat{X}_N \end{bmatrix} \tag{6.1}$$

with the ambiguity vector $\hat{X}_N$ initially solved in the real domain R^m instead of the integer domain Z^m.

The original double-differenced ambiguity vector $\hat{X}_N$ obtained from the bias-float solution is then transformed to the new ambiguities $\hat{Z}_N$,

$$\hat{Z}_N = Z\hat{X}_N \tag{6.2}$$

where $\hat{Z}_N$ is the transformed ambiguity vector and Z is an *admissible ambiguity transformation* if and only if matrix Z has *integer entries* and its *determinant equals +1*. (The integer terms of Z are required in order to preserve the integer property of the ambiguities, while the unit determinant is needed to preserve the volume in the transformation.)

The objective of LAMBDA method is to find Z which will ensure sufficient diagonalisation of $Q_{\hat{Z}_N}$, the VCV matrix of the transformed ambiguities (Teunissen, 1994), or in other words, to obtain small-valued diagonal terms and zero (or near-zero) off-diagonal terms (in order to decorrelate the ambiguities). The computations of $Q_{\hat{Z}_N}$ is done in the normal manner:

$$Q_{\hat{Z}_N} = Z.Q_{\hat{X}_N}.Z^T \tag{6.3}$$

Forming the Z matrix

Han and Rizos (1995b) describe a fast method of determining the transformation matrix Z, the steps of which are reproduced here;

i. Form the unit upper triangular factorisation of the VCV matrix:

$$Q_{\hat{X}_N} = U_1 D_1 U_1^T \tag{6.4}$$

with U_1 the upper triangular matrix, and D_1 is a diagonal matrix containing the diagonal elements of $Q_{\hat{X}_N}$.

ii. Compute the integer matrix Z_{U_1}:

$$Z_{U_1} = \left[INT(U_1)\right]^{-1} \tag{6.5}$$

where INT is an operator that rounds all elements of U_1 to its nearest integer value.

iii. Compute $Q_{\hat{Z}_{N,U_1}} = Z_{U_1} Q_{\hat{X}_N} Z_{U_1}{}^T$ (6.6)

iv. Form the unit lower triangular factorisation matrix:

$$Q_{\hat{Z}_{N,U_1}} = L_1 D_1 L_1{}^T \tag{6.7}$$

v. Compute the integer matrix:

$$Z_{L_1} = \left[INT(L_1)\right]^{-1} \tag{6.8}$$

vi. Compute $Q_{\hat{Z},L_1} = Z_{L_1} Q_{\hat{Z}_{N,U_1}} Z_{L_1}{}^T$ (6.9)

The process is repeated until both U_1 and L_1 became unit matrices. The transformation matrix Z is then computed as follows:

vii. $Z = Z_{L_{k-1}} Z_{U_{k-1}} \ldots Z_{L_1} Z_{U_1}$ (6.10)

The original ambiguity vector is then transformed to the new ambiguity vector using this Z matrix, as in equation (6.2).

6.3 The Ambiguity Search - Validation and Rejection Criteria

A simple search method of resolving the ambiguities would be just to fix the transformed ambiguities to their nearest integer values, such that;

$$Z_N = INT(\hat{Z}_N) \tag{6.11}$$

The original ambiguities can then be computed through multiplication by the inverse of the transformation matrix Z;

$$X_N = Z^{-1} Z_N \tag{6.12}$$

If the transformation matrix has successfully decorrelated the ambiguities, then this is the ideal way of resolving the ambiguities. Unfortunately in reality, it is not that easy, as the correlations between the ambiguities still exist, although they have been reduced by the transformation. In this case, a search procedure for the correct integer ambiguities still needs to be employed.

<u>The search method</u>

In the search process, a number of criteria have been used in trying to validate the selected ambiguity sets, and reject the false sets (Abidin, 1993; Abidin & Subari, 1994). This is sometimes performed in the ambiguity domain itself (e.g., FARA, LSAST, and FASF), but it also be carried out in the position (coordinate) domain (e.g., AFM, and Spectral). In the LAMBDA method the search is carried out in the *transformed ambiguity domain*.

An ambiguity search space is first constructed, depicting the volume in which the search is to be performed. In constructing the search volume, some criteria are used to ensure that the space is big enough to certain the correct ambiguity set, but not too big so that it takes too long to perform the search. The normal way to construct the search space would be (Han, 1995);

$$\hat{Z}_{N_i} - \xi_{t_f;1-\alpha/2}.m_{\hat{Z}_{N_i}} \leq (Z_i)_k \leq \hat{Z}_{N_i} + \xi_{t_f;1-\alpha/2}.m_{\hat{Z}_{N_i}} \tag{6.13}$$

where $\hat{Z}_{N_i}$ is the real-valued of the *i*'th ambiguity with $m_{\hat{Z}_{N_i}}$ as its standard deviation, $(Z_i)_k$ is the integer-value of the *i*'th ambiguity of the *k*'th set, and $\xi_{t_f;1-\alpha/2}$ is the upper and lower range-width of the two-tailed confidence range $1-\alpha$, based on Student's probability density function *t* with *f* degrees of freedom.

A straight forward implementation is then to search all the possible ambiguity sets contained within the region defined by the above equation, applying a set of validation and rejection criteria. Finally two integer ambiguity sets, representing the most and the second most likely candidate ambiguity sets, are tested using the final assurance criterion (or criteria). Since the number of ambiguity sets contained in the search space could be enormous, a long computation time may result. A method introduced by Landau & Euler (1992) as described in Han (1995), utilising a Cholesky decomposition algorithm, can reduce this computation time. The method is explained below.

In this method, the search process is done in the "transformed ambiguity domain", hence equation (5.47) can be re-written as:

$$R_k = \left(\hat{Z}_N - Z_k\right)^T Q_{\hat{Z}_N}^{-1}\left(\hat{Z}_N - Z_k\right) \tag{6.14}$$

with all parameters as explained earlier. Notice now that the original ambiguity estimation problem has been changed to search Z_k for an integer set that makes R_k minimum (Ibid, 1995).

The $Q_{\hat{Z}_N}^{-1}$ matrix can then be expressed as Cholesky factors;

$$Q_{\hat{Z}_N}^{-1} = C.C^T \tag{6.15}$$

where C is a triangular matrix. Introducing the Cholesky factor C in equation (6.14), one obtains:

$$R_k = \left[\left(\hat{Z}_N - Z_k\right)^T C\right]\left[\left(\hat{Z}_N - Z_k\right) C\right]^T \quad . \tag{6.16}$$

Computing the:

$$f_k = \left(\hat{Z}_N - Z_k\right)^T C \tag{6.17}$$

would give the final multiplication of R_k as:

$$R_k = f_k f_k^T \tag{6.18}$$

which computationally is simply the squaring and addition of the vector elements of f_k. Further advantage of the triangular shape of matrix C can be taken. Instead of performing the complete multiplication of matrices in equation (6.17) and then the vector multiplication of (6.18) for all ambiguity sets, and then applying the validation and rejection criteria, one could implement the validation and rejection process while computing both equations. In this way the rejection of the false integer set is carried out at a very early state, when the partial results of equation (6.18) already supersede the previously found second minimum value (remember that the process will select the minimum and the second minimum sets).

6.4 Assurance Criteria for the Integer Ambiguities

However, the determination of the most likely set of ambiguities is only part of the process. Once the best ambiguity set is found a procedure is needed to determine whether or not the best set is actually the correct one. Several discussions on this topic can be found in the literature (e.g., Frei & Beutler, 1990; Euler & Landau, 1992; and Abidin, 1993). A simple assurance criteria that could be used is based on computing the contrast value from the quadratic form of the residuals of the best set (minimum sum-of-weighted-squares of residuals) and the second best set.

$$contrast = \frac{\left(V^T PV\right)_{sec}}{\left(V^T PV\right)_{min}} \tag{6.18}$$

A large *contrast* value would indicate a better "separability" of the ambiguity sets, hence enabling the ambiguities to be resolved in a more confident manner, while a small contrast value would indicate otherwise. The assurance criterion would then be;

- *The contrast value, derived from the quadratic residual of the best set and the next best ambiguity set is greater than some pre-set threshold value. In this case, the value chosen is 1.5* (Han & Rizos, 1996).

If the contrast value is greater than the treshold value, the best set (with the minimum $V^T PV$), will be accepted as the correct transformed ambiguity set. The original ambiguities are computed using equation (6.12).

A schematic diagram of the total ambiguity resolution procedure employed in this research is given in Figure 6.3.

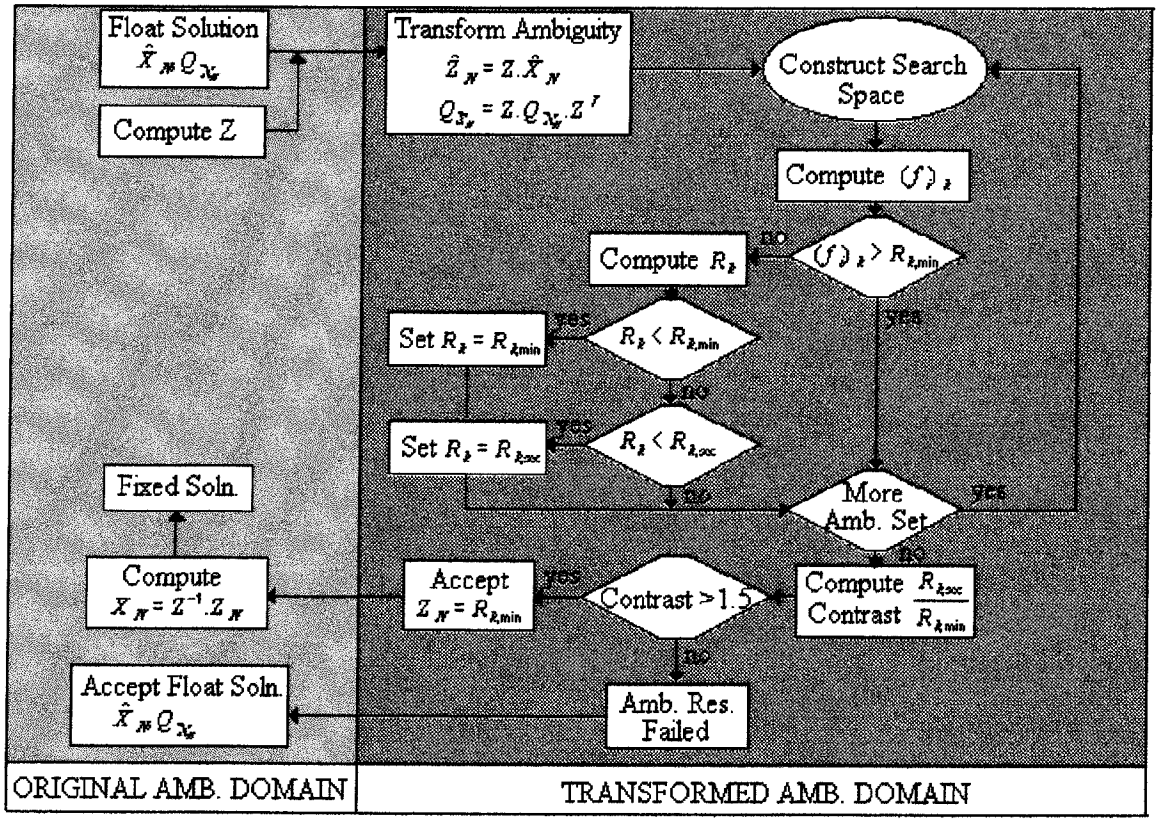

Figure 6.3: Flow-Chart for the LAMBDA ART as Implemented in software

Chapter 7

THE TESTS

Testing and calibrating surveying equipment is a common procedure undertaken by surveyors. In this regard, the GPS technology is no exception. For GPS in particular, tests are carried out for two purposes: (a) to test a category or brand of GPS instrumentation (a combination of hardware and software), or (b) to test a particular GPS instrument unit on a regular basis, or in response to a suspected problem (Rizos, 1996).

There are several system testing strategies. The most common type of test is based on the results of the baseline solution, the end product of the processing of data sets explicitly collected for this purpose. The results are compared against "ground truth" information either provided by previous GPS surveys (preferably using a technique which is of a higher accuracy than that being tested), or conventional survey techniques (Ibid, 1996).

In this research an *investigative test* was carried out. The test was designed and conducted for the explicit purpose of benchmarking the performance characteristics of a GPS system (in particular the low-cost GPS systems identified in this study) by determining the accuracy and reliability performance of the system. These performance characteristics will then be related to the observing conditions. Several low-cost GPS systems have been proposed, including a mixed system (one low-cost and one standard surveying GPS receiver). Several baselines of lengths varying from about 2 to 35 kilometres were observed. 24 hours of data were collected on each baseline to sample all satellite distribution geometries, as well as varying atmospheric contributions. The data were then processed using the BASEPACK Software, with varying observation length: single-epoch data, 1, 2, 5, 10, 30 and 60 minute data sessions. This chapter describes the test campaigns that were carried out for these investigations. Results and analysis of the data are presented in Chapter 8.

7.1 The Test Campaigns

Two campaigns have been carried out: (a) one campaign was carried out in Bandung, Indonesia, and (b) the other one in Johor Bahru, Malaysia (Figure 7.1). Both test areas were purposely selected because of their tropical and equatorial locations. The aim was to carry out the tests in an area with the 'worst' ionospheric effect, a condition that was expected in this region. It was reasoned that a higher accuracy and reliability could be expected if the GPS system is then used in other areas.

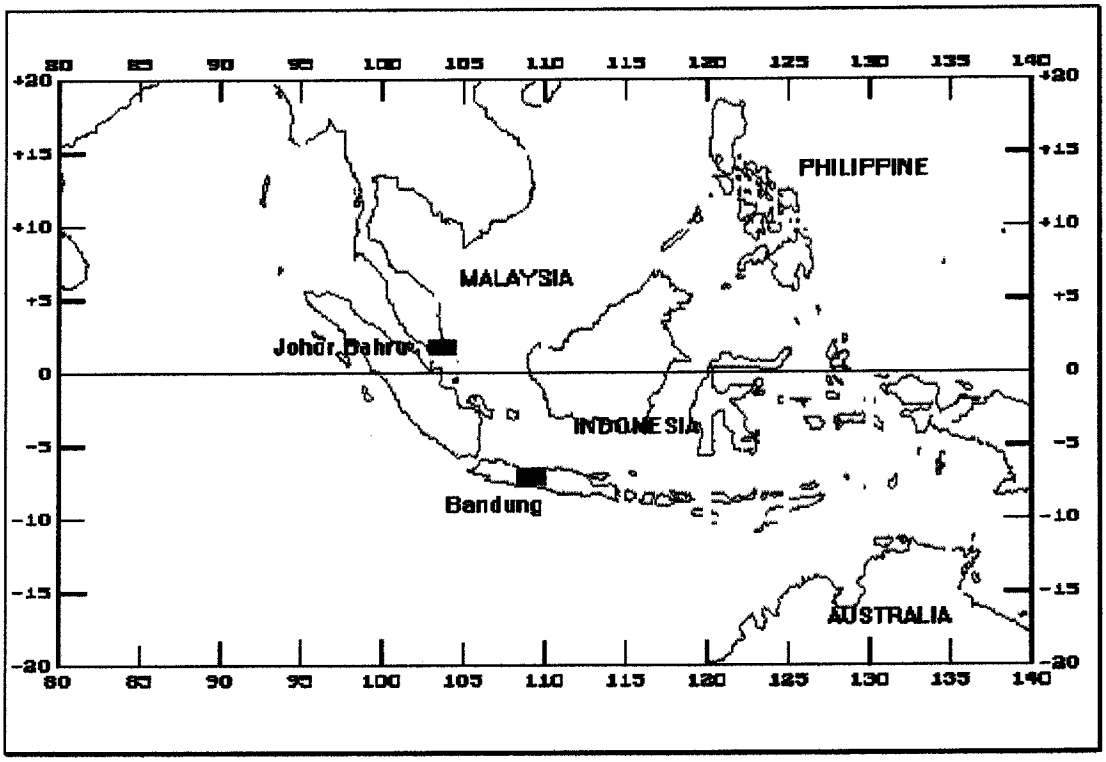

Figure 7.1: Location of the Test Areas

7.1.1 GPS Receivers Used in the Campaigns

Low-cost GPS Receivers

Two types of low-cost GPS hardware were used in the tests. The first one, the NovAtel GPSCard is priced at around AUD$6,500 (1994), and is a surveying type GPS receiver with many features of 'top-of-the-line' geodetic instrumentation. The other instrument was a Trimble SVeeSix receiver, a GPS navigation-type receiver costing around AUD$650 (1990). Both receivers required an external computer for I/O operations and data logging. Further characteristics of each receiver are described below.

1. NovAtel GPSCard Series Model 951R Receiver

This GPS receiver is an OEM board manufactured by NovAtel Communication Ltd. of Calgary, Canada, which utilises the enhanced tracking mode known as "Narrow Correlator Technology", enabling relatively precise C/A-code pseudo-ranges to be measured. The Model 951R (Figure 7.2) is also able to output the integrated carrier phase observable.

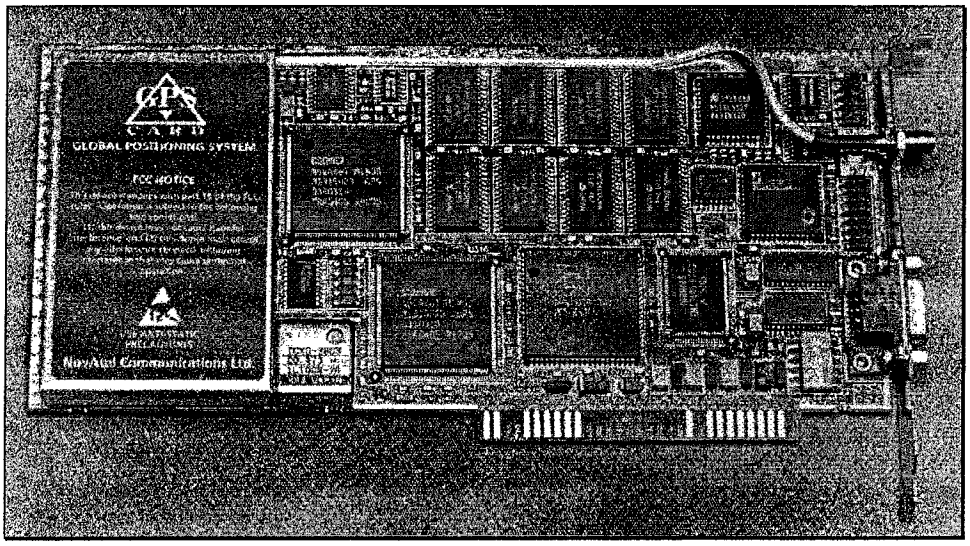

Figure 7.2: NovAtel GPSCard Series Model 951R Receiver

The model has the following features (NovAtel, 1994):

Table 7.1: NovAtel GPSCard 951R Receiver Features

Satellite tracking	10 parallel dedicated channels
Correlator	Narrow spacing
Measurement type	C/A-code, L1 and D1
Observation accuracy	C/A-code -10 cm RMS (no multipath) Phase - 3 mm RMS
Positioning accuracy (GDOP < 2)	15 metres CEP (SA off) 40 metres (SA on) 1-5 metres CEP (differential)
Data rate	Selectable, up to 20 Hz
Time tags	Steered
Antenna	Microstrip

The NovAtel GPSCard receiver used in these investigations belongs to the School of Geomatic Engineering, The University of New South Wales (UNSW). The GPSCard was housed within an NEC Portable PowerMate computer (PC), requiring a/c current to power it.

2. Trimble SVeeSix Receiver

This OEM type receiver, manufactured by Trimble Navigation Ltd., USA, is an example of ultra-low-cost GPS sensors (Figure 7.3). It can provide position and velocity information, as well as raw observation data. It is a product intended for GPS system integrators, producing products for: environtmental data acquisition, timing, tracking, geographical information systems (GIS) data capture, agriculture, marine, and communication applications, with real-time differential correction capability if needed.

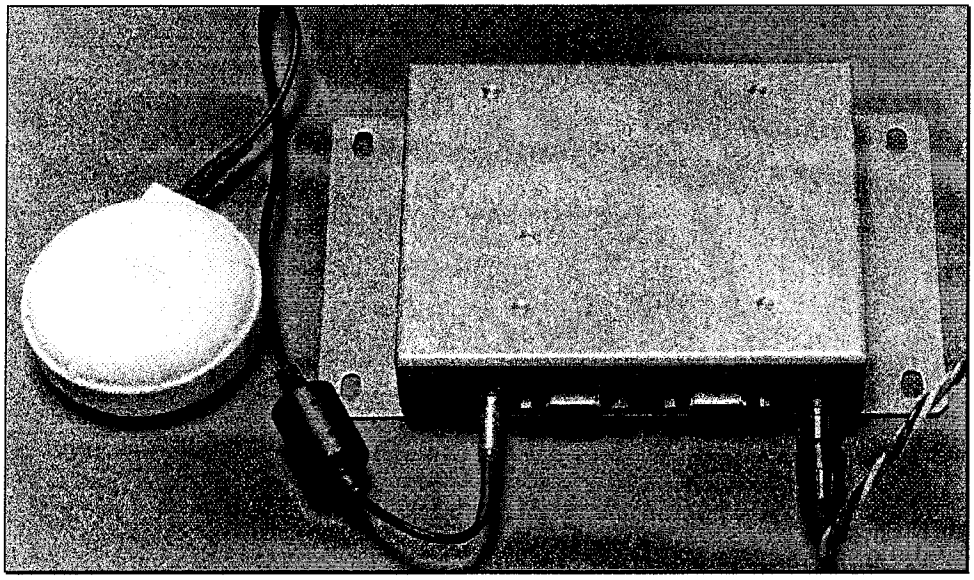

Figure 7.3: Trimble SVeeSix Receiver

Some of the features of this receiver are given in Table 7.2 (Trimble, 1990).

This GPS sensor runs on a 12 Volt dry-cell battery, with a 1.5 Volt battery permanently attached to it (to store the satellite almanac). An IPC 386 SP notebook computer was used to control the receiver and also to log data collected by the receiver. The computer was run on a/c current.

Table 7.2: Trimble SVeeSix Receiver Features

Satellite tracking	4 dedicated channels and 2 switching channels, tracking up to 8 satellites
Measurement type	C/A-code and D1
Observation accuracy	Not specified
Positioning accuracy (GDOP < 2)	25 metres SEP (SA off) 100 metres (2dRMS) <10 metres (differential)
Data rate	0.5 seconds - at 0.25 seconds and 0.75 seconds respectively
Time tags	Different measurement time for each satellite
Antenna	Low profile microstrip patch

Standard Surveying GPS Receivers

One geodetic and two surveying receivers were also used in the test campaigns: (a) The 'top-of-the-line' ASHTECH Z-XII geodetic receiver which makes all the possible observations, (b) the ASHTECH LD-XII C/A-code dual-frequency GPS receiver, and (c) the TOPCON GP-R1 C/A-code single frequency GPS receiver.

All receivers were powered by 12 Volt dry-cell batteries. Most of the time, two batteries were used together, connected in parallel, for the 24 hour operating period.

A summary of the observables possible by the GPS receivers used in this investigations is given in Table 7.3.

Table 7.3: GPS Receivers Measurement Types

Receiver	Measurements
ASHTECH Z-12	PC/A, P1, P2, L1, L2, D1, D2
ASHTECH LD-XII	C/A, L1, L2, D1
TOPCON GP-R1	C/A, L1, D1
NovAtel GPSCard	C/A, L1, D1
SVeeSix	C/A, D1

The C/A-Code Observable

Due to the significant difference in quality of the C/A-code measurements made by these receivers, for the purpose of system identification in these investigations, the C/A-code is classified into two categories:

Table 7.4: Types of C/A-Code and Its Accuracy

C/A-Type	Receivers	Designated Std. deviation
Precise C/A-code (PC/A-code)	Ashtech Z-XII, NovAtel	0.7 m
Standard C/A-code (C/A-code)	SVeeSix, Ashtech LD-XII	1.7 m

The Ashtech Z-XII and the NovAtel GPSCard 951R receivers measure a relatively precise C/A-code pseudoranges (PC/A-code). The measurement noise for the NovAtel in particular has been reported as being around 30 cm (Erickson, 1992b; Lachapelle et el., 1992). Taking into consideration the other measurement biases, and studying the magnitude of the double-difference of the two PC/A-codes (Figure 7.4 (b)), the standard deviation for the PC/A-codes was set to about 70 cm. The other GPS receivers, the SVeeSix, the Ashtech LD-XII and the TOPCON GP-R1, measure the standard C/A-code pseudo-ranges, with Figure 7.4 showing a precision of around 1.5 - 1.7 m. Obviously, when a mixed combination of the PC/A-code and the standard C/A-code is used, the latter precision is assigned (e.g., see double-difference residuals of Ashtech LD-XII and NovAtel C/A-code in Figure 7.4 (a)).

7.2 Low-Cost GPS System Configurations

In order to facilitate system identification in these investigations, several low-cost GPS systems have been identified:

System 1 **: PC/A-Code System**
Measurement Type : Precise C/A-code pseudo-range
Data processing algorithm : Double-differenced observables
System formation : NovAtel + Ashtech Z-XII

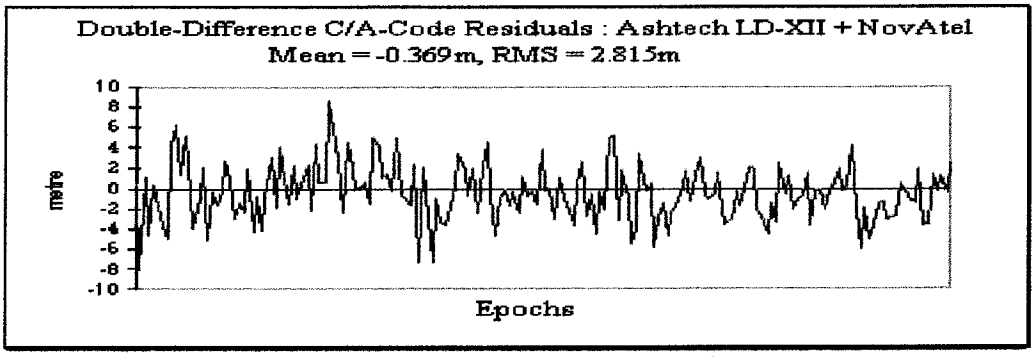

(a) Ashtech LD-XII + NovAtel

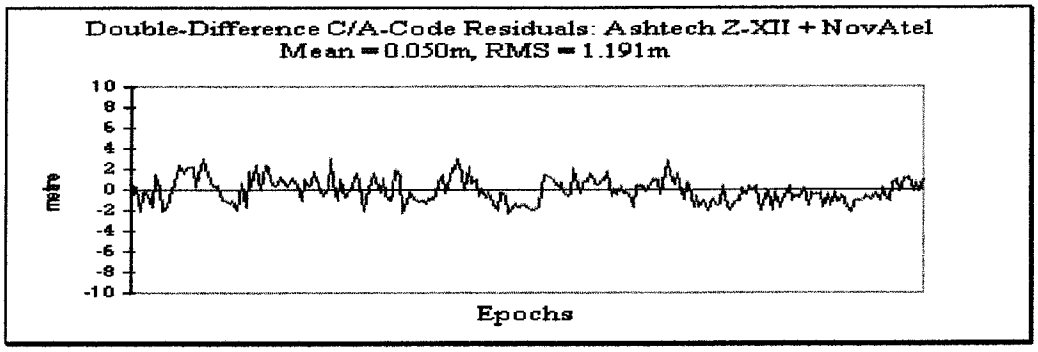

(b) Ashtech Z-XII + NovAtel

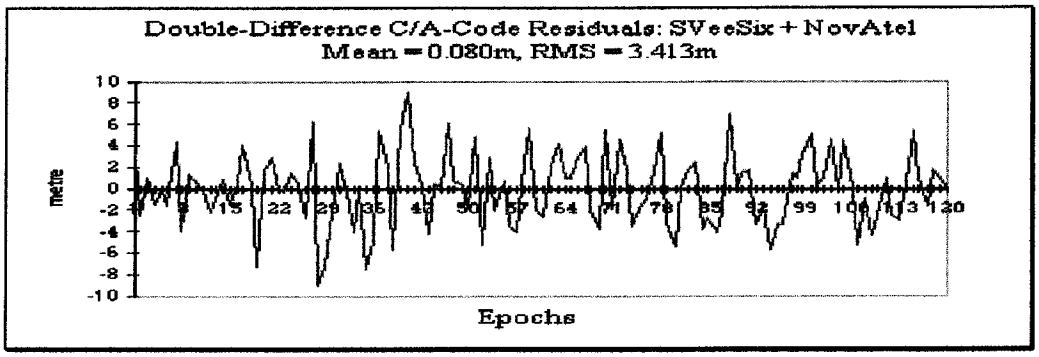

(c) NovAtel + SVeeSix

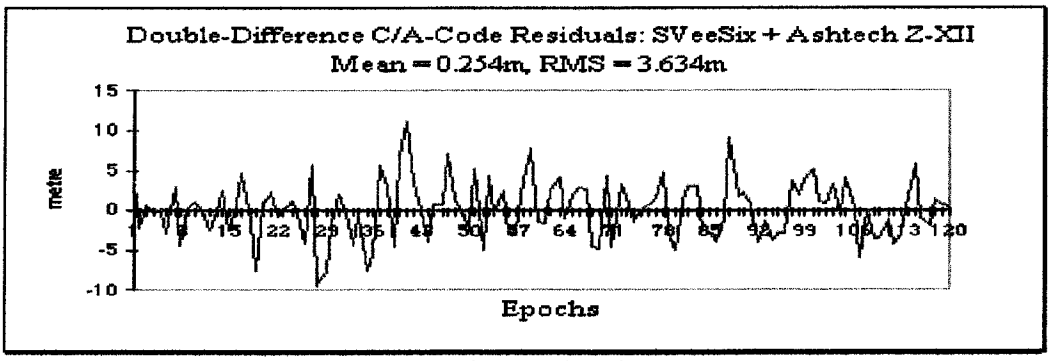

(d) SVeeSix + Ashtech Z-XII

Figure 7.4: Double-Difference Residuals of Different Types C/A-Code Measurements

System 2	**: C/A-Code System**
Measurement Type	: Standard C/A-code pseudo-range
Data processing algorithm	: Double-differenced observables
System formations	: SVeeSix + Ashtech Z-XII, SVeeSix + NovAtel.

Note that mixing a C/A-code receiver with a PC/A-code receiver is equivalent to a C/A-code system.

System 3	**: L1 Phase System**
Measurement Type	: L1-carrier phase
Data processing algorithm	: Double-differenced observables
System formations	: NovAtel + Ashtech Z-XII, NovATel + Topcon GP-R1, NovAtel + Ashtech LD-XII

System 4	**: Triple-Difference L1 Phase System**
Measurement Type	: L1-carrier phase
Data processing algorithm	: Triple-differenced phase observable
System formations	: Same as system 3

System 5	**: Mixed PC/A-Code and L1 Phase System**
Measurement Type	: Precise C/A-code pseudo-range and L1-carrier phase
Data processing algorithm	: Double-differenced observables
System formation	: NovAtel + Ashtech Z-XII

System 6	**: Mixed C/A-Code and L1 Phase System**
Measurement Type	: C/A-code pseudo-range and L1-carrier phase
Data processing algorithm	: Double-differenced observables
System formations	: NovAtel + Ashtech LD-XII, NovATel + Topcon GP-R1

System 7	**: RSP-L1 System**
Measurement Type	: Precise C/A-code pseudo-range and L1-carrier phase
Data processing algorithm	: Double-differenced observables (ambiguity fixed solution)
System formations	: NovAtel + Ashtech Z-XII

7.3 Campaign I

The observations in this campaign was collected around the city of Bandung, on the island of Java, in Indonesia (Figure 7.1). The area is bounded by Latitude $6^{o} - 7^{o} S$ and Longitude $111^{o} - 115^{o} E$. The overall area is mountainous with height ranging between 100 - 1500 km above mean sea level.

7.3.1 Stations

The site selection, except for the PASC site which was a geodetic pillar on top of the four-story PASCA Building, on the campus of the Institute of Technology Bandung (ITB), was made according to the following 'non-scientific' criteria;

- Easy accessibility,
- Access to electrical supply to power the host computers,
- Security for 24 hours unattended operations.

For a combination of these reasons most of the sites that were selected were atop houses and bungalows. A short description of each site is given below.

Site 1: PASC

The antenna was set up on a survey pillar atop the four-story PASCA Building, located on the campus of ITB. The station had been surveyed previously and its coordinates in the WGS-84 system are known. The surrounding buildings were of varying heights but a cut-off elevation angle of about 5° was possible. During the course of the observations an amateur radio transmitter was being erected about 5 metres away from the station, but was still not in use. The receiver was kept in the building, connected to the antenna via a 5 m cable.

Site 2: CIGA

The antenna was located on top of a cylindrical stainless steel water tank about 2 m diameter, located on the roof of a house. The antenna was connected via a 3 m antenna cable to the receiver located at the base of the water tank. The area was within a housing estate, with detached houses neighbouring the house used for the observations. The surroundings were the rooftops of other houses, and some large trees, which allowed elevation angle mask angles of about 5°-10°.

Site 3: ISHA

The antenna was mounted on a standard surveying tripod placed on the roof of a bungalow house. The receiver was located in the house, with a cable connecting it to the antenna. The surroundings were an open area with low vegetations. Observations down to the horizon were possible at this site.

Site 4: TONO

The antenna was mounted on a standard surveying tripod placed on the roof of a terrace house. The receiver was located in the house, with a cable connecting it to the antenna. The surroundings were the rooftops of other houses of the same height. The cut-off elevation angle was about 5^{o}.

Site 5: DIDI

The antenna was mounted on a standard surveying tripod, placed on the roof of a terrace house. The receiver was located in the house, with a cable connecting it to the antenna. The house is located within a housing area, and the surroundings were rooftops of other houses of the same height. The cut-off elevation angle was again about 5^{o}.

Site 6: EKAK

The antenna was mounted on a standard surveying tripod placed on high ground, in the backyard of a village house. The receiver was located in the house, with a cable connecting it to the antenna. The surroundings were four village houses, some with 'atap' rooftops, and some with zinc roofing. Several large trees around the site meant that elevation mask angles of around 5^{o}-10^{o} were necessary.

7.3.2 Baselines Observed

A total of seven baselines, ranging in length from 1.9 to 16.5 km, have been observed in this campaign (Figure 7.5). The baselines were observed to test the performance of mixed use of a low-cost GPS receiver with a standard surveying receiver, as well as a stand alone low-cost GPS system. The low-cost GPS receivers used in this campaign were the NovAtel GPSCard 951R receiver and the Trimble SVeeSix receiver. The Ashtech Z-XII GPS receiver was the geodetic instrument. Due to the limited memory capacity of the Ashtech Z-XII receiver, 15 second data rate was selected for data collection.

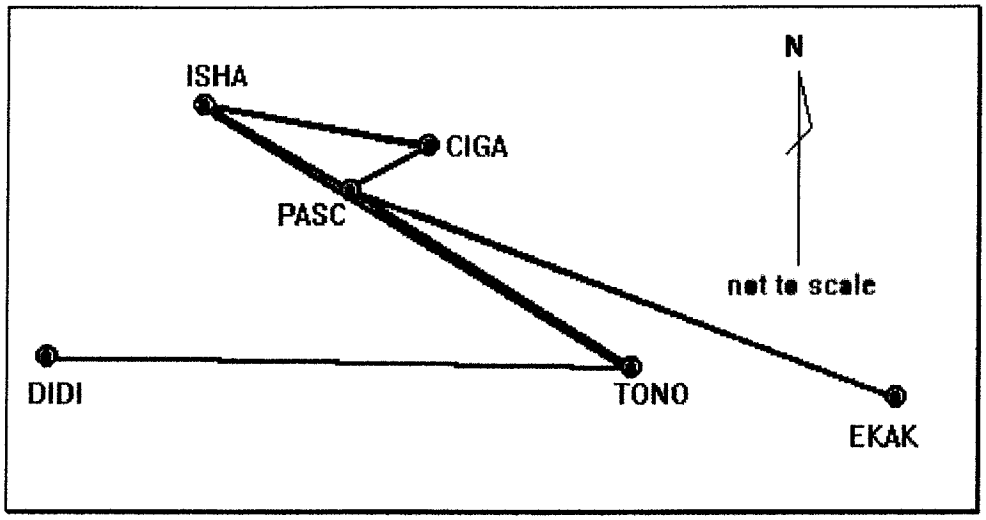

Figure 7.5: Indonesian Campaign Baselines

A total of 5 days, of 24 hour observation tests were carried out, corresponding to GPS daynumbers 227, 229, 231, 233 and 235 in 1995. On day 227, one baseline, the Ashtech Z-XII receiver at site PASC and NovAtel receiver at site EKAK, was observed. Due to several electricity failures, the observations at site EKAK, which uses a/c to power the NEC computer hosting the NovAtel receiver, were not a full 24 hour span. On day 229, another observation campaign was organised. Initially, three receivers were deployed; the Ashtech Z-XII at site PASC, the NovAtel at site TONO and the SVeeSix at site CIGA. An electricity black-out in the middle of the day caused the loss of data of the SVeeSix at CIGA. As a result, only one baseline was observed. On day 231, the same instrumentation was used; with the Ashtech Z-XII at site PASC, the NovAtel at site ISHA, and the SVeeSix at site CIGA. On this day the 12 Volt dry-cell battery that powered the Ashtech Z-XII went flat at around 18:00 hour. Despite this mishap, 24 hours of data was successfully collected for the CIGA and the ISHA sites. Three baselines were successfully observed on that day; 24 hours data for the CIGA-ISHA baseline, and 18 hours data for both the CIGA-PASC and ISHA-PASC baselines. On day 233 only one baseline was observed, connecting the Ashtech Z-XII receiver at site TONO and the NovAtel receiver at site ISHA. 24 hour of data were observed. Another baseline was observed on day 235, between site DIDI using the Ashtech Z-XII receiver, and site TONO, using the NovAtel. Again, 24 hours of data were collected. A summary of the baselines observed, baseline length, sites and GPS receivers used, and the amount of data collected, is given in Table 7.5.

Table 7.5: Campaign I Baseline Summary

No.	GPSDAY	BASELINE	SITES + RECEIVER USED	OBSERVATION LENGTH
1.	DAY231	1.9 km	PASC - Ashtech Z-12 + CIGA - SVeeSix	18 hours
2.	DAY231	4.3 km	PASC - Ashtech Z-12 + ISHA - NovAtel	18 hours
3.	DAY231	6.2 km	ISHA - NovAtel + CIGA - SVeeSix	24 hours
4.	DAY229	8.2 km	PASC - Ashtech Z-12 + TONO - NovAtel	24 hours
5.	DAY233	12.0 km	ISHA - Ashtech Z-12 + TONO - NovAtel	24 hours
6.	DAY235	14.7 km	DIDI - Ashtech Z-12 + TONO - NovAtel	24 hours
7.	DAY227	16.1 km	PASC - Ashtech Z-12 + EKAK - NovAtel	24 hours - segmented

7.4 Campaign II

The second campaign took place around the area of Johor Bahru, in Malaysia (Figure 7.1). The area is bound by Latitude $0.5^{o} - 1.5^{o} N$ and Longitude $115^{o} - 116^{o} E$. The overall area is flat land with height ranging around 50-100 m above mean sea level.

7.4.1 Stations

For the same reasons as in the first campaign, the sites were selected mainly on the basis of 'non-scientific' criteria. A short description of each site is given below.

Site 1: HASS

The antenna was mounted on a pole about 1.5 m in height, placed on the roof of a terrace house. The receiver was located in the house, with a cable connecting it to the antenna. The house is located within a housing area, and the surroundings were the rooftops of houses of similar height. A cut-off elevation angle of about 5^{o} was possible.

Site 2: BAHR

The antenna was mounted on a standard surveying tripod placed on the balcony of a double-storey terrace house. The receiver was located in the house, with a cable connecting it to the antenna. The house is located within a housing area, and the

surroundings were other houses of similar height. A cut-off elevation angle of about 5° on the southern part of the sky was possible.

Site 3: MAJI

The antenna was mounted on a standard surveying tripod placed on the roof of a bungalow house. The receiver was located in the house, with a cable connecting it to the antenna. The house is located within a housing area, and the surroundings were the rooftops of other houses of similar height, a small distance apart, as well as several large trees, resulting in an elevation mask angle of about 5°.

Site 4: MUKR

The antenna was mounted on a pole about 1.5 m in height placed on the roof of a terrace house. The receiver was located in the house, with a cable connecting it to the antenna. Again, the house is located within a housing area.

Site 5: SYED

The antenna was mounted on a standard surveying tripod, placed on a rooftop of a terrace house in an environment similar to the other sites.

7.4.2 Baselines Observed

A total of three baselines, of length 5.5, 17.8 and 34.9 km, were observed in this test campaign (Figure 7.6). The longest baseline was observed in order to probe the limit of the low-cost GPS system configuration. The low-cost GPS receivers used in this campaign were the NovAtel GPSCard 951R receiver and the Trimble SVeeSix receiver. The Ashtech LD-XII and the Topcon GP-R1 were the surveying standard receivers tested. 20 second data rate was selected for the data collection in this campaign, mainly due to the limited capacity of the surveying standard receivers.

Two days of 24 hour long observation campaign were carried out, corresponding to GPS daynumbers 245, and 258 in 1995. On day 245 three receivers were employed; the Ashtech LD-XII at site BAHR, the NovAtel at site HASS and the Topcon GP-R1 at site MAJI. The intermittent requirement to download the data collected by both the surveying receivers at site BAHR and MAJI, resulting in segmented 24 hour data being collected at both sites. On day 258 one baseline was observed, connecting site SYED and site MUKR. An Ashtech LD-XII receiver was used at site SYED and the NovAtel receiver was used at site MUKR. Again, segmented 24 hour data sets were collected with the surveying receiver at site SYED.

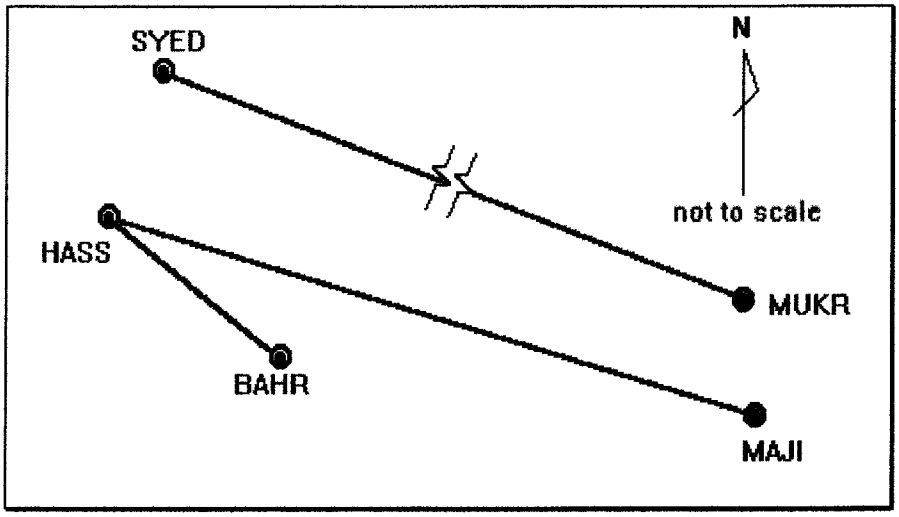

Figure 7.6: Malaysian Campaign Baselines

A summary of the baselines observed, the baseline length, sites involved and GPS receiver employed, and the length of observations is given in Table 7.6.

Table 7.6: Campaign II Baseline Summary

No.	GPSDAY	BASELINE	SITES + RECEIVERS USED	OBSERVATION LENGTH
8.	DAY245	5.5 km	BAHR - Ashtech LD-XII + HASS - NovAtel	24 hours - segmented
9.	DAY245	17.8 km	MAJI - Topcon GP-R1 + HASS - NovAtel	24 hours - segmented
10.	DAY258	34.9 km	SYED - Ashtech LD-XII + MUKR - NovAtel	24 hours - segmented

7.5 Comments on Observations

Although it was intended to collect 24 hours of data for each baseline, some technical problems prevented this from always happening. Some of them were:

1. Frequent intermittent electricity failure has affected the continuous observations of the low-cost receivers. These has affected the NovAtel and the SVeeSix receivers differently:

- In the case of the NovAtel receiver, a re-initialisation program was used to automatically restart the receiver and to continue to log the data, although to

different data files. This has resulted in several blank sessions in the 24 hour data sets.

- In the case of the SVeeSix receiver the problem was worse, having to do with the I/O characteristics of the SVeeSix. The I/O program used for data logging will only write the observed data to the data file if the data file is first closed at the end of the observation session. At re-start, all the data collected to date is lost.

2. The logistics of the surveying receivers.

Two problems arose because of this:

- The size of the RAM of the receivers did not support high data rate observations. The Ashtech Z-XII has a RAM of about 4 Mbyte, hence a 15 second data rate will barely be sufficient for a continuous 24 hours observation span. The other GPS receivers have only 1 Mbyte RAM, which would only allow a 60 second data rate for the intended span. In the case of 20 second data rate only about 8 hours data can be stored. For this reason the tracking needed to be stopped and periodically the data downloaded to a computer. Thus an uninterrupted 24 hour data set was not possible.

- The surveying receivers required 12 Volt dry-cell batteries, but this could only support experiments of a few hours in length. Interruptions in the power supply, as happened at site BAHR, have caused further segmentation of the data sets collected.

7.6 Data Processing

Procedures for processing the data were done as follows (Figure 7.7):

Data pre-processing:

1. Ashtech data files were first converted to RINEX files using the ASHTORIN utility program.
2. Timetags for the Ashtechs and Topcon data were corrected using program TIMETAG, written by the author and new RINEXO files are created.
3. SVeeSix data is converted to RINEX files using a conversion program TBP2RNX written by Mr. B.Hirsch (UNSW).

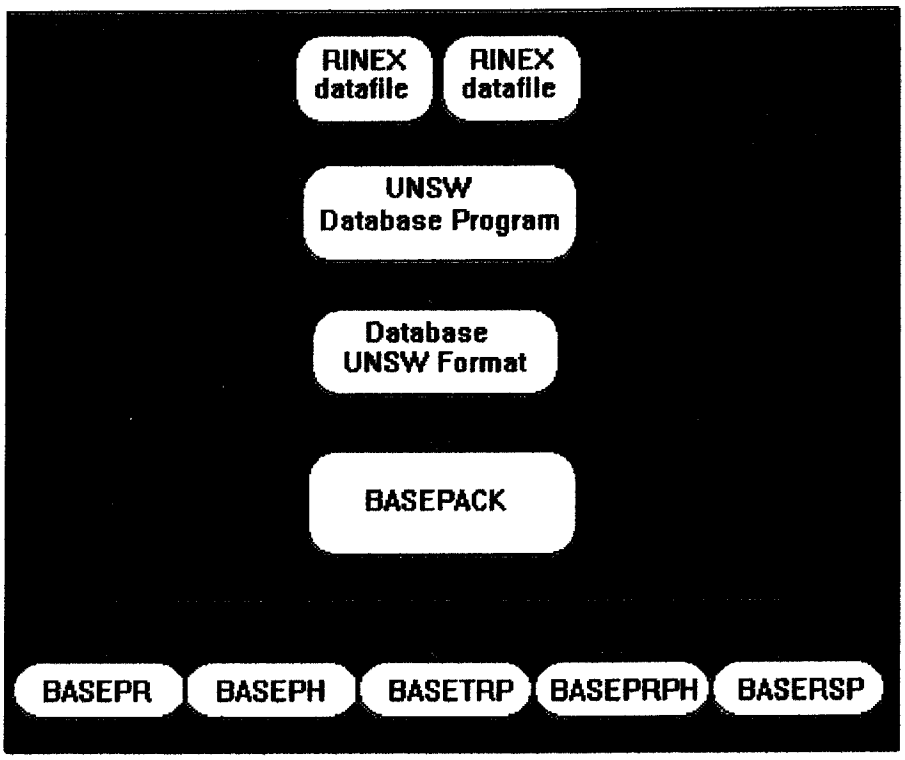

Figure 7.7: Data Processing Strategies Used in this Research

Data-base creation

The two RINEXO files (for each baselines), were then merged using the program DBCREATE, written by Mr. B.Hirsch, and a database for the baseline was then formed.

Data processing:

Data processing was then carried-out using all the algorithm options in the BASEPACK software. A batch file was written by Mr. B.Hirsch to enable the sessions (i.e., single-epoch, 1, 2, 5, 10, 30 and 60 minute spans) to be automatically processed in a continuous fashion. A PC486 computer was used for the data processing.

Results and analysis:

Results of the data processing and the analyses of these are presented in Chapter 8.

Chapter 8

RESULTS AND ANALYSES

8.1 Quantifying System Performance Characteristics

In quantifying the performance characteristics of low-cost GPS systems, following the discussion in Chapter 4, two parameters need to be defined: ***accuracy*** and ***reliability***.

System accuracy in this study is defined in terms of the ***positional error*** i.e., the ***level of "closeness"*** of the results given by the system ***to the "true" value*** (Rizos, 1996). ***Reliability*** on the other hand is considered to be ***a measure of the degree of repeatability*** of the accuracy of the results. If the obtainable positioning accuracy is stable, it suggests that the reliability of the system is high, on the other hand if the obtainable positioning accuracy is highly variable, then the reliability of the system can be considered to be low.

Hence, given a certain reliability level, say 95%, two things remain to be specified: (1) the level of accuracy which this corresponds to, and (2) the operational constraints that must be specified to ensure this accuracy and reliability (Rizos et al., 1995).

8.1.1 Analysing the Results

The analyses was carried out to achieve the objectives of the research, that is, to quantify:

- The accuracy, and the
- Level of Reliability,

of low-cost GPS systems under certain

- Operational constraints.

System Accuracy

In these investigations, system accuracy is computed via the deviation of the computed baseline results from the 'true value' (in other words, the positional error). The deviation was further catagorised to indicate different levels of accuracy, as depicted in Table 8.1.

Table 8.1: Accuracy Classification for Performance Analyses

Accuracy classification
< 10 cm
< 20 cm
< 50 cm
< 1 m
< 2 m
< 5 m

The standard deviation of the positional error can be then be computed, if required, according to the following formula:

$$\sigma_{gsv} = \sqrt{\frac{\sum_{i=1}^{n}(X_i - \tilde{X})^2}{n-1}} \qquad (8.1)$$

where

σ_{gsv} is the standard deviation of the positional error

X_i is the *i*'th baseline solution

$\tilde{X}$ is the 'true-value' of the baseline

n is the number of baseline solutions.

System Reliability

The level of reliability, corresponding to a specific accuracy level, is given by the *ratio* of the number of baseline solutions in a certain accuracy band over the total number of solutions. While system reliability, is given by the overall level of reliability of the different levels of accuracy.

The operational constraints can be divided into two groups;

- User controllable parameters, which include;
  - Length of the observation session
  - Baseline length

- Non-user controlled parameters
  - Satellite geometry
  - Atmospheric disturbances

The user-controllable parameters were analysed through the use of a variety baselines (with varying length) and the different observation session lengths adopted in the processing. The non-user controlled parameters, on the other hand, were treated as discussed below.

Satellite Geometry

The effect of satellite geometry on the results is investigated through noting the number of satellites used in the data processing. Although the *BDOP1* value is an indicator of satellite geometry (Merminod and Rizos, 1994), noting the number of satellites is a more practical and straightforward measure.

Atmospheric Disturbances

Atmospheric disturbances are effects of the ionospheric delay and the tropospheric delay on the GPS signals. The ionospheric delay, which is the largest between the two delays (Klobuchar (1991), has a worse effect on daytime compared to night time (see the approximate ionospheric *cosine model* by Klobuchar (1987), as represented in Figure 8.1).

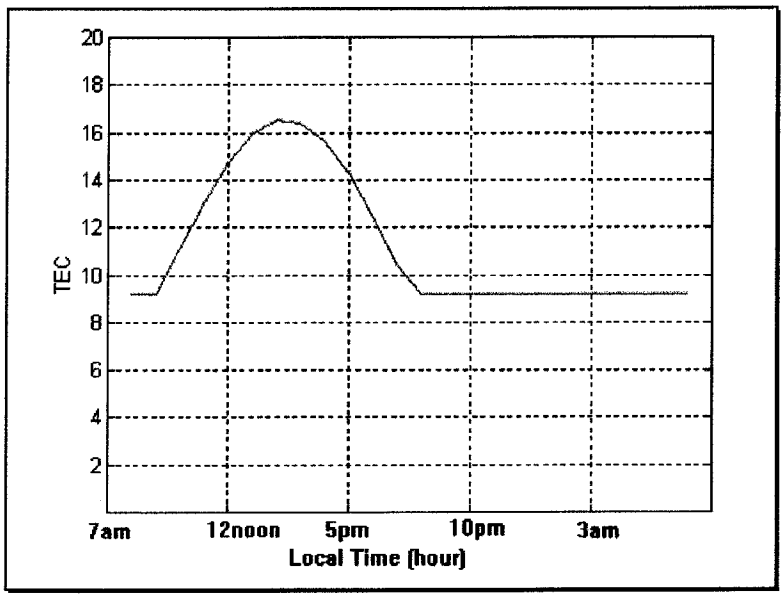

Figure 8.1: Ionospheric delay in 24 hours (adapted from Klobuchar, 1987)

Hence the analyses method employed in this investigations has taken this into account by dividing the results into DAYTIME and NIGHTIME periods. The daytime period (between 7:00 am - 7:00 pm) is the 'normal' period for conducting surveying work, but considered to experience the 'worst' ionospheric effect, while the night time period (between 7:00 pm - 7:00 am) was considered the best period as far as the ionospheric influence is concerned.

8.1.2 Computing the True Baseline Values

The accuracy of the computed baselines is expressed in terms of the solution deviation from the true component values. The true component values (distance, etc.) were obtained by processing the baselines using the Ashtech's GPPS™ software. Since all baselines involved different receiver types, a non-Ashtech receiver paired with an Ashtech receiver (or Ashtech type GPS receiver like the Topcon), some pre-processing steps are necessary before the data can be input into the GPPS™ software. It should be noted here that Ashtech and Topcon receivers allow the timetags to "drift", sometimes by as much as 0.3 seconds over a 24 hour period (as in Figure 8.2), causing the code measurements to have a negative value! These need to be "corrected" prior to merging such files with data files such as those produced by the NovAtel GPSCard receiver, which generate "steered" timetags.

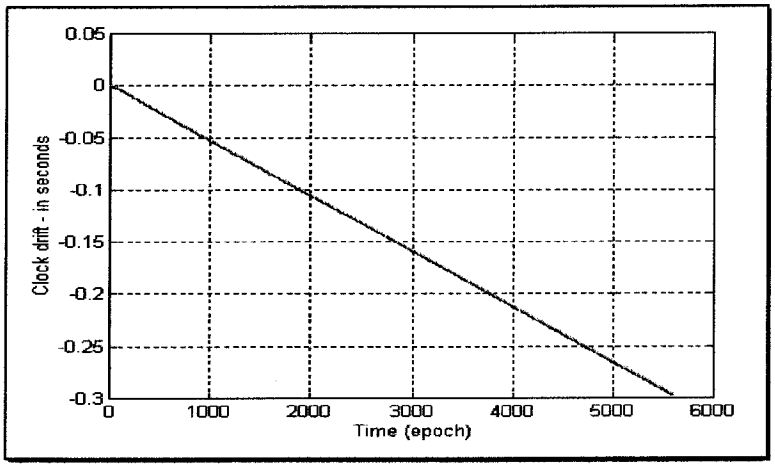

Figure 8.2: Clock Drift of the Ashtech Z-XII Receiver Over 24 Hours.

The following procedures were applied when processing the data in order to compute the true baseline component values;

1. Ashtech and Topcon data files were converted to RINEXO files using the ASHTORIN utility.
2. RINEXO files are then timetag-corrected using program TIMETAG, developed by the author.
3. Corrected RINEXO files, and the other RINEXO files (produced by the NovAtel receiver), are converted to the Ashtech format using the RINTOASH utility.
4. The L1 double-difference (fixed) solution results obtained from GPPS™ processing are considered as the true baseline values.

In the case of baselines observed with the SVeeSix receiver, as there are no carrier-phase data recorded, the true baseline is assumed to be the mean of the 60 minute session C/A-code pseudo-range solutions for the baseline.

8.2 Campaign I

In this campaign, the following six low-cost GPS system were tested;

1. System 1: PC/A-code system
2. System 2: C/A-code system
3. System 3: L1 carrier-phase system
4. System 4: Triple-difference L1 carrier-phase system
5. System 5: Mixed PC/A-code and L1 carrier-phase system
6. System 7: RSP-L1 system

System configurations were as discussed earlier in Chapter 7.

8.2.1 System 1 : PC/A-Code System

In this campaign, five baselines were observed. Details of the baselines are as listed in Table 8.2.

Table 8.2: Baselines for the PC/A-Code System in Campaign 1

No.	GPSDAY	BASELINE LENGTH	SITE + RECEIVER	OBSERVATION LENGTH
1	DAY231	4.3 km	PASC - Ashtech Z-XII ISHA - NovAtel	18 hours
2	DAY229	8.2 km	PASC - Ashtech Z-XII ISHA - NovAtel	24 hours
3	DAY233	12.1 km	PASC - Ashtech Z-XII ISHA - NovAtel	24 hours
4	DAY235	14.7 km	PASC - Ashtech Z-XII ISHA - NovAtel	24 hours
5	DAY227	16.1 km	PASC - Ashtech Z-XII ISHA - NovAtel	24 hours - segmented

The PC/A-code pseudo-range data for these baselines has been processed using the BASEPR program utilising the double-differenced algorithm (see Chapter 4 for software description). Different observation session lengths were processed. The number of baseline solutions for each observation session length is given in Table 8.3. As indicated in Table 8.2, the length of the observation session for baseline 1 was only 18 hours, hence the total number of solutions for this baseline (Table 8.3) are less than that of the

other baselines. The reason why the number of single-epoch solutions for baseline 2 is about half the number for other baselines is because a 30 second data rate was used for data collection, as opposed to 15 second for the other baselines.

Table 8.3: Total Baseline Solutions for Various Observation Session

Session length / Baseline (km)	single-epoch	1 min	2 min	5 min	10 min	30 min	60 min
4.3	4544	1135	568	225	113	38	19
8.2	2756	1386	695	279	140	47	24
12.1	5751	1440	720	288	144	48	24
14.7	5744	1437	720	288	144	48	24
16.1	5403	1352	680	271	136	47	24

For each observation session, the 'spread' of the baseline solutions was analysed. The positional error for each baseline solution was computed (i.e., the difference with respect to the 'true' value) and the solutions are then grouped according to the 'accuracy' (i.e., the error) classifications specified in Table 8.1.

The ratio of the number of solutions for each accuracy 'band', over the total number of baseline solutions for the whole day, is then computed, to give the level of reliability of the system, in terms of percentage of the 'spread' for each accuracy band. Results for different observation session, are given in Table 8.4.

Performance vs Observation Spans

The following conclusions are drawn from the tabulated value of reliability performance in Table 8.4:

- Single-epoch session solutions deliver accuracies under 2 m at the 95% level of reliability for baselines under 15 km, with some baselines even higher, at the 99% level.
- The 1 and 2 minute session solutions give accuracy of about 1-2 m at the 95% level, with almost all baselines having an accuracy under 2 m at the 99% level.
- The 10 minute session solutions have accuracy under 1 m at the 95% level.
- The 30 and 60 minute session solutions give accuracy under 1 m at the 100% reliability level.

Table 8.4: Reliability Performance (in %) of the PC/A-Code System for Different Observation Spans

	Baseline Length (km)				
Accuracy	4.3	8.2	12	14.7	16.1
< 1m	69	77	80	86	65
< 2m	95	98	98	99	92
< 5m	100	100	100	100	99

(a) Single Epoch Session Solutions

	Baseline Length (km)				
Accuracy	4.3	8.2	12	14.7	16.1
< 1m	79	84	87	88	74
< 2m	98	98	99	99	95
< 5m	100	100	100	100	100

(b) 1 Minute Session Solutions

	Baseline Length (km)				
Accuracy	4.3	8.2	12	14.7	16.1
< 1m	82	88	91	92	82
< 2m	99	99	99	100	97
< 5m	100	100	100	100	100

(c) 2 Minute Session Solutions

	Baseline Length (km)				
Accuracy	4.3	8.2	12	14.7	16.1
< 50cm	60	66	72	70	89
< 1m	94	94	94	97	99
< 2m	100	99	100	100	100

(d) 5 Minute Session Solutions

	Baseline Length (km)				
Accuracy	4.3	8.2	12	14.7	16.1
< 50cm	71	71	78	74	72
< 1m	96	97	97	99	93
< 2m	100	99	100	100	99

(e) 10 Minute Session Solutions

	Baseline Length (km)				
Accuracy	4.3	8.2	12	14.7	16.1
< 20cm	29	40	40	31	30
< 50cm	79	83	85	81	72
< 1m	100	100	100	100	100

(f) 30 Minute Session Solutions

	Baseline Length (km)				
Accuracy	4.3	8.2	12	14.7	16.1
< 20cm	37	46	33	33	33
< 50cm	74	83	88	79	88
< 1m	100	100	100	100	100

(g) 60 Minute Session Solutions

Performance vs Baseline Length

For better visual analyses, the figures in Table 8.4 are plotted in Figure 8.3, from which the following conclusions can be drawn:

- The single-epoch, 1, 2 and 10 minute session solutions, clearly show horizontal trendlines for both accuracy groups plotted. This indicate comparable reliability performance of the system for all baselines.
- The 5 minute session solutions show an 'increase' of reliability performance in the < 50 cm accuracy group, but the overall accuracy performance (< 1 m) is still the same.
- The 30 minute session solutions show a slight 'decrease' in the reliability performance with baseline length, as well as the < 20 cm accuracy group in the 60 minute session solutions. On the other hand, the < 50 cm accuracy group in the 60 minute session solutions, shows a slight 'increase' of the reliability performance. The validity of this performance is suspected, as it may caused by the noise in the observation data.

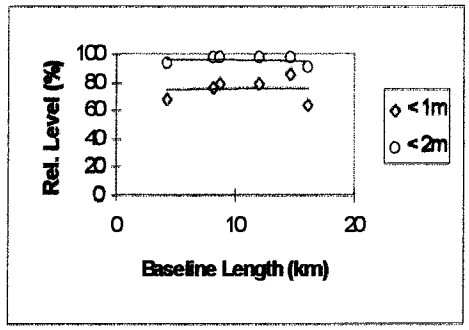

(a) Single Epoch Session Solutions

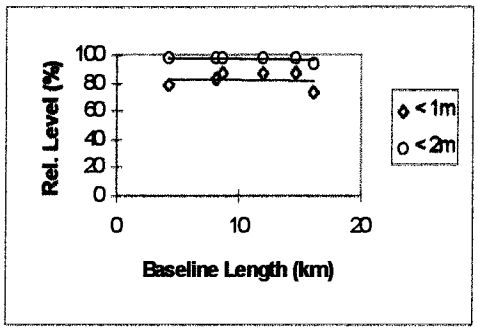

(b) 1 Minute Session Solution

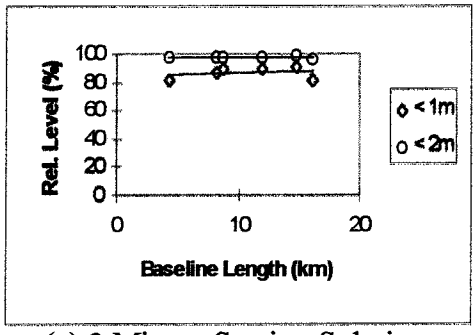

(c) 2 Minute Session Solutions

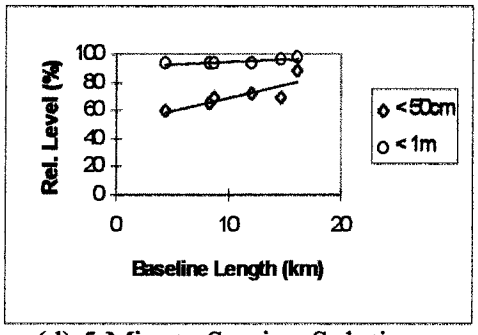

(d) 5 Minute Session Solution

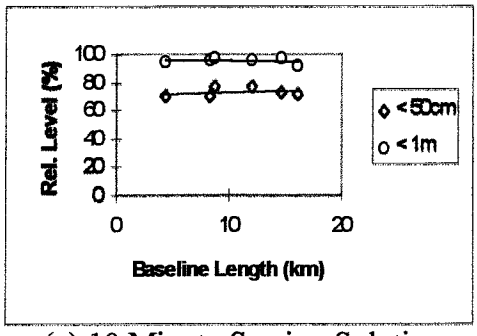

(e) 10 Minute Session Solution

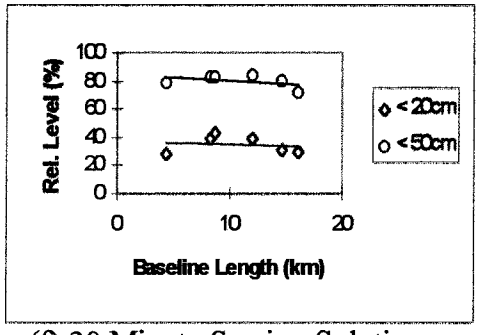

(f) 30 Minute Session Solution

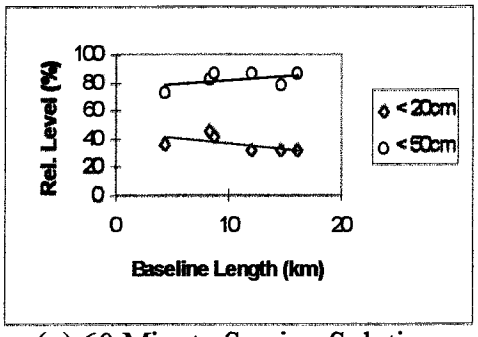

(g) 60 Minute Session Solutions

Figure 8.3: Plots of Reliability Performance (in %) of the PC/A-Code System for Different Observation Spans

Concluding the analyses, it seems that the performance of the PC/A-code system, for all observation spans, does not appear to vary with the baseline length. The reason for this

could be that, for short baseline separations, the biases which vary as a function of baseline length, such as the ionospheric residuals (i.e., those remaining after data differencing), are significantly less than the observation noise. Hence, for these baselines, the observation noise may dominate the position error budget. For longer baselines (> 50 km), it is expected that the performance will degrade with baseline length.

Performance vs Different Ionospheric Influences

The 24 hour baseline solutions were divided into two sessions. The DAY session covers the first half of the day (7:00 am - 7:00 pm), and the NIGHT session for the remaining half day (7:00 pm - 7:00 am the next day). Similar analyses were carried out for to both the DAY and NIGHT solutions. The results of the analyses are plotted in Figure 8.4.

Comparing the two session results, the following analyses can be drawn;

- Short observation sessions (single-epoch, 1, 2, 5, and 10 minutes), indicate better DAY time performance than the NIGHT time (up to about 10%). This occurs for all baselines (Figure 8.4 (a, b, c, d and e)).
- Longer observation sessions (30 and 60 minutes) on the other hand, indicate better NIGHT time performance than for the DAY time, for baselines longer than 10 km, with the 60 minute session showing the more significant improvement (Figure 8.4 (f and g)).

Drawing conclusions from these analyses can be a bit difficult. Understanding that the observation noise of the differenced code measurement could still be significantly larger than the ionospheric residual (within the baseline length involved in this research), the analyses might not be that meaningful (as in the performance vs baseline length case). For example, in the short observation sessions results, the apparent better DAY time performance might be due to the level of noise in the data, rather than the DAY time factor. In the longer observation sessions, the longer baselines (>10 km) give the expected 'normal' result with NIGHT time sessions giving better performance than the DAY time sessions, but the shorter baselines give result otherwise. One possible explanation is that, ionospheric residual will only be significantly larger than the measurement noise on longer baselines, hence its effect being realised in the longer baselines result. While on the shorter baselines, the result is mainly due to the level of the measurement noise.

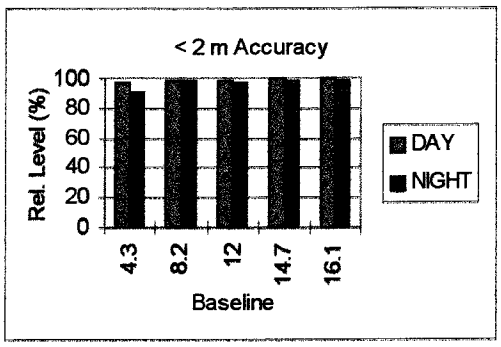

(a) Single-Epoch Session Solutions

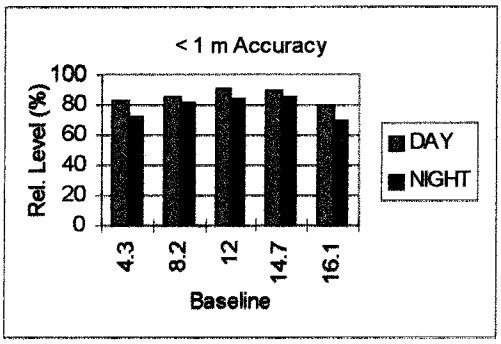

(b) 1 Minute Session Solutions

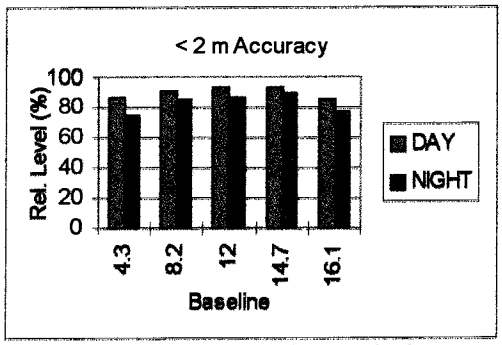

(c) 2 Minute Session Solutions

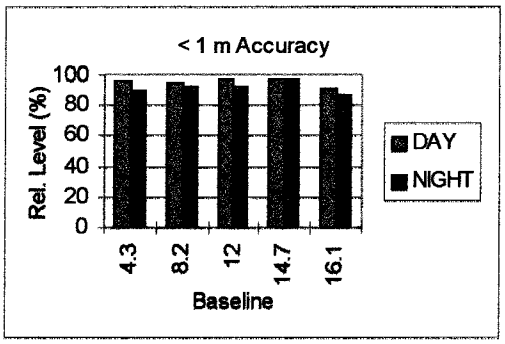

(d) 5 Minute Session Solutions

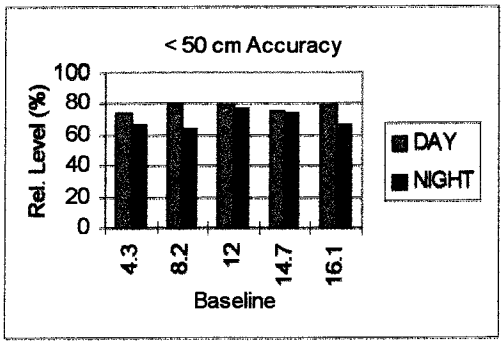

(e) 10 Minute Session Solutions

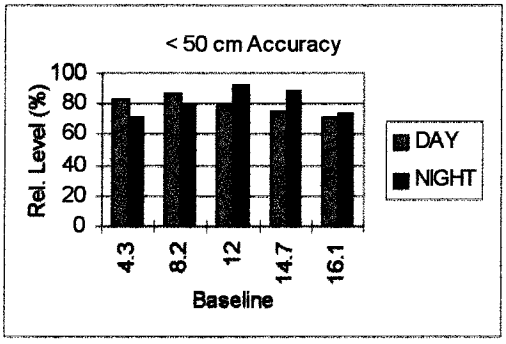

(f) 30 Minute Session Solutions

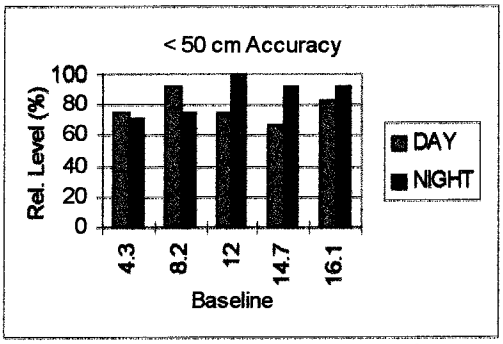

(g) 60 Minute Session Solutions

Figure 8.4: Plots of Reliability Performance (in %) of the PC/A-Code System - Comparing DAY and NIGHT Session Solutions

Performance vs Satellite Geometry

The 24 hour baseline solutions were then grouped according to the number of observed satellites during the session (in most cases, especially for shorter observation spans, the number of satellites for the whole span is constant, otherwise the number indicated is for more than 50% of the time). Then, for each group of solutions, the same analyses were done. Only in this case the percentage (or the reliability level) was computed over the number of solutions for each group, and not over the total solutions for the 24 hour span. In this regard, the number of baseline solutions for each group (of number of observed satellites) would approximately correspond to Figure 2.4 in Chapter 2.

The performance for each group (of number of observed satellites) are then plotted for each baseline, as in Figure 8.5, for the different observation spans. The following conclusions are drawn:

- A general rule that the more observed satellites during the session, the better the accuracy is verified with these results.
- Sessions with only four observed satellites seem to be inferior to those sessions with more than four observed satellites. An additional satellite therefore appears to improve the accuracy of solutions by more than 30%. However, due to the fact that the number of baseline solutions with only four observed satellites is less than 1% in the 24 hour span (refer to Chapter 2 for the discussions), these conclusions may not be very concrete.
- Accuracy improvement when the number of satellites increases from five to six is less than 10%; from six to seven less than 5%; while from seven to eight sometimes hardly noticeable.

However, only a general trend can be deduced from these results, since the relationship between accuracy and the number of observed satellites is complex (as discussed earlier in Chapter 2).

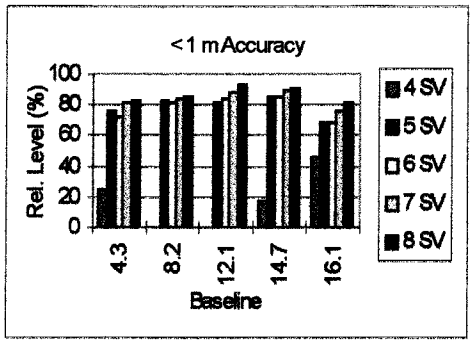

(a) 1 Minute Session Solutions

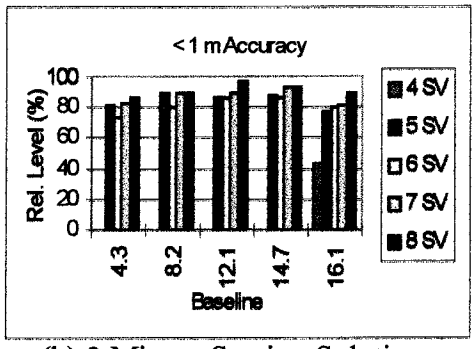

(b) 2 Minute Session Solutions

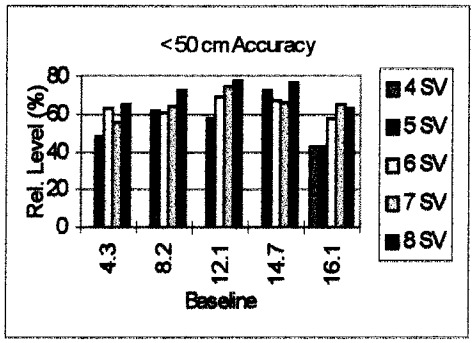

(c) 5 Minute Session Solution

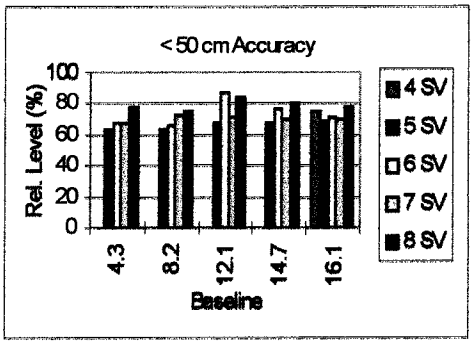

(d) 10 Minute Session Solutions

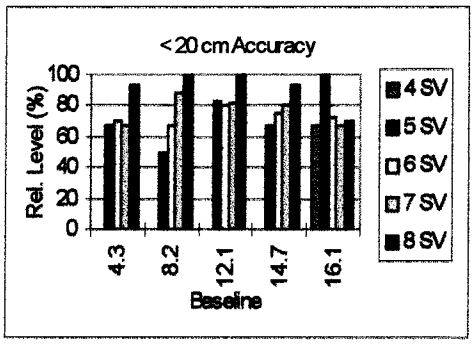

(e) 30 Minutes Session Solution

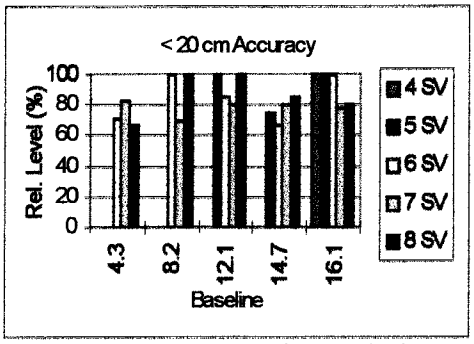

(f) 60 Minutes Session Solution

Figure 8.5: Plots of Reliability Performance of the PC/A-Code System vs Number of Satellites

8.2.2 System 2 : C/A-Code System

In the first campaign, two baselines have been observed, with characteristics as listed in Table 8.5.

Table 8.5: Baselines for System 2 in Campaign I

No.	GPSDAY	BASELINE LENGTH	SITE + RECEIVER	OBSERVATION LENGTH
1	DAY231	1.9 km	PASC - Ashtech Z-XII CIGA - SVeeSix	18 hours
2	DAY231	6.2 km	ISHA - NovAtel CIGA - SVeeSix	24 hours

The C/A-code pseudo-range data for these baselines has been processed using the BASEPR program utilising the double-differenced algorithm (see Chapter 4 for software description). Different observation session lengths were processed, namely single-epoch, 1, 2, 5, 10, 30 and 60 minutes. The total number of baseline solutions for each of the observation session lengths is given in Table 8.6. As indicated in Table 8.2, the observation data for baseline 1 was only about 18 hours, hence the total number of solutions for this baseline is less than that of the other baseline.

Table 8.6: Total Baseline Solutions for Various Observation Sessions

Session length / Baseline (km)	single-epoch	1 min	2 min	5 min	10 min	30 min	60 min
1.9	4511	1134	566	228	114	38	19
6.2	5249	1317	659	264	132	44	23

The same analyses were performed on the results. The reliability performance of the system for the different observation spans is indicated in Table 8.7.

Performance vs Observation Spans

Analysing the system performance in relation of the observation span, the following conclusions are drawn from Table 8.7:

- Single-epoch session solutions cannot fulfil the anticipated accuracy of DGPS which is stated to be at the 2-5 m at 95% level of reliability (Rizos, 1996).
- The 1 and 2 minute session solutions give accuracy at about 2-5 m, at the 95% level of reliability.

- The 2 minute session solutions are slightly better than the 1 minute ones, giving accuracy under 5 m at the 99% level.
- The 10 and 30 minute session solutions give accuracy of about 1-2 m, at the 95% level.
- The 60 minute session solutions are only slightly better than the 10 and 30 minute sessions, with accuracy under 2 m, at the 95% level.

Table 8.7: Reliability Performance (in %) of the C/A-Code System for Different Observation Spans

	Baseline (km)	
Accuracy	1.9	6.2
< 1m	27	26
< 2m	49	50
< 5m	89	89

(a) Single-Epoch Session Solutions

	Baseline (km)	
Accuracy	1.9	6.2
< 1m	41	42
< 2m	71	71
< 5m	98	98

(b) 1 Minute Session Solutions

	Baseline (km)	
Accuracy	1.9	6.2
< 1m	54	51
< 2m	84	83
< 5m	99	99

(c) 2 Minute Session Solutions

	Baseline (km)	
Accuracy	1.9	6.2
< 50cm	34	44
< 1m	61	69
< 2m	91	94
< 5m	100	100

(d) 5 Minute Session Solutions

	Baseline (km)	
Accuracy	1.9	6.2
< 50cm	30	44
< 1m	73	80
< 2m	96	97
< 5m	100	100

(e) 10 Minute Session Solutions

	Baseline (km)	
Accuracy	1.9	6.2
< 20cm	21	23
< 50cm	58	59
< 1m	82	91
< 2m	97	100

(f) 30 Minute Session Solutions

	Baseline (km)	
Accuracy	1.9	6.2
< 20cm	16	48
< 50cm	58	61
< 1m	84	96
< 2m	95	100

(g) 60 Minute Session Solutions

Performance vs Baseline Length

Reliability figures in Table 8.7, for specific accuracy groups are plotted in Figure 8.6. However, due to the limited number of baselines observed by this system, firm conclusions cannot be drawn. Nevertheless, some analyses can be reported;

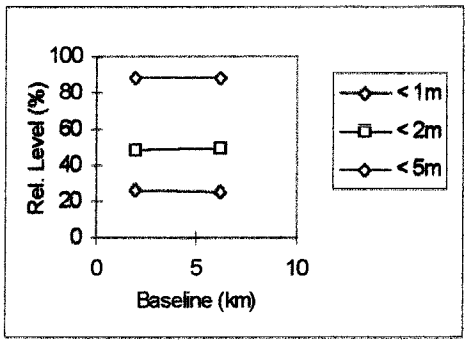

(a) Single-Epoch Session Solutions

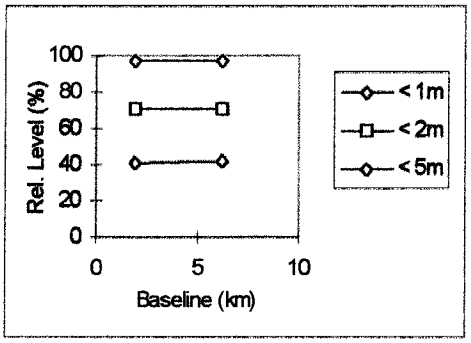

(b) 1 Minute Session Solution

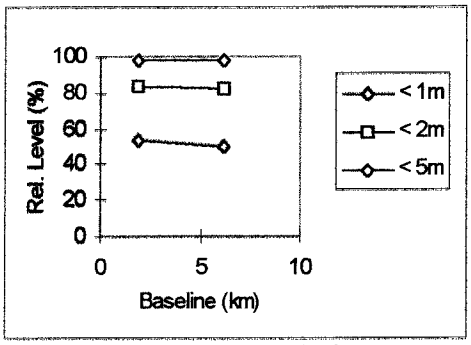

(c) 2 Minute Session Solutions

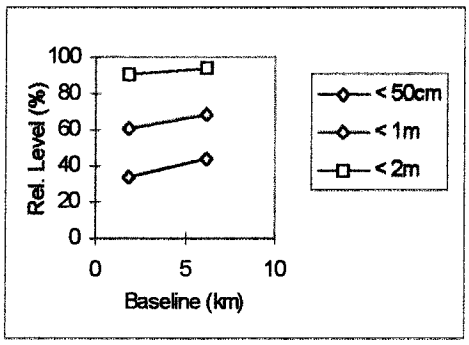

(d) 5 Minute Session Solution

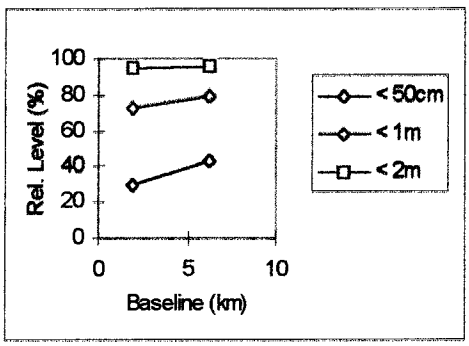

(e) 10 Minute Session Solutions

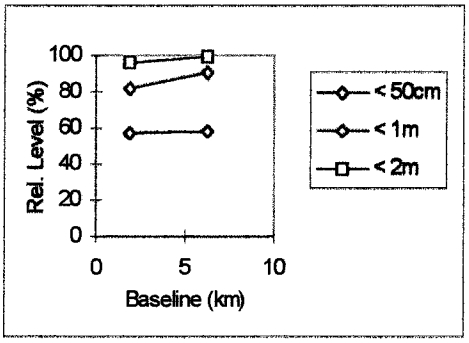

(f) 30 Minute Session Solution

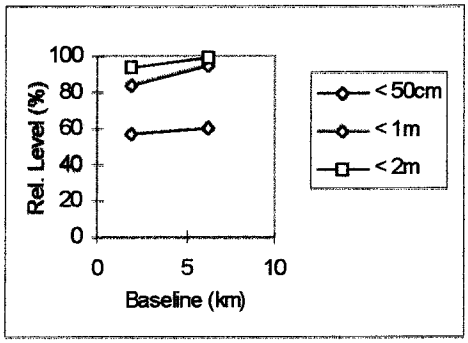

(g) 60 Minute Session Solutions

Figure 8.6: Plots of Reliability Performance (in %) of the C/A-Code System for Difference Observation Spans

- For baselines between 2 to 6 km in length, similar performance of the system can be expected, though sometimes the system gave slightly better performance for the 6 km baseline. However it is suspected that this only due to the variable quality of the data.

Performance vs Different Ionospheric Influences

As done earlier, the 24 hour baseline solutions were divided into DAY and NIGHT sessions, and similar analyses were done to both groups of solutions.

Comparing the two bar plots in Figure 8.7, the following conclusions are drawn;

- For short observation sessions (single-epoch, 1 and 2 minutes), comparable performance between the DAY and NIGHT sessions can be seen (except for the 1.9 km baseline in Figure 8.6(c)). Better DAY performance can sometimes be noticed (e.g., Figure 8.6(b)).
- For observation spans of 5 minutes and longer, two distinct phenomenon can be noted:

  (1) For the 1.9 km baseline, DAY session solutions show better reliability performance, by up to about 20%.

  (2) For the 6.2 km baseline, NIGHT session solutions show better reliability performance, by up to about 5%.

Similar conclusions as in the PC/A-code system performance can be said here, where the measurement noise of the C/A-code data might have contributed more significantly to the performance of the system, rather than the different ionospheric factor.

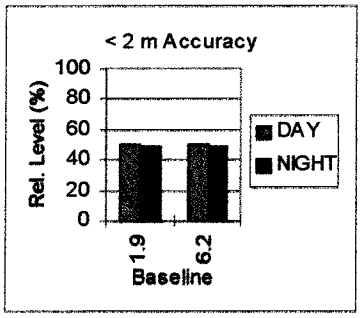

(a) Single-Epoch Solutions

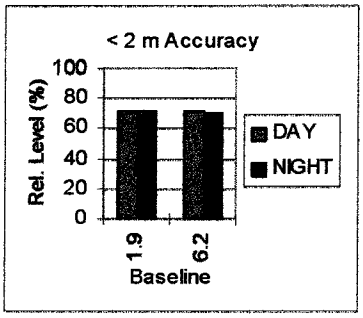

(b) 1 Min. Session Solutions

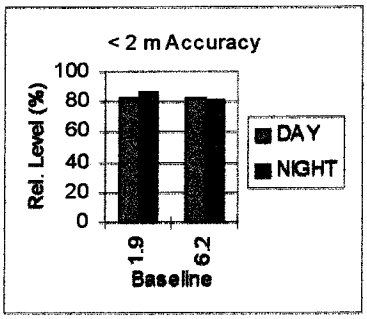

(c) 2 Min. Session Solutions

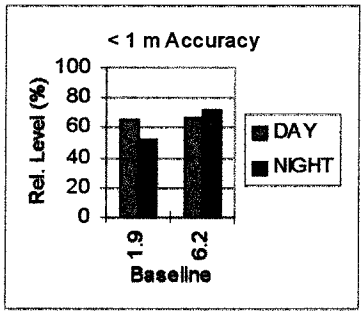

(d) 5 Min. Session Solutions

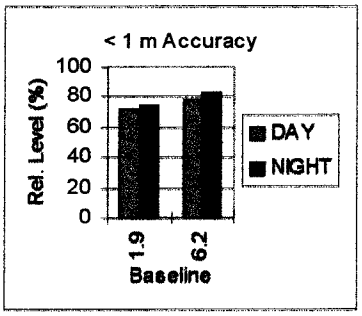

(e) 10 Min. Session Solutions

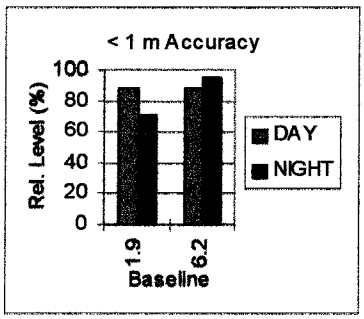

(f) 30 Min. Session Solutions

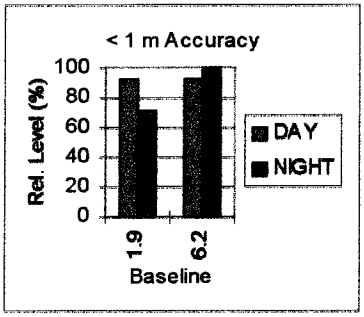

(g) 60 Min. Session Solutions

Figure 8.7: Reliability Performance (in %) of the C/A-Code System - Comparing DAY and NIGHT Session Solutions

Performance vs Satellite Geometry

As for earlier analyses, the baseline solutions were then grouped according to the number of observed satellites. Note that since the SVeeSix GPS receiver only observes a maximum of six satellites, the analyses have been restricted up to this number. As indicated in Figure 8.8, the majority of the baseline solutions for the 24 hour span were computed using six observed satellites (more than 80% of the time), while five observed satellites were only available for about 15% of the time, and four observed satellites for less than 1% of the spans.

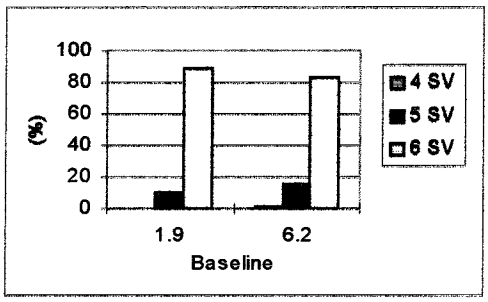

Figure 8.8: Percentage of Baseline Solutions vs Number of Observed Satellites for Baseline Involving SVeeSix GPS Receiver

The reliability performance for each group (of number of observed satellites) are then plotted for each baseline, as in Figure 8.9, for different observation spans. The following conclusions were drawn from these figures:

- Sessions with only four observed satellites seem to be inferior to those sessions involving more than four observed satellites (Figure 8.9 (a and b) for baseline 6.2 km). An additional satellite appears to improve the accuracy of solutions significantly.
- Accuracy improvement when the number of satellites increases from five to six is less than 10% in some observation session (Figure 8.9 (c for 1.9 km), (d) and (e for 1.9 km)), while in others it is hardly noticeable (Figure 8.9 (a and b)).

Some of the figures indicate a degradation of the reliability performance with an increase in the number of observed satellites from five to six (Figure 8.9 (c for 6.2 km), (e for 6.2 km), and (f)). No concrete explanation can be provided.

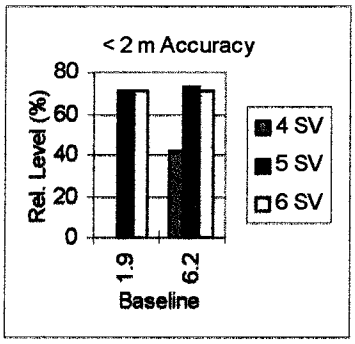

(a)1 Minute Session

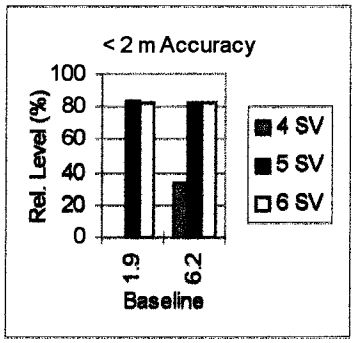

(b) 2 Minute Session

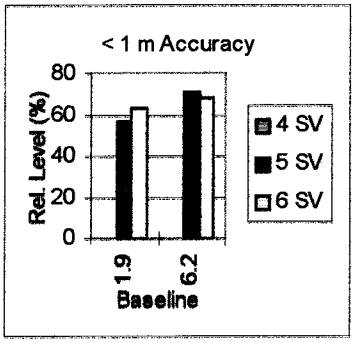

(c) 5 Minute Session

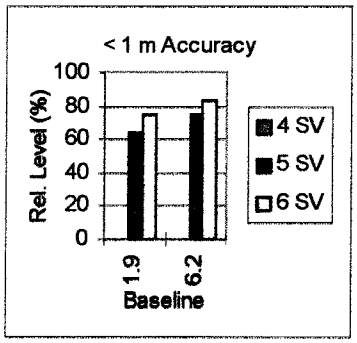

(d)10 Minute Session

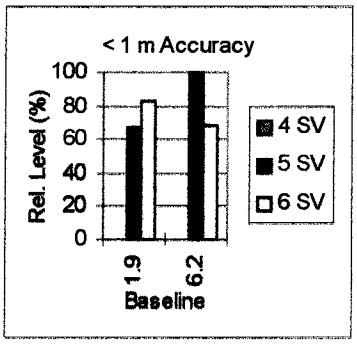

(e)30 Minute Session

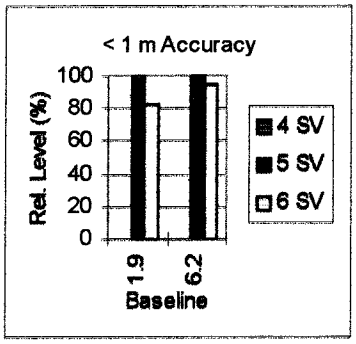

(f) 60 Minute Session

Figure 8.9: Plots of Reliability Performance of the C/A-Code System vs Number of Satellites

8.2.3 System 3 : L1 Phase System

The baselines observed for this system's evaluation are the same as in Table 8.2. The L1 carrier-phase data were processed using the program BASEPH, which utilises the double-differenced data algorithm. The algorithm was described in Chapter 4. The result of the double-differenced ambiguity float solution is used in these analyses. The number of baseline solutions for each of the observation spans is given in Table 8.8. An explanation of the number of solutions was given earlier.

Table 8.8: Total Baseline Solutions for Various Observation Session

Session length / Baseline (km)	1 min	2 min	5 min	10 min	30 min	60 min
4.3	1138	569	228	114	38	19
8.2	1386	694	278	139	47	24
12.1	1440	720	288	144	47	23
14.7	1433	719	288	144	48	24
16.1	1350	678	269	132	39	19

The same analyses were carried out as for the other systems. The reliability performance of the system for different observation spans is indicated in Table 8.9.

Performance vs Observation Spans

Since carrier-phase is an ambiguous range measurement with an unknown full-cycle ambiguity (equation (2.2)), the change in receiver-satellite geometry must be significant to permit reliable baseline computations.

The following conclusions are drawn from the results presented in Table 8.9:

- For short observation sessions, e.g., 1 minute, at the 95% level of reliability, the accuracy obtained was only in the order of 2-5 m for all baselines.
- For 2 minute session solutions, at the same level of reliability, an improvement of the accuracy to the level of 2 m was achieved.
- For the 5 minute session solutions, significant improvement was noticed with submetre accuracy achieved at the 95% level.

Table 8.9: Reliability Performance (in %) of the L1-Phase System for Different Observation Spans

	Baseline Length (km)				
Accuracy	4.3	8.2	12	14.7	16.1
< 1m	56	58	58	56	55
< 2m	85	87	85	82	83
< 5m	99	100	99	98	98

(a) 1 Minute Session Solutions

	Baseline Length (km)				
Accuracy	4.3	8.2	12	14.7	16.1
< 1m	75	84	74	74	74
< 2m	96	99	94	94	91
< 5m	100	100	100	100	100

(b) 2 Minute Session Solutions

	Baseline Length (km)				
Accuracy	4.3	8.2	12	14.7	16.1
< 20cm	29	43	38	40	37
< 50cm	72	83	74	80	69
< 1m	95	98	94	93	91
< 2m	99	100	100	100	96

(c) 5 Minute Session Solutions

	Baseline Length (km)				
Accuracy	4.3	8.2	12	14.7	16.1
< 20cm	61	60	59	56	57
< 50cm	94	93	88	90	80
< 1m	99	100	99	98	92
< 2m	100	100	100	100	96

(d) 10 Minute Session Solutions

	Baseline Length (km)				
Accuracy	4.3	8.2	12	14.7	16.1
< 10cm	68	81	68	63	54
< 20cm	92	91	85	88	67
< 50cm	100	100	98	98	85

(e) 30 Minute Session Solutions

	Baseline Length (km)				
Accuracy	4.3	8.2	12	14.7	16.1
< 10cm	84	88	91	88	50
< 20cm	100	100	96	100	83
< 50cm	100	100	100	100	100

(f) 60 Minute Session Solutions

For longer observation sessions, carrier-phase positioning will deliver higher baseline accuracy than the PC/A-code pseudo-range data. The accuracy is, however, dependent on the baseline length. The following levels of accuracy, at the 95% level of reliability, were obtained:

- The 5 minute session solutions deliver about 1 m accuracy for baseline lengths less than 10 km, and about 1-2 m for baseline lengths greater than that.
- The 10 minute session solutions deliver about 50 cm - 1 m for all baselines.
- The 30 minute session solutions deliver about 20-50 cm accuracy for baseline lengths less than 15 km.
- The 60 minute session solutions deliver accuracy of 10-20 cm for baseline lengths less than 15 km, and about 20-50 cm for the longer baselines.

Performance vs Baseline Length

Plots of the accuracy levels in Table 8.9, for the 5, 10, 30 and 60 minute observation sessions, are shown in Figure 8.10. Trendlines for these accuracy level are also indicated.

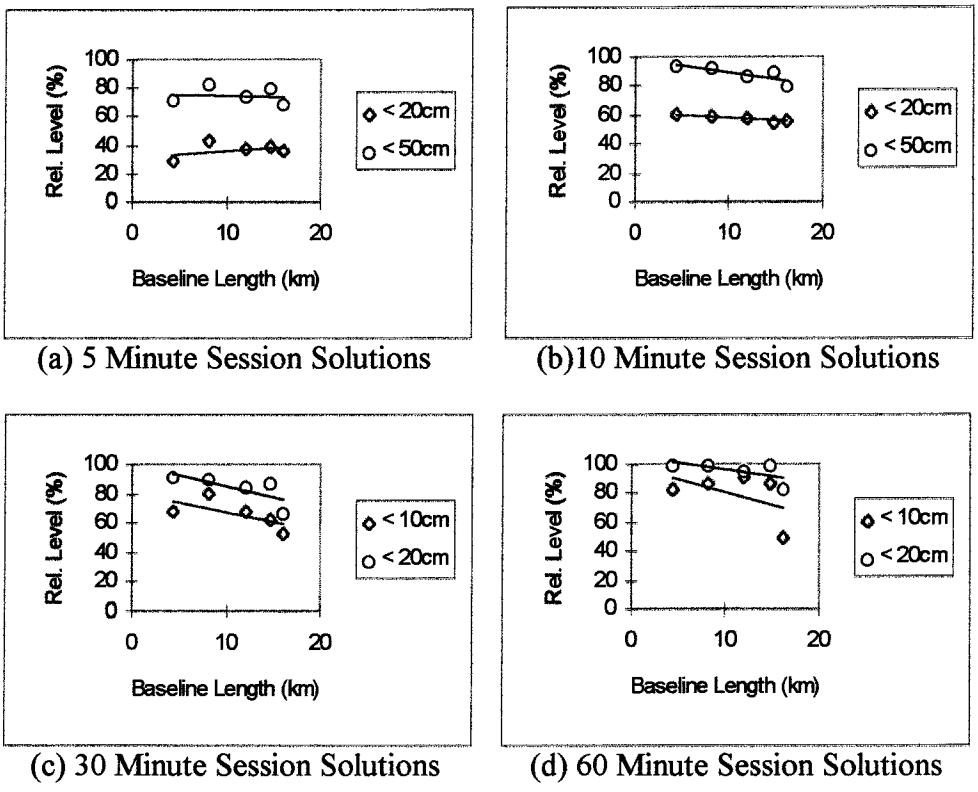

(a) 5 Minute Session Solutions (b)10 Minute Session Solutions

(c) 30 Minute Session Solutions (d) 60 Minute Session Solutions

Figure 8.10: Plots of Reliability Performance (in %) of the L1-Phase System for Different Observation Spans

The following additional conclusions are drawn:

- The trend of decreasing reliability performance with increasing baseline length for the L1-phase system, is quite apparent in these investigations, even though only limited baseline separations were investigated in this research.

- The trend of decreasing reliability performance with increasing baseline length is more apparent in the longer observation spans (> 30 minutes) than in the shorter ones (< 10 minutes). This may be due to the fact that longer observation span give more 'stable' reliability performance (see Table 8.9 (c, d, e and f)).
- The 5 minute observation span does not clearly show a degradation of reliability for baseline greater than 16 km length (note the trendline of the < 50 cm accuracy), but the 30 minute spans indicate a clearer sloping trendline (Figure 8.10 (a and b)).
- The 30 and 60 minute observation session, on the other hand, indicate a definite trendline slope of reliability degradation (Figure 8.10 (c and d)).

Performance vs Different Ionospheric Influences

For the purpose of analysing the different ionospheric influence on solutions, the 24 hour baseline solutions are divided into DAY and NIGHT sessions, and the data are then subjected to the same analyses, as indicated previously. The reliability performance of both the DAY and NIGHT session solutions are given in Figure 8.11, which are plots of the reliability level, of a specific accuracy, from which the following conclusions are drawn:

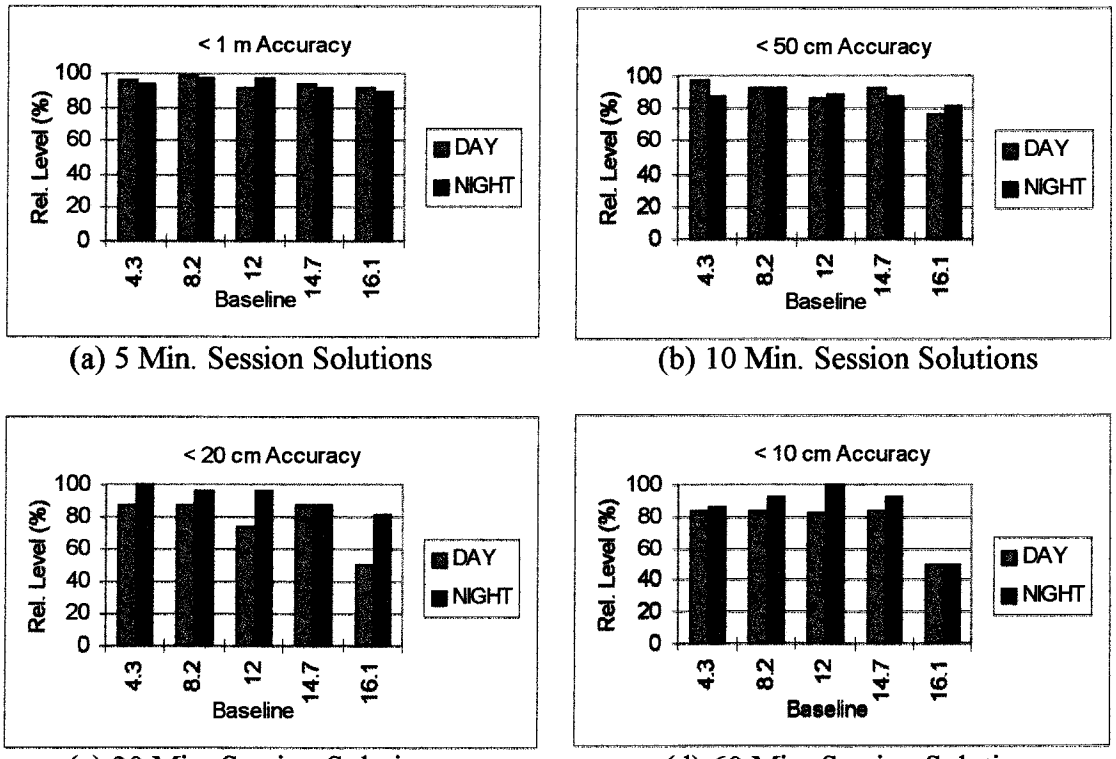

(a) 5 Min. Session Solutions (b) 10 Min. Session Solutions

(c) 30 Min. Session Solutions (d) 60 Min. Session Solutions

Figure 8.11: Plots of Reliability Performance (in %) of the L1-Phase System - Comparing DAY and NIGHT Sessions

- The longer observation spans (30 and 60 minutes) clearly show a distinct improvement of the NIGHT sessions over the DAY sessions.
- The night session improvement can sometimes be up to about 25% (Figure 8.11 (c and d)), but generally it is of the order of 10-15%.
- The shorter observation span (5 and 10 minutes) results show a mixture of performance, some baselines having a better DAY reliability level, while other baselines indicate the opposite trend. This might be due to the 'instability' of the baseline solutions which use a small amount of observation data.

Performance vs Satellite Geometry

The 24 hour baseline solutions were further grouped according to the number of observed satellites during the session (refer to earlier system analyses). Then for each group of solutions, the same reliability analyses was carried out. The performance for each group (of number of observed satellites) are then plotted for each baseline, as in Figure 8.12, for the different observation spans.

The following conclusions are then drawn from these figures:

- A general rule that the more observed satellites during the session, the better the accuracy will be, is more strongly verified for the L1 phase system. This is most apparent for the shorter observation span solutions (5, 10, and 30 minutes).
- Sessions with only four observed satellites are inferior to those sessions with more than four observed satellites (see plot in Figure 8.12 (b)).
- The accuracy improvement when the number of observed satellites increases from five to six is also significant, of the order of 15-20%.
- The improvement from six to seven observed satellites is around 5-10%.
- The improvement from seven to eight observed satellite is only apparent on shorter observation sessions (5 and 10 minutes).

Generally, for shorter observation spans, the contribution of an additional observed satellites is very significant, while the contribution reduces with an increase in the length of the observation span.

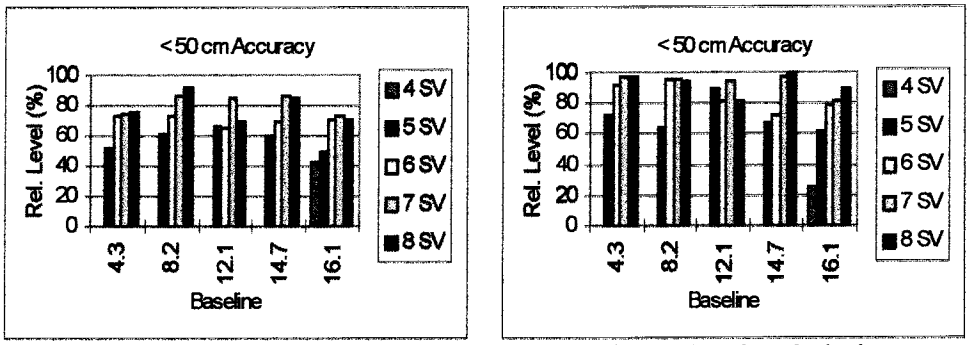

(a) 5 Minute Session Solutions (b) 10 Minute Session Solutions

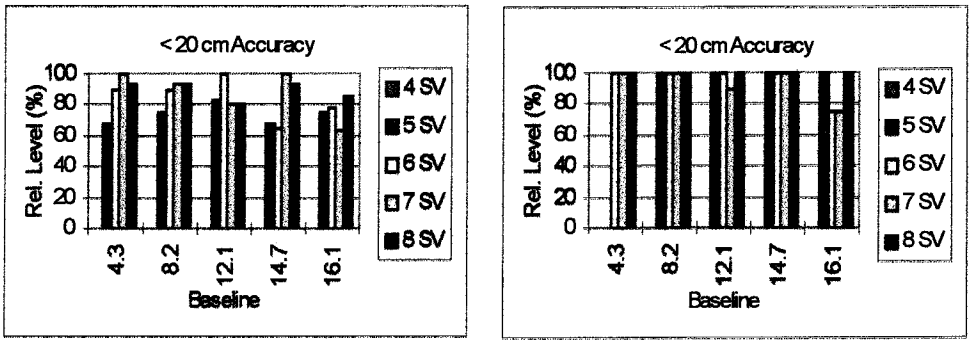

(c) 30 Minute Session Solutions (d) 60 Minute Session Solutions

Figure 8.12: Plots of Reliability Performance (in %) of the L1-Phase System vs Number of Satellites

8.2.4 System 4 : Triple-Difference L1 Phase System

The baselines in Table 8.2 were used for this system's evaluation. The L1 carrier-phase data were processed using the program BASETRP, which utilises the triple-difference data processing algorithm. Further explanation of the program and the algorithm are in Chapters 4 and 5. The number of baseline solutions, for the various observation spans, are given in Table 8.10.

Table 8.10: Total Baseline Solutions for Various Observation Sessions

Session length / Baseline (km)	1 min	2 min	5 min	10 min	30 min	60 min
4.3	1138	569	228	114	38	19
8.2	1382	694	279	139	47	24
12.1	1440	720	288	144	48	24
14.7	1435	719	288	144	48	24
16.1	1349	678	269	133	47	22

The same analyses were performed on the results. The reliability performance of the system, for different observation spans, is indicated in Table 8.11.

Performance vs Observation Spans

Theoretically, L1 carrier-phase triple-differencing will give results equivalent to the L1 double-difference ambiguity float solution only when full correlation between the data is taken into account. In these investigations only correlations between the data within the same epoch are taken into account, but not the between-epoch correlation. Thus a degradation in the accuracy compared to the L1 carrier-phase ambiguity float solutions (System 3) is expected. However, the general performance trend of the phase-based system should be the same.

Table 8.11: Reliability Performance (in %) of the Triple-Difference L1 Phase System or Different Observation Spans

	Baseline Length (km)				
Accuracy	4.3	8.2	12	14.7	16.1
< 1m	54	57	58	57	53
< 2m	84	87	86	85	82
< 5m	99	99	99	99	97

(a) 1 Minute Session Solutions

	Baseline Length (km)				
Accuracy	4.3	8.2	12	14.7	16.1
< 1m	75	81	76	77	72
< 2m	96	98	95	96	91
< 5m	100	100	100	100	99

(b) 5 Minute Session Solutions

	Baseline Length (km)				
Accuracy	4.3	8.2	12	14.7	16.1
< 50cm	75	85	71	78	71
< 1m	96	98	93	94	90
< 2m	100	100	100	98	97

(c) 5 Minute Session Solutions

	Baseline Length (km)				
Accuracy	4.3	8.2	12	14.7	16.1
< 20cm	63	63	58	60	50
< 50cm	96	98	89	92	83
< 1m	100	100	99	99	95
< 2m	100	100	100	100	99

(d) 10 Minute Session Solutions

	Baseline Length (km)				
Accuracy	4.3	8.2	12	14.7	16.1
< 10cm	55	68	56	60	40
< 20cm	87	89	81	88	70
< 50cm	100	98	100	100	94

(e) 30 Minute Session Solutions

	Baseline Length (km)				
Accuracy	4.3	8.2	12	14.7	16.1
< 10cm	74	75	67	63	55
< 20cm	95	83	88	92	86
< 50cm	100	100	100	96	95

(f) 60 Minute Session Solutions

The following conclusions are drawn from reliability performance in Table 8.11:

- For 1 minute session solutions, at the 95% level of reliability, the accuracy obtained was only of the order of 2-5 m for all baselines.
- For 2 minute session solution, at the same level of reliability, an improvement of the accuracy to the level of 2 m was achieved, for baselines under 15 km in length.

- For 5 minute session solutions, submetre accuracy can be achieved, at the 95% reliability level, for baselines under 10 km in length, while for longer baselines the accuracy level remains at about 1-2 m.
- The 10 minute session solutions give an accuracy of about 20-50 cm, at the 95% reliability level, for baselines under 10 km; about 50 cm - 1 m for baselines between 10-15 km; while only about 1-2 m accuracy for all baselines longer than 15 km.
- The 30 minute session solutions give about 20-50 cm accuracy for baselines shorter than 15 km.
- The 60 minute session solutions deliver an accuracy of under 20 cm, for baseline less than 5 km; about 10-20 cm accuracy for baselines between 5-15 km; and about 20-50 cm accuracy for longer baselines longer than 15 km, at the 95% level of reliability.

Performance vs Baseline Length

Plots of the accuracy levels in Table 8.11, for the 5, 10, 30 and 60 minute observation sessions, are given in Figure 8.13. Trendlines for these accuracy levels are also shown.

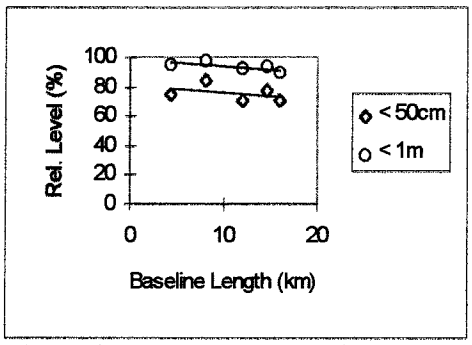

(a) 5 Minute Session Solutions

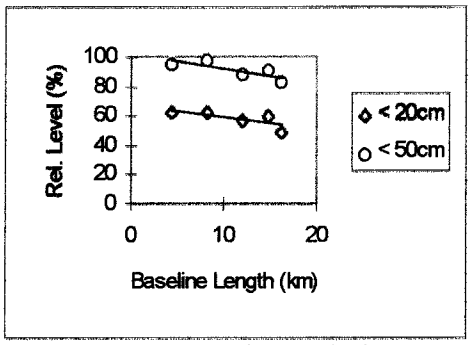

(b) 10 Minute Session Solutions

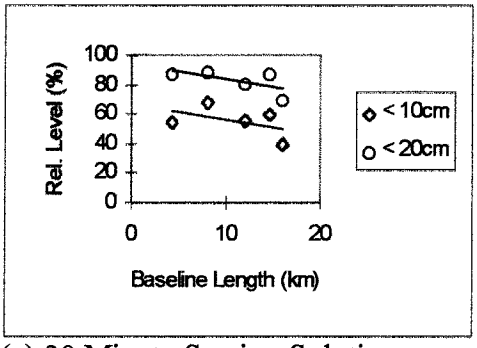

(c) 30 Minute Session Solutions

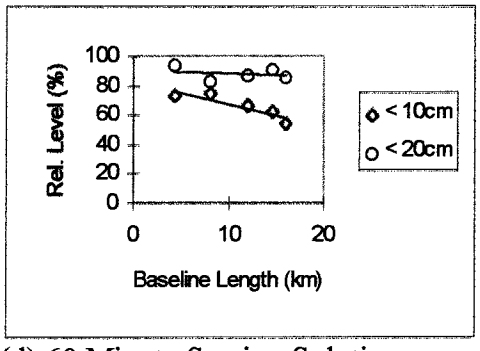

(d) 60 Minute Session Solutions

Figure 8.13: Plots of Reliability Performance (in %) of the Triple-Difference L1 Phase System for Difference Observation Spans

The following additional conclusions can be drawn from the plots:

- The trend of decreasing reliability performance with longer baseline length for the triple-difference L1-phase system, is the same as for the ambiguity-float double-difference system.
- The trend of decreasing reliability performance with increasing baseline length is more apparent in the longer observation spans (> 10 minutes) than in the shorter ones (< 10 minutes).
- The 5 minute observation span solutions do not indicate degradation of reliability for baseline longer than 16 km (note the trendline of the < 50 cm accuracy, Figure 8.12 (a)); however the 10 and 30 minute span solutions do indicate a clear sloping trendline (Figure 8.13 (b and c)).
- The 60 minute session solutions on the other hand, do not have a significant degradation slope for the trendline of the < 20 cm accuracy, nevertheless, it is apparent (Figure 8.13 (d)) on the < 10 cm accuracy band.

Performance vs Different Ionospheric Influences

Following the same procedures as implemented in the earlier system testing, the baseline solutions were grouped into DAY and NIGHT sessions. Then, for a specific accuracy group, the reliability performance is plotted for both sessions as in Figure 8.14.

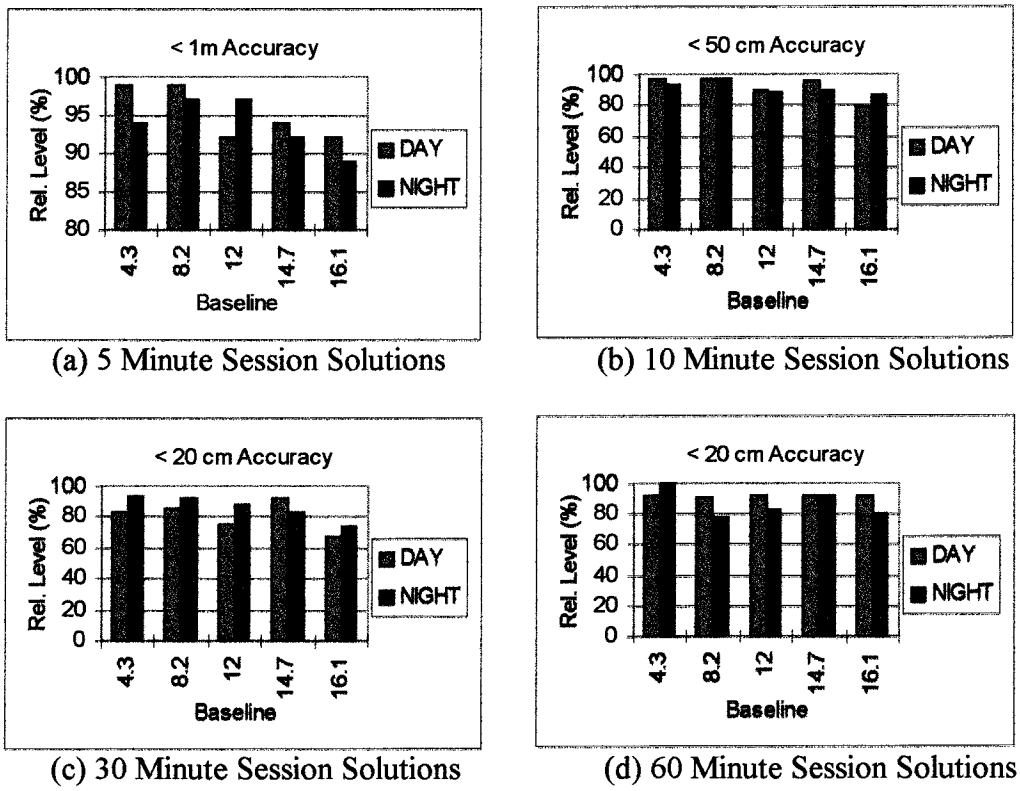

(a) 5 Minute Session Solutions (b) 10 Minute Session Solutions

(c) 30 Minute Session Solutions (d) 60 Minute Session Solutions

Figure 8.14: Plots of Reliability Performance (in %) of the Triple-Difference L1 Phase System - Comparing DAY and NIGHT Sessions.

From Figure 8.14, the following points are noted:

- The 30 minute session solutions show a distinct improvement of the NIGHT sessions over the DAY sessions (except for the 14.7 km baseline).
- The 60 minute session solutions, however, do not show the same trend. Rather, the majority of the baselines indicate the opposite conclusions! No explanation can be given for this.
- The shorter observation spans (5 and 10 minute session solutions) show a mixture of performance, some baselines having a better NIGHT time reliability level, though the majority of them indicate the opposite.

Performance vs Satellite Geometry

The solutions for each baseline and each observation span, were further grouped according to the number of observed satellites during the session (refer to earlier system analyses). The performance for each group (of number of observed satellites) was then plotted for the baselines, as in Figure 8.15, for different observation spans.

The following conclusions were then drawn from these figures:

- A general rule that the more observed satellites during a session, the better the accuracy is also true for this system.
- For shorter observation spans (5, 10, and 30 minutes), the impact of additional observed satellites is more significant, compared to its impact on longer observation spans (60 minutes). (See Figure 8.15 (a) of the 5 minute session solutions, for the impact of increasing from five to six, and from six to seven observed satellites).
- Sessions with only four observed satellites (which fortunately are only very few) are inferior to those sessions with more observed satellites. A five satellite session appears to improve the accuracy of the solutions significantly (see plot in Figure 8.15 (a, b and c for the 16.1 km baseline)).
- Accuracy improvement when the number of satellites increases from five to six, and from six to seven, are also significant, especially for longer baselines.
- Improvements due to an increase from seven to eight observed satellites is only apparent on some baselines (e.g., Figure 8.15 (a) and (b) for the 8.2 km baseline).

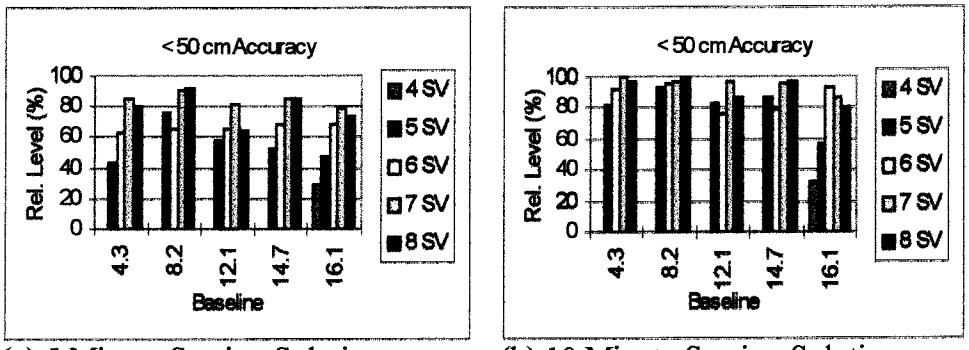

(a) 5 Minute Session Solutions (b) 10 Minute Session Solutions

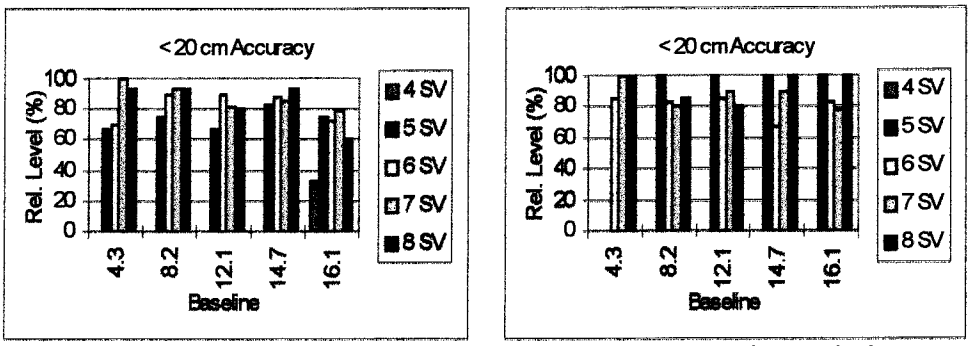

(c) 30 Minute Session Solutions (d) 60 Minute Session Solutions

Figure 8.15: Plots of Reliability Performance of the Triple-Difference L1 Phase System vs Number of Satellites

8.2.5 System 5 : Mixed PC/A-Code and L1 Phase System

The baselines used for this system's evaluation are the same as in Table 8.2. The data were processed using program BASEPRPH, utilising the mixed PC/A-code and L1 carrier-phase ambiguity-float double-differenced data algorithm. Further explanation of the program and the algorithm can be found in Chapters 4 and 5. The number of baseline solutions for different observation spans are given in Table 8.12.

Table 8.12: Total Baseline Solutions for Various Observation Session

Session length / Baseline (km)	single-epoch	1 min	2 min	5 min	10 min	30 min	60 min
4.3	4544	1138	569	228	114	38	19
8.2	2756	1388	695	274	139	47	24
12.1	5751	1440	720	288	144	47	23
14.7	5744	1437	719	288	144	48	24
16.1	5403	1354	679	270	132	39	18

The same analyses were carried out on the results. The reliability performance of the system for different observation spans is shown in Table 8.13.

Performance vs Observation Spans

This mixed GPS system combined the unambiguous, high noise PC/A-code measurements with the ambiguous, low noise carrier-phase measurements. For shorter observation spans the solution is dominated by the contribution of the pseudo-range data, while the carrier-phase data dominates the baseline solutions of the longer observation spans.

Table 8.13: Reliability Performance (in %) of the Mixed PC/A-Code and L1 Phase System for Different Observation Spans

	Baseline Length (km)				
Accuracy	4.3	8.2	12	14.7	16.1
< 50cm	49	59	61	62	50
< 1m	84	89	90	92	82
< 2m	99	99	100	100	99
< 5m	100	100	100	100	100

(a) 1 Minute Session Solutions

	Baseline Length (km)				
Accuracy	4.3	8.2	12	14.7	16.1
< 50cm	61	71	69	74	65
< 1m	92	95	97	97	91
< 2m	100	100	100	100	100
< 5m	100	100	100	100	100

(b) 2 Minute Session Solutions

	Baseline Length (km)				
Accuracy	4.3	8.2	12	14.7	16.1
< 20cm	40	52	47	53	43
< 50cm	80	92	86	89	80
< 1m	99	100	98	100	96
< 2m	100	100	100	100	99

(c) 5 Minute Session Solutions

	Baseline Length (km)				
Accuracy	4.3	8.2	12	14.7	16.1
< 20cm	59	67	61	67	59
< 50cm	96	95	93	94	85
< 1m	100	100	99	100	95
< 2m	100	100	100	100	98

(d) 10 Minute Session Solutions

	Baseline Length (km)				
Accuracy	4.3	8.2	12	14.7	16.1
< 10cm	66	79	70	67	53
< 20cm	95	91	85	92	68
< 50cm	100	100	98	98	85

(e) 30 Minute Session Solutions

	Baseline Length (km)				
Accuracy	4.3	8.2	12	14.7	16.1
< 10cm	84	88	91	88	56
< 20cm	100	100	96	100	78
< 50cm	100	100	100	100	100

(f) 60 Minute Session Solutions

Further conclusions are drawn from the reliability performance values in Table 8.13:

- Single-epoch session solutions give equivalent reliability performance as the PC/A-code system. In this case, the single-epoch carrier-phase data (due to the unknown integer ambiguity) has not contributed any information to the baseline solution, and hence the solution is influenced entirely by the geometric information content of the pseudo-range data.
- 1 minute sessions deliver about 1-2 m accuracy at the 95% level of reliability, for all baselines; while at the 99% level under 2 m accuracy can be expected.

- The 2 minute sessions give submetre accuracy for baselines under 15 km.
- The 5 minute sessions give submetre accuracy for all baselines.
- The 10 minute sessions give 20-50 cm accuracy at the 95% level, for baselines under 10 km in length.
- The 30 minute sessions give 20-50 cm accuracy at the same level of reliability for baselines under 15 km.
- The 60 minute sessions give about 10-20 cm accuracy for baselines under 15 km.

Note that for longer observation sessions (30 and 60 minutes), the performance of the mixed system are approaching the same quality as the ambiguity-float L1 carrier-phase system (compare Table 8.9 (e and f) and Table 8.13 (e and f)).

Performance vs Baseline Length

Plots of certain accuracy groups from Table 8.13, for the 1, 2, 5, 10, 30 and 60 minute observation sessions, are illustrated in Figure 8.16. Trendlines for these accuracy level are also shown.

The following conclusions are drawn from the plots:

- The trend of decreasing reliability performance with longer baseline length for the mixed-system is only apparent for the longer observation session spans (10, 30 and 60 minutes). The reason for this is that for the shorter observation sessions (single-epoch, 1, 2 and 5 minutes), the solution are dominated by the pseudo-range data, which does not indicate a degradation of accuracy with increasing baseline length (at least for the range of baselines considered in this investigations, as concluded from the analysis of System 1 discussed earlier).
- On the other hand, the trend of accuracy degradation with increasing baseline length for longer observation sessions (30 and 60 minutes) is significant. This is perhaps due to the dominate influence of the carrier-phase data in the baseline solutions for these longer data spans.

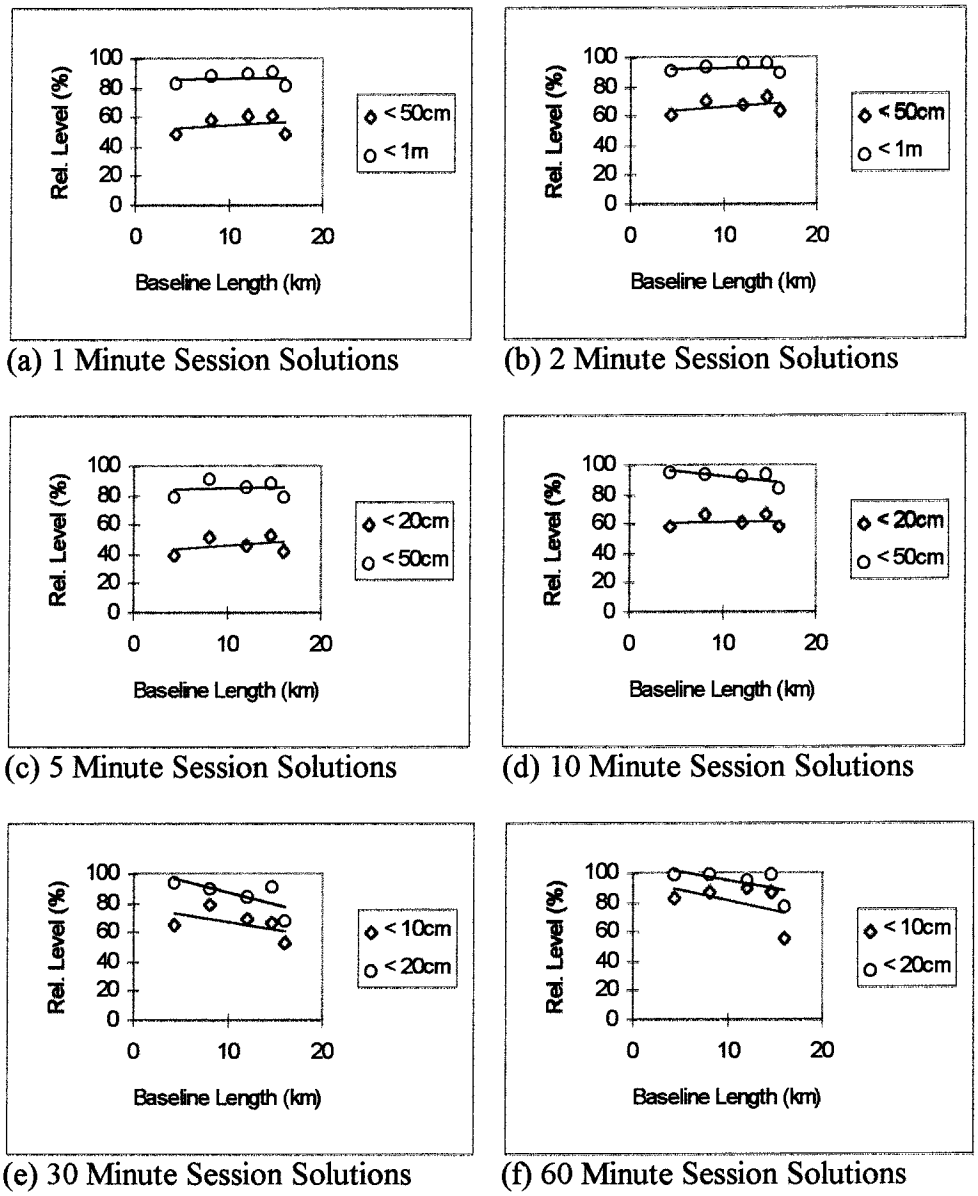

(a) 1 Minute Session Solutions (b) 2 Minute Session Solutions

(c) 5 Minute Session Solutions (d) 10 Minute Session Solutions

(e) 30 Minute Session Solutions (f) 60 Minute Session Solutions

Figure 8.16: Plots of Reliability Performance (in %) of the Mixed PC/A-Code and L1 Phase System for Different Observation Spans

Performance vs Different Ionospheric Influences

The DAY and NIGHT sessions were extracted from the 24 hour solutions according to the same division as used in the earlier analyses. Similar analyses were then carried out on both the DAY and NIGHT session group of solutions. Plots of some accuracy groups, for both sessions, are illustrated in Figure 8.17.

Analysing the results of the two sessions, the following conclusion can be drawn:

- Short observation spans (1, 2, 5 and 10 minutes) follow the trend of the earlier PC/A-code solutions, where the DAY time reliability performance appears to be better than the NIGHT session.

- Longer observation spans (30 and 60 minutes), follow the trend of the L1 carrier-phase solutions, where NIGHT time has better reliability performance than the DAY time solutions.

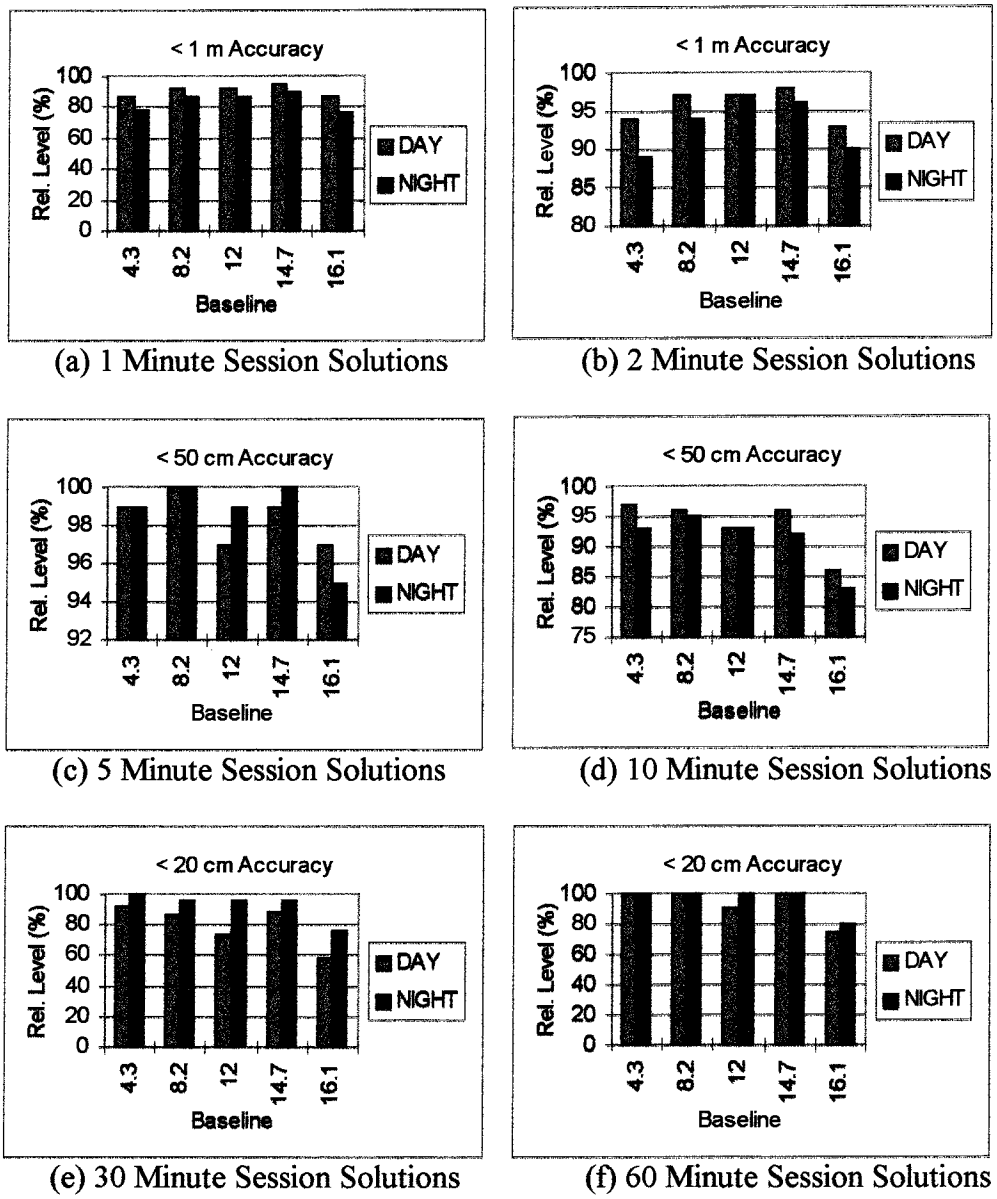

Figure 8.17: Plots of Reliability Performance (in %) of the Mixed PC/A-Code and L1 Phase System - Comparing DAY and NIGHT Sessions.

Performance vs Satellite Geometry

The 24 hour baseline solutions for the mixed PC/A-code and the L1 carrier-phase ambiguity-float double-difference system, for each baseline and each observation span, were further grouped according to the number of observed satellites during the session. Then for each group of baseline solutions, the same analyses were carried out. The

performance for each group (of number of observed satellites) are then plotted for each baseline, as in Figure 8.18, for different observation spans.

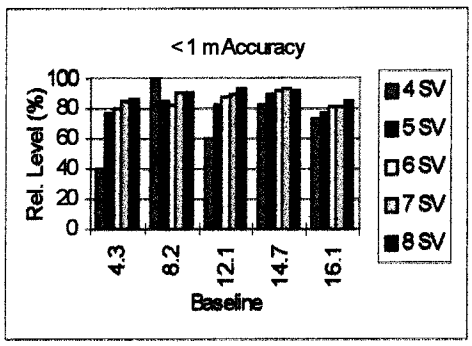

(a) 1 Minute Session Solutions

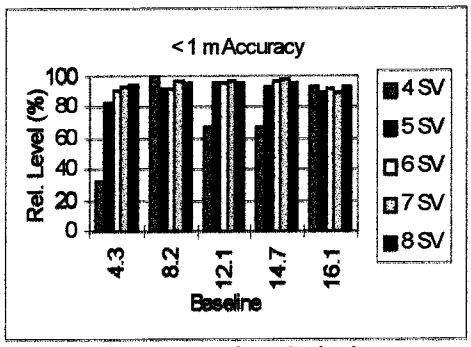

(b) 2 Minute Session Solutions

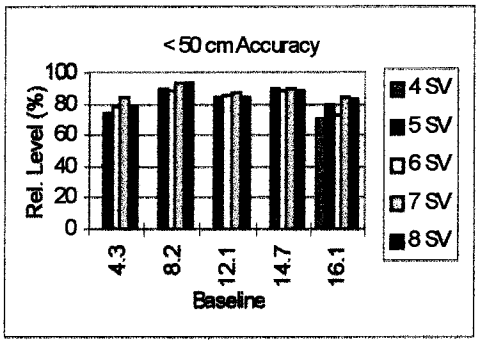

(c) 5 Minute Session Solutions

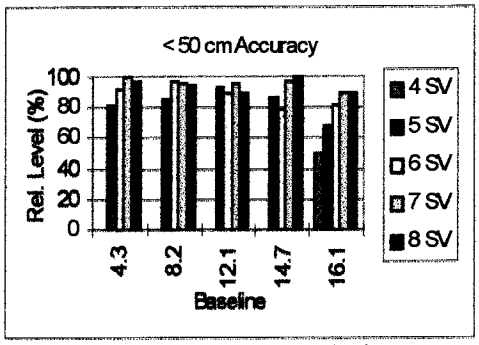

(d) 10 Minute Session Solutions

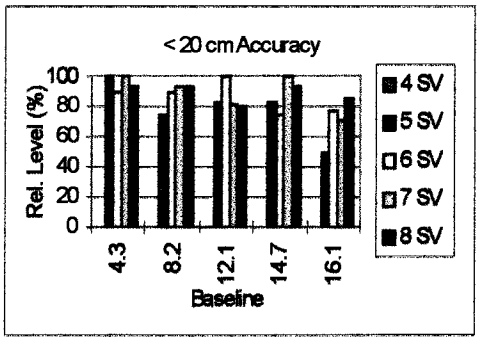

(e) 30 Minute Session Solutions

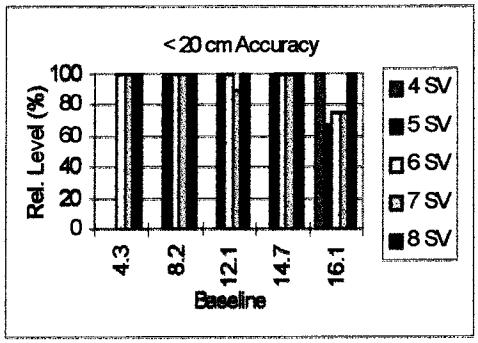

(f) 60 Minute Session Solutions

Figure 8.18: Plots of Reliability Performance of the Mixed PC/A-Code and L1 Phase System vs Number of Satellites

Conclusions which can be drawn from these figures are:.

- A general rule that the more observed satellites during a session the better the accuracy will be, is also true for this system.
- For shorter observation spans (1, 2, 5 and 10 minutes), the impact of additional observed satellites is more significant, then in the case of the longer observation spans (30 and 60 minutes) (See Figure 8.18 (a, b, c and d) and Figure 8.20 (e and f)).

- With short observation spans, sessions with only four satellites (which are very few, less than 1% of the total) appear to be inferior to those sessions with more observed satellites (notice in Figure 8.18 (a) for baselines 4.3 and 12.1 km, and Figure 8.18 (b) for baselines 4.3, 12.1 and 14.7 km). Five satellite sessions appear to have significantly improved accuracy. However for some other baselines (Figure 8.18 (a) for baselines 8.2, 14.7 and 16.1 km, and Figure 8.18 (b) for baselines 8.2 and 16.1 km), the improvement was not significant.
- For short observation spans, the improvement in the reliability performance from five to six, six to seven and seven to eight observed satellites, are only of the order of 5-10%.

8.2.8 System 7 : RSP-L1 System

The baselines used for this system's evaluation are as listed in Table 8.2. Two types of measurement are used for this system: the PC/A-code and the L1 carrier phase. At first, the mixed PC/A-code and the L1 carrier-phase double-difference ambiguity-float solutions were carried out. Then, the ambiguity resolution technique utilising the LAMBDA method is employed (Chapter 6). The procedures are carried out within the BASERSP program. The software was described in Chapters 4 and 5, while the LAMBDA algorithm was explained in Chapter 6. Results of the baseline solutions with fixed double-differenced ambiguities, are then recorded.

The number of solutions for each baseline, for the various observation sessions, are shown in Table 8.14. Shorter observation spans (1 and 2 minute) were also processed, but the results were worse than the ones shown here (for observation sessions of 5 minutes and longer).

Table 8.14: Total Baseline Solutions for Various Observation Sessions

Session length / Baseline (km)	5 min	10 min	30 min	60 min
4.3	228	115	39	19
8.2	274	140	47	24
12.1	-	144	47	23
14.7	-	144	48	24
16.1	-	132	39	18

Table 8.15: Reliability Performance of the RSP-L1 System vs Different Observation Spans for Various Baseline Lengths

Obs. Span	Number of Solutions (nf)	Number Resolved (nc)	nc/nf (%)	DAY (%)	NIGHT (%)
5	228	118	52	48	58
10	115	92	78	71	90
30	39	36	95	92	100
60	19	19	100	100	100

(a) 4.3 km Baseline

Obs. Span	Number of Solutions (nf)	Number Resolved (nc)	nc/nf (%)	DAY (%)	NIGHT (%)
5	274	107	39	42	35
10	140	84	60	56	64
30	47	44	94	87	100
60	24	24	100	100	100

(b) 8.2 km Baseline

Obs. Span	Number of Solutions (nf)	Number Resolved (nc)	nc/nf (%)	DAY (%)	NIGHT (%)
10	144	71	49	49	50
30	47	39	83	77	88
60	23	21	91	80	100

(c) 12.1 km Baseline

Obs. Span	Number of Solutions (nf)	Number Resolved (nc)	nc/nf (%)	DAY (%)	NIGHT (%)
10	144	78	54	53	56
30	48	39	81	71	92
60	24	22	92	83	100

(d) 14.7 km Baseline

Obs. Span	Number of Solutions (nf)	Number Resolved (nc)	nc/nf (%)	DAY (%)	NIGHT (%)
10	132	51	39	36	41
30	39	28	72	67	76
60	18	16	89	88	90

(e) 16.2 km Baseline

The baseline solutions with fixed double-differenced ambiguities are then compared to the true baseline component values. Baseline components that differ by less than 10 cm are considered as to have had their double-differenced ambiguities correctly resolved. The number of 'correct' baseline solutions and their ratio to the total number of baseline solutions are computed to give an indication of the reliability performance of this system. The results are illustrated in Table 8.15.

Performance Characteristics

For baseline length of less than 10 km, it has been noted that:

- 30 minutes of observation data will give about 95% level of reliability in the ambiguity resolution, while for 60 minute observation spans, 100% reliability can be achieved.
- In the case of night sessions (Tables 8.15), when the ionospheric activity is least, 100% level of reliability can be achieved with 30 minutes worth of observation data, but during day time sessions, the level of reliability degrades to about 87% only.
- For shorter observation sessions, e.g., 10 and 5 minute sessions, ambiguity resolution with single frequency data is not reliable, even for baselines under 5 km in length.

For baselines longer than 10 km;

- 60 minutes of observation data could only give about 90% level of reliability.
- Although for night time sessions, for baseline length between 10-15 km, 100% level of reliability could be achieved, the level of reliability for day time sessions is only about 80%.

It seems that to reliably resolve the ambiguities at these baseline lengths, more than 1 hour of observation data is needed.

Performance vs Satellite Geometry

The baseline solutions were then grouped according to the number of observed satellites in the session. Similar analyses as previously were then carried out for each group of solutions. The results are summarised in Table 8.16, from which further conclusions can be drawn:

- The number of observed satellites does not significantly affect the ambiguity resolution process, as long as five or more satellites are observed (see Tables 8.16). This is especially true for longer observation spans (30 and 60 minutes). For shorter observation spans (5 and 10 minutes), the affect would be more slightly apparent.

- The most important factors for successful ambiguity resolution seem to be the quality of the data (rather than the number of observed satellites at each epoch), and the length of the observation span.

Table 8.16: Reliability Performance (in %) of the Ambiguity Resolution vs Number of Satellites for Various Observation Spans

No of SV / Obs. Span	5	6	7	8
5	39	51	49	57
10	45	88	82	75
30	100	100	89	87
60	100	100	100	100

(a) 4.3 km Baseline

No of SV / Obs. Span	5	6	7	8
5	25	38	45	35
10	43	64	60	60
30	75	100	88	100
60	100	100	100	100

(b) 8.2 km Baseline

No of SV / Obs. Span	5	6	7	8
5	28	12	42	35
10	67	55	50	52
30	83	63	85	86
60	50	100	100	100

(c) 14.7 km Baseline

No of SV / Obs. Span	5	6	7	8
5	34	22	34	27
10	38	47	39	34
30	25	78	75	100
60	67	100	88	100

(d) 16.1 km Baseline

8.3 Campaign II

Four low-cost GPS systems (see Chapter 7 for system configuration) have been tested in this campaign:

1. System 2: C/A-Code System
2. System 3: L1-Phase System
3. System 4: Triple-Difference L1-Phase System
4. System 6: Mixed C/A-Code and L1-Phase System

Note that systems 2, 3 and 4 have also been tested in the first campaign.

8.3.1 System 2 : C/A-Code System

During the second campaign three baselines were observed using this system. The baselines are listed in Table 8.17.

Table 8.17: Baselines for the C/A-Code System in Campaign II

No.	GPSDAY	BASELINE LENGTH	SITES + RECEIVER USED	OBSERVATION LENGTH
1	DAY245	5.5 km	BAHR - Ashtech LD-XII HASS - NovAtel	24 hours - segmented
2	DAY245	17.8 km	MAJI - Topcon GP-R1 HASS - NovAtel	24 hours - segmented
3	DAY258	34.9 km	SYED - Ashtech LD-XII MUKR - NovAtel	24 hours - segmented

The C/A-code data for these baselines has been processed using the BASEPR program (see Chapter 4 for software description), for different observation session lengths. The total number of baseline solutions for each observation span are given in Table 8.18. Note that the number is less than that in the first campaign due to the lower data rate selected for this campaign (20 seconds as compared to 15 seconds). The other reason is the greater number of data breaks in the 24 hour observing span due to hardware problems (refer to Chapter 7).

The same analyses were carried out as for the earlier systems. The result of the analyses in terms of reliability performance of the system, for various observation spans, are shown in Table 8.20.

Table 8.18: Total Baseline Solutions for Various Observation Sessions

Session length / Baseline (km)	single-epoch	1 min	2 min	5 min	10 min	30 min	60 min
5.5	4055	1366	687	273	137	45	21
17.8	4137	1383	695	280	141	47	24
34.9	4239	1416	710	283	142	47	23

Looking at the reliability performance in Table 8.20 one is immediately struck by the exceptional performance of the 34.9 km baseline (the longest baseline in the tests!), compared to the other two baselines. For example, the single-epoch session solutions give an accuracy better than 2 m, at the 95% level of reliability, comparable to the PC/A-code system tested in campaign I, while for the other two baselines only an accuracy under 5 m is achieved.

On closer inspection of the double-differenced residuals of the C/A-code for this baseline, as shown in Figure 8.19, it is obvious they are comparable in magnitude or even lower than the double-differenced residuals of the PC/A-code system (see Figure 7.4 (b)).

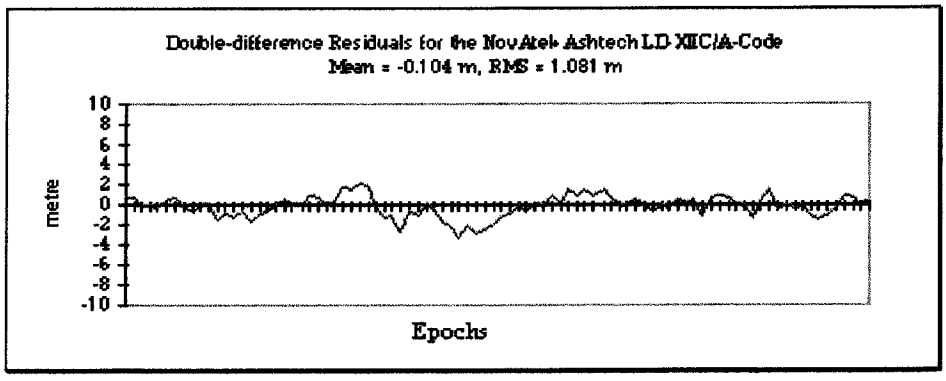

Figure 8.19: Double-Differenced Residuals of the C/A-Code on Baseline 34.9 km

No explanation can be given for this. Based on the GPS receivers used in this baseline (Ashtech LD-XII and NovAtel), the standard C/A-code performance would be expected. Furthermore, the sites involved are similar to the other sites, i.e., rooftop of houses, hence similar multipath effects would be expected. However, the results are obviously not typical of a C/A-code type receiver.

Unfortunately, another anomalous result was found on the 5.5 km baseline. Inspecting the baseline solutions for the 60 minute sessions for System 2 (double-difference C/A-code) and System 4 (double-difference L1 carrier-phase float), a "constant" offset of about 1.1 m in the baseline length was noted (Table 8.19). On closer inspection of the baseline component differences appears that the offset is the result of differences in the DX and DY components of the baselines;

delta DX = 1.240 m
delta DY = 0.447 m
delta DZ = 0.001 m.

Table 8.19: Differences in the Double-Difference C/A-Code and the Double-Difference L1 Carrier-Phase Float Baseline Solutions.

	C/A-Code Solution				L1 Float Solution			
GPSSec	DX	DY	DZ	Baseline	DX	DY	DZ	Baseline
522000	4374.1	1015.3	3183.7	5504.545	4372.7	1016.0	3183.8	5503.668
525600	4373.8	1015.4	3184.0	5504.545	4372.8	1016.1	3183.7	5503.700
529200	4374.0	1016.2	3183.6	5504.663	4372.5	1016.0	3183.6	5503.363
532800	4374.8	1014.6	3183.8	5505.024	4372.8	1015.5	3183.5	5503.429
536400	4373.0	1015.8	3183.8	5503.852	4372.6	1015.5	3183.7	5503.406
540000	4374.2	1015.9	3184.0	5504.956	4372.5	1015.7	3183.5	5503.290
547200	4374.3	1015.5	3183.4	5504.624	4372.9	1014.5	3183.9	5503.546
550800	4373.9	1015.9	3183.7	5504.529	4373.1	1015.9	3183.7	5503.919
565460	4374.1	1017.0	3184.1	5505.138	4373.1	1014.6	3183.8	5503.693
568800	4373.9	1016.4	3183.6	5504.507	4373.0	1015.0	3183.8	5503.697
576000	4374.1	1016.6	3183.3	5504.615	4372.9	1016.0	3183.5	5503.659
586800	4373.8	1016.2	3183.5	5504.387	4372.9	1015.2	3183.7	5503.593
594000	4373.7	1017.3	3183.6	5504.565	4372.8	1015.2	3183.8	5503.586
601200	4375.1	1014.8	3183.7	5505.281	4372.9	1015.3	3183.9	5503.740
Mean	4374.1	1015.9	3183.7	5504.659	4372.8	1015.5	3183.7	5503.593
Stdev.	0.504	0.780	0.221	0.355	0.194	0.521	0.137	0.171

Since the test area is nearly on the Equator, this offset indicates a 'height' problem in the baselines. Again, the GPS receivers used and the sites involved in this baseline are similar to those of the other baselines. Hence, no concrete explanation can be offered. Apart from this problem, the baselines of the C/A-code solutions (plus offset) are of a comparable level of precision as the other C/A-code baseline solutions (see figures in bracket for the 5.5 km baseline in Table 8.20).

Finally, plots of the solutions over the 24 hour spans for the 17.8 km baseline indicate a strong existence of multipath (see Figure 8.20), the magnitude of which is more than 5 metres! This may be due to the strong effect of multipath at site MAJI, because, although the GPS antenna was located on a tripod, the tripod was set quite low.

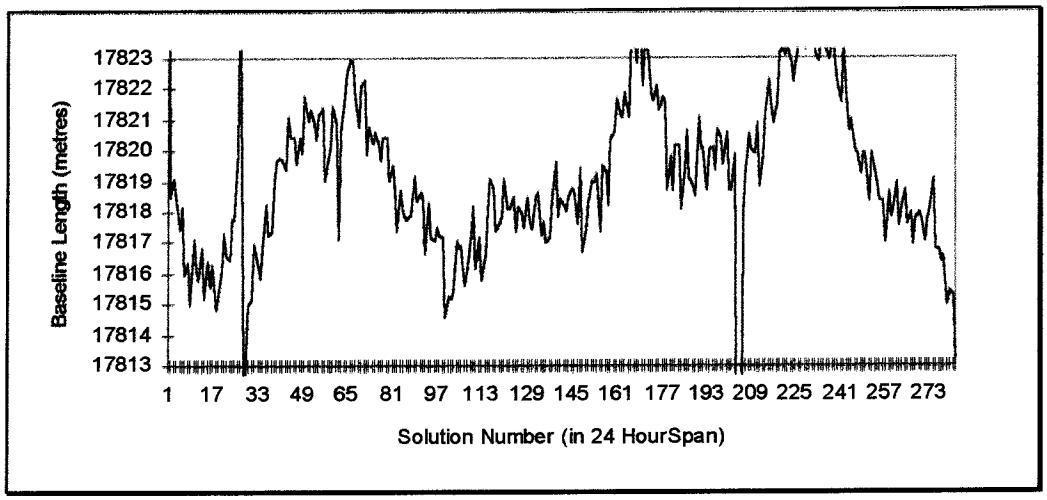

Figure 8.20: Baseline Solutions of the 5 Minute Sessions showing strong Multipath disturbances in the 17.8 km Baseline.

Performance vs Observation Spans

Despite all the 'anomalies' in these results, analyses of system performance was carried out and some conclusions drawn from Table 8.20 are:

- Single-epoch solution, cannot fulfil the anticipated accuracy of DGPS (except for the 34.9 km baseline, for reason discussed earlier). The same result was obtained with the same system in campaign I.
- The 1 and 2 minute solutions give an accuracy of about 2-5 m at 95% reliability level. The 2 minute solutions are slightly better than the 1 minute solutions, with accuracies under 5 m obtained at the 100% reliability level (again, neglecting the result of the 34.9 km baseline).
- The 5, 10, 30 and 60 minute sessions give accuracies around 1-2 m, at the 95% reliability level (the value in brackets for the 5.5 km baseline).
- The 30 and 60 minute session solutions only deliver a slight improvement in performance compared to the 5 and 10 minute sessions.

These conclusions are similar to the ones made for the same system earlier in campaign I.

Table 8.20: Reliability Performance (in %) of the C/A-Code System for Different Observation Spans

	Baseline (km)		
	5.5	17.8	34.9
< 1m	28 (30)	25	69
< 2m	51 (55)	47	95
< 5m	90 (92)	87	100

(a) Single-Epoch Solutions

	Baseline (km)		
	5.5	17.8	34.9
< 1m	39 (49)	33	75
< 2m	70 (79)	60	97
< 5m	99 (99)	100	100

(b) 1 Minute Session Solutions

	Baseline (km)		
	5.5	17.8	34.9
< 1m	46 (60)	34	81
< 2m	79 (90)	63	98
< 5m	100 (100)	100	100

(c) 2 Minute Session Solutions

	Baseline (km)		
	5.5	17.8	34.9
< 50cm	21 (49)	20	57
< 1m	47 (80)	37	86
< 2m	92 (98)	63	100

(d) 5 Minute Session Solutions

	Baseline (km)		
	5.5	17.8	34.9
< 50cm	20 (63)	23	63
< 1m	50 (92)	37	93
< 2m	96 (100)	66	100

(e) 10 Minute Session Solutions

	Baseline (km)		
	5.5	17.8	34.9
< 50cm	4 (51)	21	70
< 1m	49 (84)	33	98
< 2m	100 (100)	70	100

(f) 30 Minute Session Solutions

	Baseline (km)		
	5.5	17.8	34.9
< 50cm	5 (48)	29	83
< 1m	62 (90)	33	100
< 2m	100 (100)	76	100

(g) 60 Minute Session Solutions

Performance vs Baseline Length

With only one baseline to consider (due to the 'anomalous' results discussed earlier), this analysis are not made. However, comparing the 5.5 km baseline performance against the same system in campaign I earlier, comparable reliability level is noted.

Performance vs Different Ionospheric Influences

The 24 hour baseline solutions were divided into DAY and NIGHT sessions according to the procedure described earlier. Similar analyses were carried out on both group of solutions. Although 'discrepancies' are present in the results of the baseline processing, for the purpose of analysing the different performance between DAY and NIGHT session solutions, all baselines except the 17.8 km baseline, which has a strong multipath effect, were used. Plots of a specific accuracy band were made (Figure 8.21), from which the following conclusions were drawn:

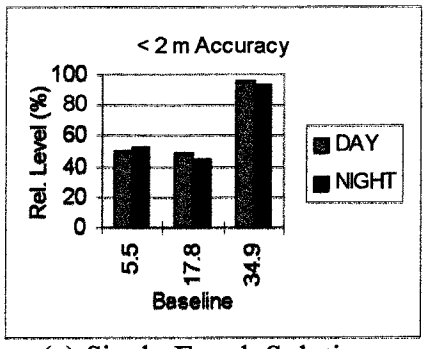

(a) Single-Epoch Solutions

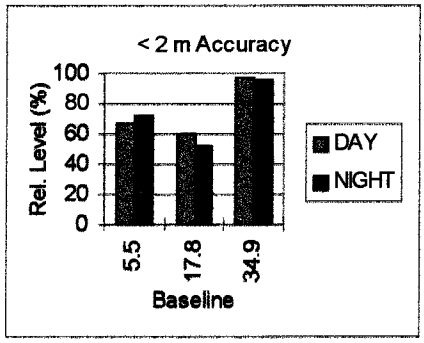

(b) 1 Minute Session Solutions

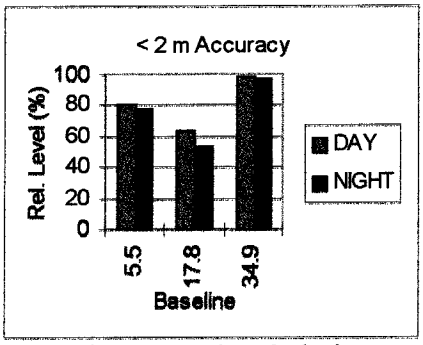

(c) 2 Minute Session Solutions

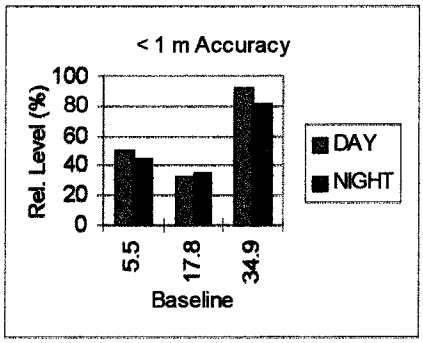

(d) 5 Minute Session Solutions

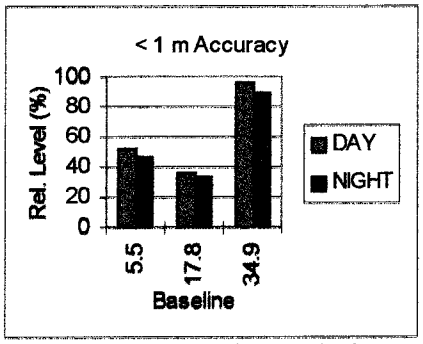

(e) 10 Minute Session Solutions

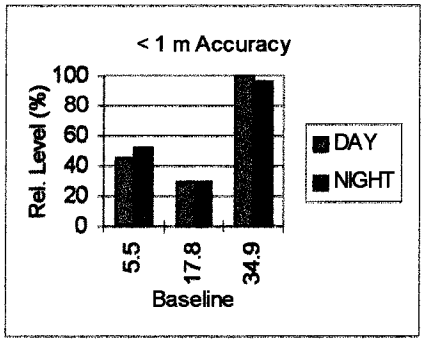

(f) 30 Minute Session Solutions

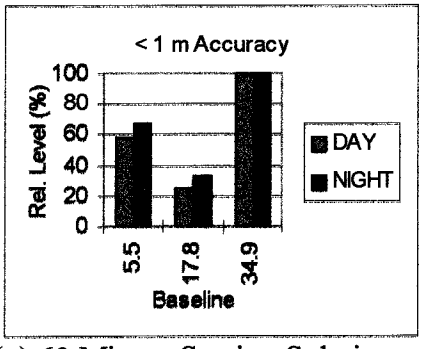

(g) 60 Minute Session Solutions

Figure 8.21: Plots of Reliability Performance (in %) of the C/A-code System - Comparing DAY and NIGHT Sessions.

- The single-epoch, 1 and 2 minute session solutions have a comparable DAY and NIGHT performance, with only a few percentage differences.
- The 5 and 10 minute session solutions have better DAY session performance, by up to about 10%.
- The 30 and 60 minute session solutions on the other hand, have better NIGHT session performance, especially for the 5.5 km baseline.

Performance vs Satellite Geometry

The same procedures were followed in these analyses, whereby the 24 hour baseline solutions have been grouped according to the number of observed satellites. The reliability performance of each group of data are computed for each accuracy band. A specific accuracy band was then plotted in Figure 8.22, for all the observation sessions.

Conclusions which are drawn from this figure are:

- For the shorter observation spans (1, 2, 5 and, partially the 10 minute sessions), the same trend of better performance with more observed satellites is evident.
- On some plots, a significant improvement from four to five observed satellites (e.g., Figure 8.22 (b and c) for the 5.5 km baseline) can be clearly seen.
- The other trends are similar, e.g., the increase in performance from five to six satellites is generally greater than six to seven; and from seven to eight the improvement is hardly noticeable.
- For longer observation spans (30 and 60 minutes), the trend is not obvious due to the smaller number of baseline solutions to analyse. Furthermore, as concluded earlier, the large amount of data used in the processing would have contributed the satellite-receiver geometrical strength, rather than the addition of satellites in the constellation.

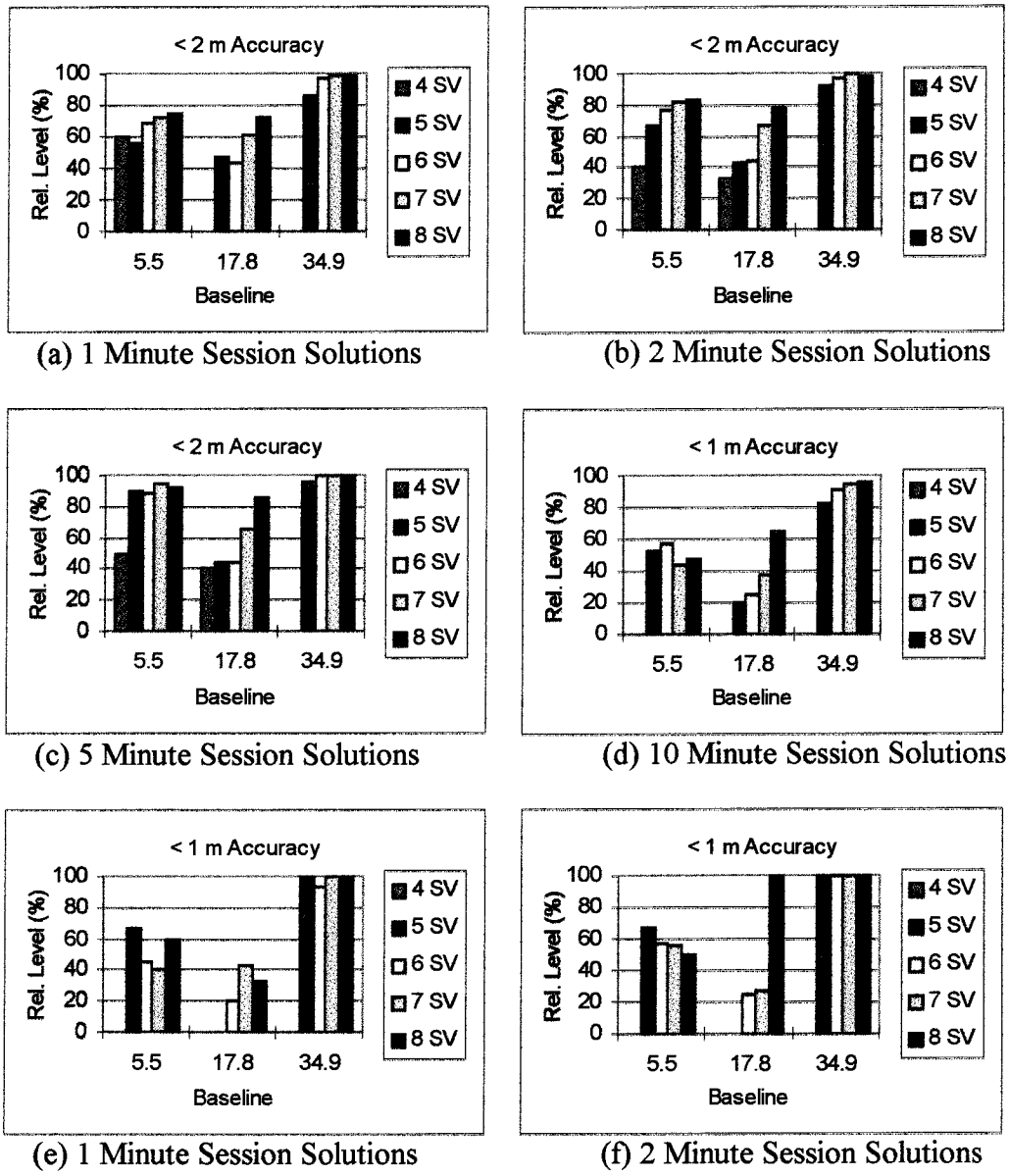

Figure 8.22: Plots of Reliability Performance of the C/A-Code System vs Number of Satellites

8.3.2 System 3 - L1 Phase System

The three baselines observed in the second campaign, as listed in Table 8.17, were used for testing the system. The L1 carrier-phase data for these baselines has been processed using the BASEPH program (see Chapter 4), for different observation session lengths.

The total number of baseline solutions, for each observation span, are given in Table 8.21. The different number of baseline solutions is due to the intermittent gaps in the observation sessions of each baseline, as well as the number of rejected solutions due to

small amounts of observation data and incorrect baseline determinations (e.g., failure to correct cycle-slips).

Table 8.21: Total Baseline Solutions for Various Observation Sessions

Session length / Baseline (km)	1 min	2 min	5 min	10 min	30 min	60 min
5.5	1124	680	272	133	39	17
17.8	1377	691	278	137	42	19
34.9	1412	709	282	140	44	20

The same analyses as described earlier were carried out for this system. The results of the analyses, in the form of the reliability performance level (as a percentage) for various observation spans, are given in Table 8.22.

Performance vs Observation Spans

Analysing the level of reliability in Table 8.22, the performance of the shortest baseline appears to be rather 'poor' compared to the other two longer baselines. Nevertheless, the following conclusions may be drawn:

- The 1 minute session solutions give an accuracy between 2-5 m, at the 95% level of reliability.
- The 2 minute session solutions give an accuracy under 2 m, at the 95% level, except in the case of the 5.5 km baseline.
- The 5 minute session solutions give an accuracy between 1-2 m, at the same reliability level.
- The 10 minute session solutions give submetre accuracy, at the same level of reliability, except for the 5.5 km baseline. The reliability level is also higher for the 17.8 km baseline compared to the 34.9 km baseline.

Leaving aside the 5.5 km baseline, further conclusions are made:

- The 30 minute session solutions give an accuracy of 20-50 cm, at the 95% level, for the 17.8 km baseline, and 50 cm-1 m for the 34.9 km baseline.
- The 60 minute session solutions give an accuracy of 20-50 cm, at the 95% level, for both baselines.

Note that the reliability performance of the double-difference L1 carrier-phase float solution system in this campaign is poorer than the first campaign.

Table 8.22: Reliability Performance (in %) of the L1 Carrier-Phase System for Different Observation Spans

	Baseline (km)		
	5.5	17.8	34.9
< 1m	58	61	60
< 2m	87	89	87
< 5m	99	98	99

(a) 1 Minute Session Solutions

	Baseline (km)		
	5.5	17.8	34.9
< 1m	71	81	77
< 2m	91	95	96
< 5m	98	100	100

(b) 2 Minute Session Solutions

	Baseline (km)		
	5.5	17.8	34.9
< 50cm	49	72	67
< 1m	79	92	91
< 2m	95	99	99

(c) 5 Minute Session Solutions

	Baseline (km)		
	5.5	17.8	34.9
< 50cm	60	88	81
< 1m	86	99	96
< 2m	95	100	99

(d) 10 Minute Session Solutions

	Baseline (km)		
	5.5	17.8	34.9
< 20cm	36	64	73
< 50cm	87	100	93
< 1m	100	100	100

(e) 30 Minute Session Solutions

	Baseline (km)		
	5.5	17.8	34.9
< 10cm	53	32	50
< 20cm	53	79	80
< 50cm	100	100	100

(f) 60 Minute Session Solutions

Performance vs Baseline Length

Plots of the reliability level, of some accuracy bands, are given in Figure 8.23 for the 5, 10, 30 and 60 minute session solutions. The 1 and 2 minute session solutions were not considered since the carrier-phase solutions for very short observation spans were not stable (as indicated from earlier analyses).

Some of the conclusions that can be drawn are:

- The trend of accuracy degradation with increasing baseline length is apparent, although not very distinct. The 5 and 10 minute session solutions have this trend for all accuracy bands.
- The 30 and 60 minute session solutions indicate that this trend exists only in some accuracy bands (eg in Figure 8.23 (e) for the < 50 cm accuracy).

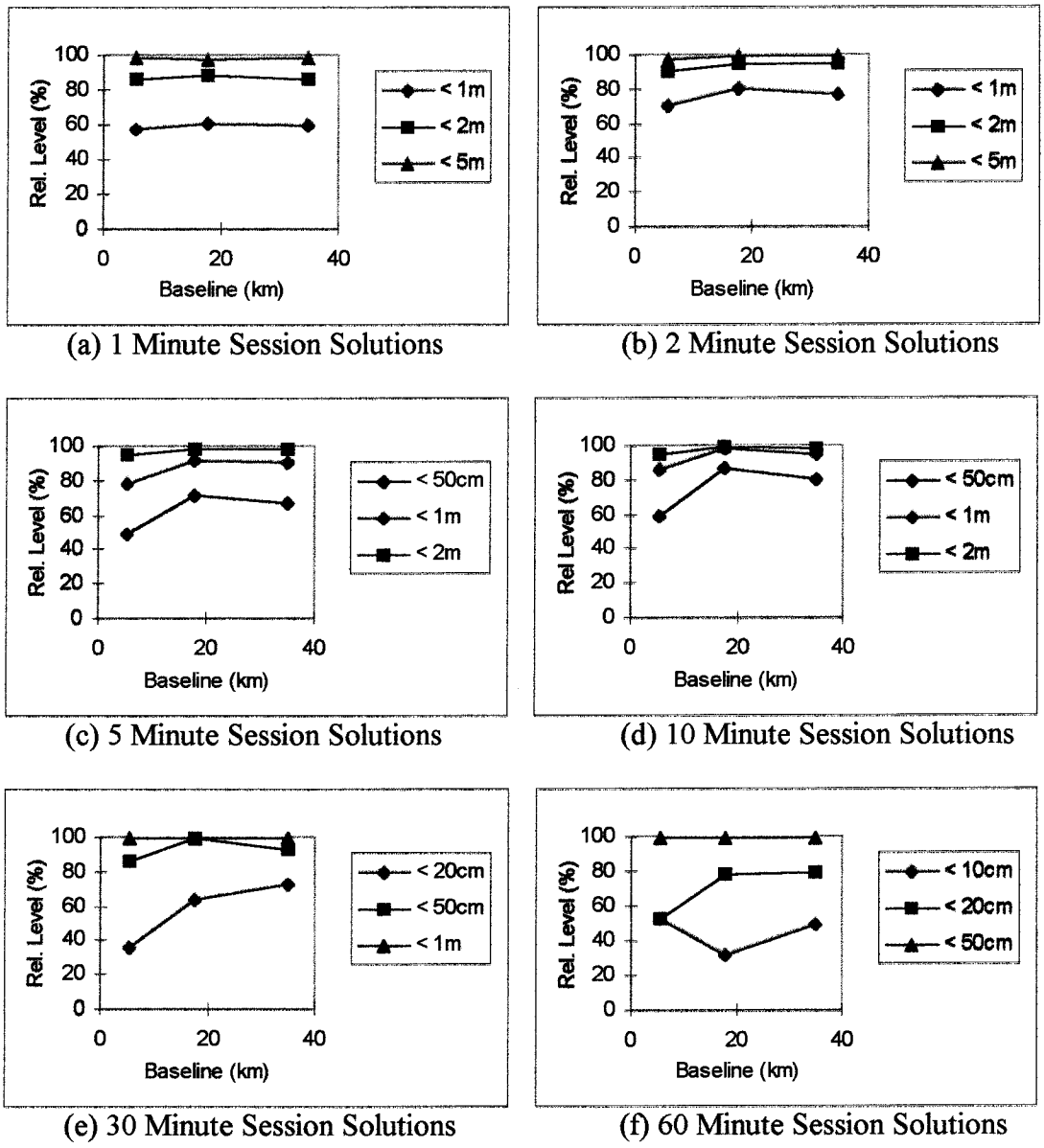

Figure 8.23: Plots of Reliability Performance (in %) of the L1 Carrier-Phase System for Different Observation Spans

Performance vs Difference Ionospheric Influence

The 24 hour baseline solutions were divided into DAY and NIGHT sessions as described previously. Plots of the reliability level for specific accuracy band are presented in Figure 8.24.

Analysing these plots, the following conclusions are drawn:

- The short observation session solutions (5 and 10 minute) shows a mixture of performance, with most baselines having a better DAY time reliability level. The same phenomenon has also been noted in the first campaign.

- The 30 minute session solutions shows an improvement of the NIGHT sessions over the DAY sessions (except for the shortest baseline).
- However, the 60 minute session solutions shows the opposite result, where the 5.5 km baseline show a better NIGHT performance while the longer baselines shows a better DAY performance.

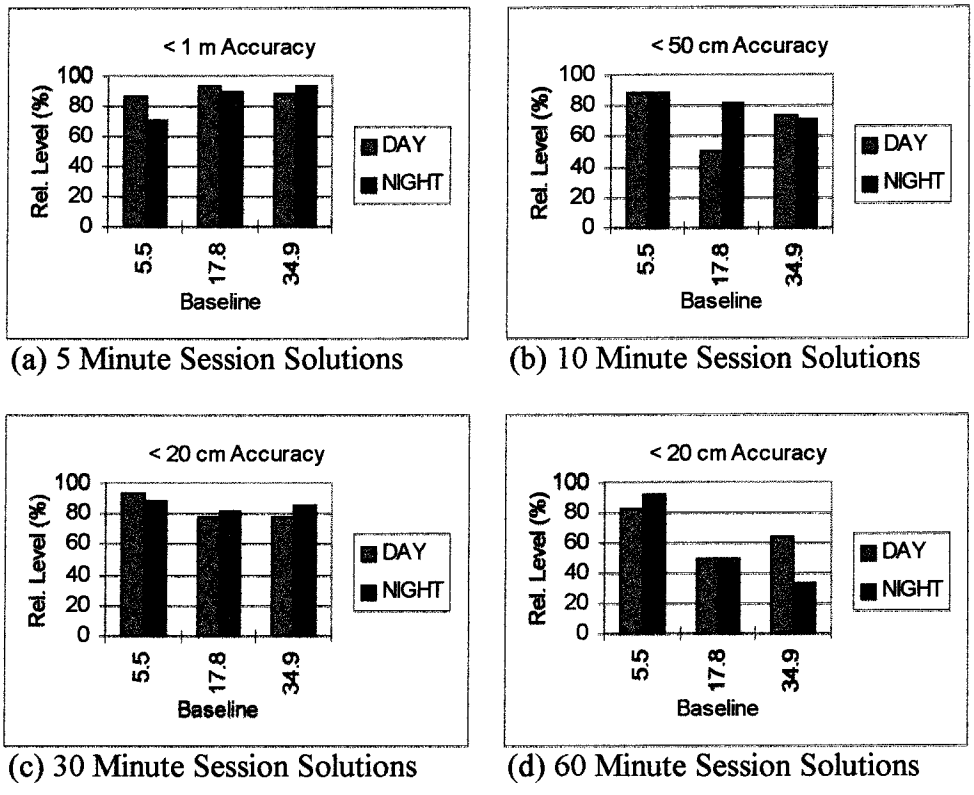

(a) 5 Minute Session Solutions (b) 10 Minute Session Solutions

(c) 30 Minute Session Solutions (d) 60 Minute Session Solutions

Figure 8.24: Plots of Reliability Performance (in %) of the L1 Carrier-Phase System - Comparing DAY and NIGHT Sessions.

Performance vs Satellite Geometry

The 24 hour baseline solutions were then grouped according to the number of observed satellites. The group were then subjected to the same analyses. The reliability level for specific accuracy bands were then plotted (Figure 8.25).

Some conclusions which can be drawn:

- A general rule that the more satellites observed during a session, the better the performance, is also verified here.
- The 5, 10 and 30 minute session solutions clearly shows higher reliability level with more observed satellites. Except for the 34.9 km baseline, the 60 minute session solutions also shows the same trend.

- Accuracy improvement when the number of satellite increases from five to six is seen to be more significant (eg Figure 8.25 (a) and (b), for the 17.8 km baseline, Figure 8.25 (c), for all baseline and Figure 8.25 (d), for the 5.5 km baseline).
- Improvements due to an increase from seven to eight observed satellites is apparent on some baselines (e.g., the 5.5 and 34.9 km in Figure 8.25 (a and c), the 17.8 and 34.9 km in Figure 8.25 (b), and the 5.5 km in Figure 8.25 (d)).

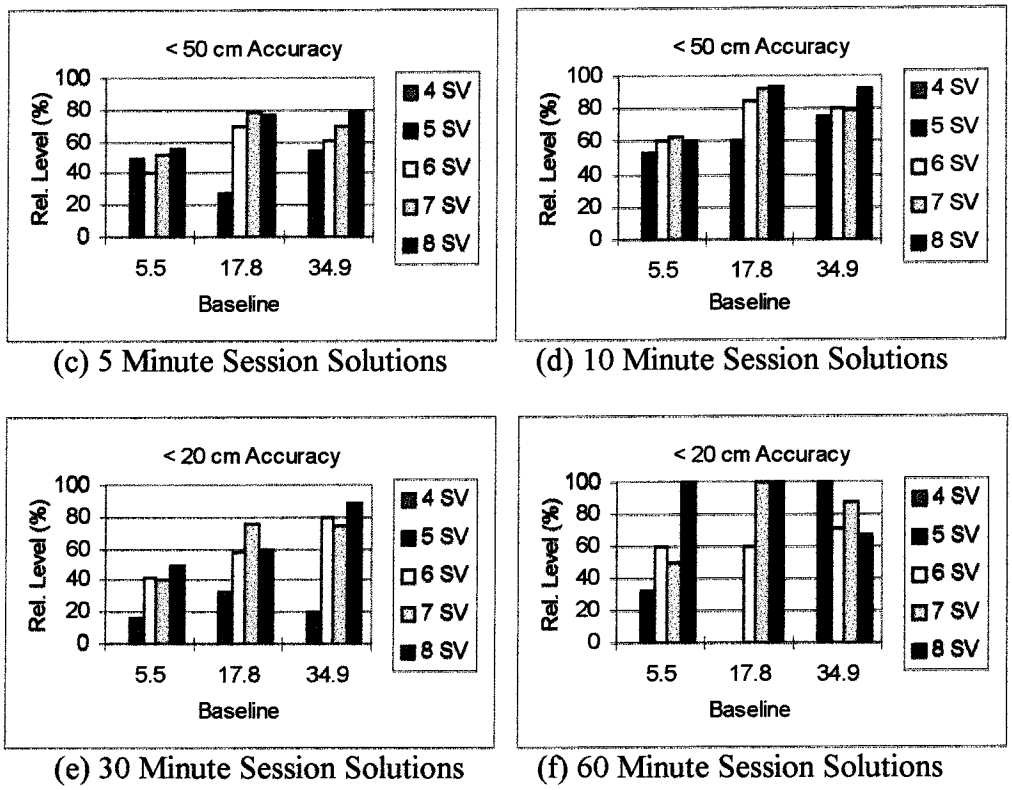

(c) 5 Minute Session Solutions (d) 10 Minute Session Solutions

(e) 30 Minute Session Solutions (f) 60 Minute Session Solutions

Figure 8.25: Plots of Reliability Performance of the L1 Carrier-Phase System vs Number of Satellites

8.3.3 System 4 - Triple-Difference L1 Phase System

The baselines observed in this campaign, as listed in Table 8.17, were used for testing. The L1 carrier-phase data for these baselines has been processed using the BASETRP program (see Chapter 4), for different observation session lengths.

The total number of baseline solutions, for each observation span, are given in Table 8.23. The reasons for the different number of solutions for the baselines were due to the intermittent gaps in the observation sessions for each baseline, as well as the number of rejected solutions due to the small amount of observation data involved.

Table 8.23: Total Baseline Solutions for Various Observation Sessions

Session length / Baseline (km)	1 min	2 min	5 min	10 min	30 min	60 min
5.5	1359	686	271	140	47	24
17.8	1379	695	282	143	48	24
34.9	1414	709	281	142	48	24

The results of the analyses, in the form of the reliability performance level, for various observation spans, are summarised in Table 8.24.

Performance vs Observation Spans

Table 8.24 gives the performance of the system, in terms of the level of reliability for specific accuracy bands, for each observation span.

Table 8.24: Reliability Performance (in %) of the Triple-Difference L1 Carrier-Phase System for Different Observation Spans

	Baseline (km)		
	5.5	17.8	34.9
< 1m	61	60	60
< 2m	90	90	86
< 5m	99	99	99

(a) 1 Minute Session Solutions

	Baseline (km)		
	5.5	17.8	34.9
< 1m	76	81	76
< 2m	95	96	96
< 5m	100	100	100

(b) 2 Minute Session Solutions

	Baseline (km)		
	5.5	17.8	34.9
< 50cm	56	72	66
< 1m	87	93	91
< 2m	98	98	98

(c) 5 Minute Session Solutions

	Baseline (km)		
	5.5	17.8	34.9
< 20cm	34	47	40
< 50cm	67	85	86
< 1m	92	96	99

(d) 10 Minute Session Solutions

	Baseline (km)		
	5.5	17.8	34.9
< 10cm	23	29	38
< 20cm	40	65	69
< 50cm	85	90	94

(e) 30 Minute Session Solutions

	Baseline (km)		
	5.5	17.8	34.9
< 10cm	21	42	46
< 20cm	38	83	71
< 50cm	83	92	96

(f) 60 Minute Session Solutions

Some conclusions that can be drawn from Table 8.24 are:

- The 1 minute session solutions give an accuracy between 2-5 m, at the 95% level, for all baselines.
- The 2 minute session solutions give an accuracy of 1-2 m, again at the same level of reliability. The 5.5 km baseline, however, shows a slightly lower reliability level.

- The 5 minute session solution give an accuracy of 1-2 m at 95% level also, only slightly better than the 2 minute session solutions.
- The 10 minute session solutions give submetre accuracy at the 95% level, except for the case of the 5.5 km baseline.
- Surprisingly, the 30 and 60 minute session solutions also give the same performance as the 10 minute session solutions, with the exception of the 34.9 km baseline which gives under 50 cm accuracy at the 95% level.

Note that the performance of the same system in the first campaign was better.

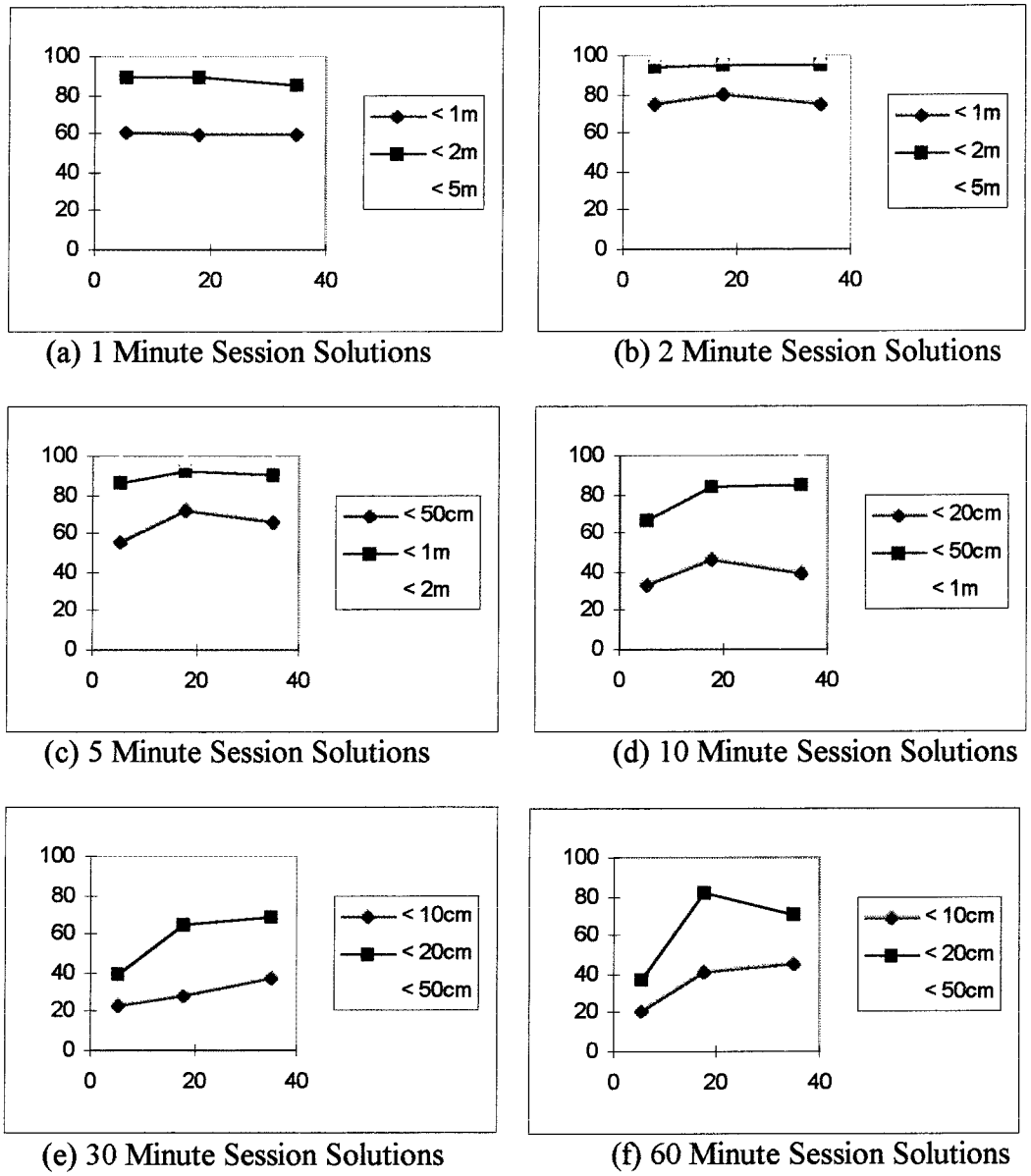

(a) 1 Minute Session Solutions

(b) 2 Minute Session Solutions

(c) 5 Minute Session Solutions

(d) 10 Minute Session Solutions

(e) 30 Minute Session Solutions

(f) 60 Minute Session Solutions

Figure 8.26: Plots of Reliability Performance (in %) of the Triple-Difference L1 Carrier-Phase System for Different Observation Spans

Performance vs Baseline Length

The reliability level for specific accuracy bands in Table 8.24, are plotted in Figure 8.26. From these plots, the following conclusions are made:

- With the exception of the 5.5 km baseline, the trend of decreasing performance with increasing baseline length can be noted in almost all plots.
- The short observation spans (1, 2, 5, and 10 minute) indicate this trend, albeit not as significantly.
- The 30 and 60 minute session solutions, however, do not show such trend (except for the < 50 cm accuracy in Figure 8.26 (f)).

Performance vs Different Ionospheric Influences

The 24 hour baseline solutions for all the various observation spans, were then divided into the DAY and NIGHT sessions. The reliability levels are then plotted in Figure 8.27.

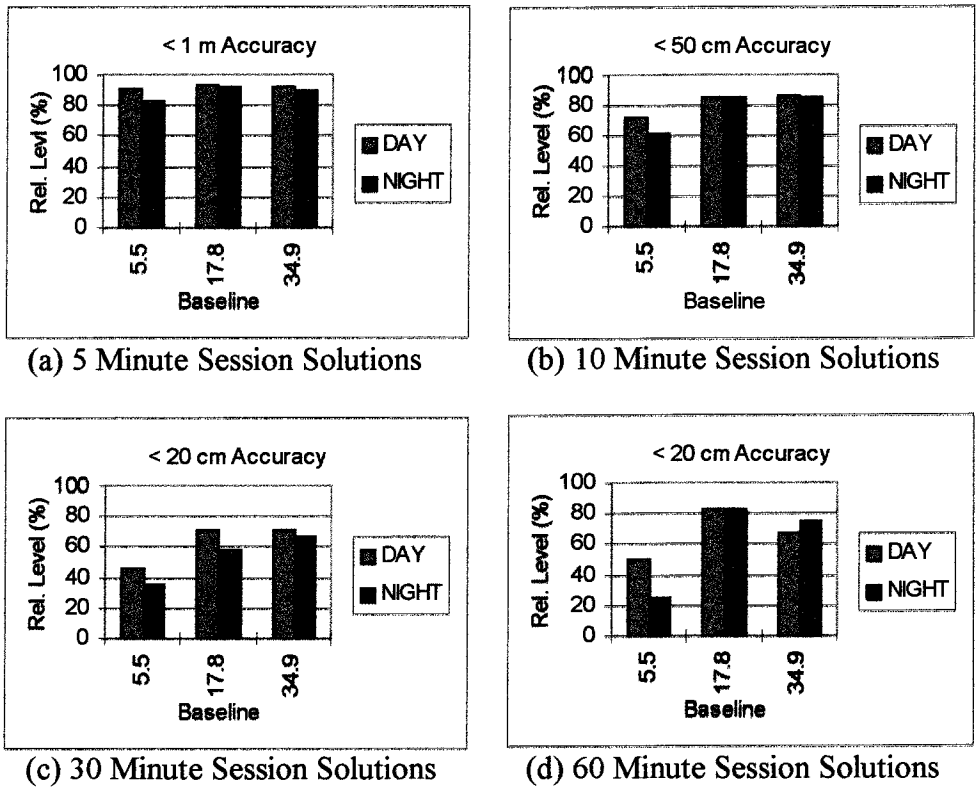

(a) 5 Minute Session Solutions (b) 10 Minute Session Solutions

(c) 30 Minute Session Solutions (d) 60 Minute Session Solutions

Figure 8.27: Plots of Reliability Performance (in %) of the Triple-Difference L1 Carrier-Phase System - Comparing DAY and NIGHT Sessions.

Studying the DAY and NIGHT plots in Figure 8.27, the following points are noted:

- The 5 and 10 minute session solutions do not show any significant difference in performance between the DAY and the NIGHT sessions.

- The 30 minute session solutions surprisingly show a better DAY than NIGHT performance.
- The 60 minute session solutions indicate better NIGHT performance for the 34.9 km baseline, but not for the 17.8 km baseline.

Performance vs Satellite Geometry

The 24 hour baseline solutions for each baseline and each observation span, were grouped according to the number of observed satellites. Then, for each group of solutions, the same analyses were carried out. The performance for each group (of number of observed satellites) were plotted in Figure 8.28.

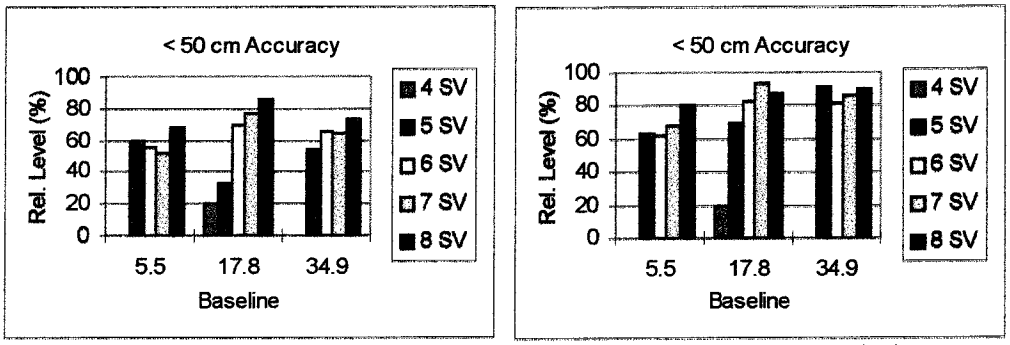

(a) 5 Minute Session Solutions (b) 10 Minute Session Solutions

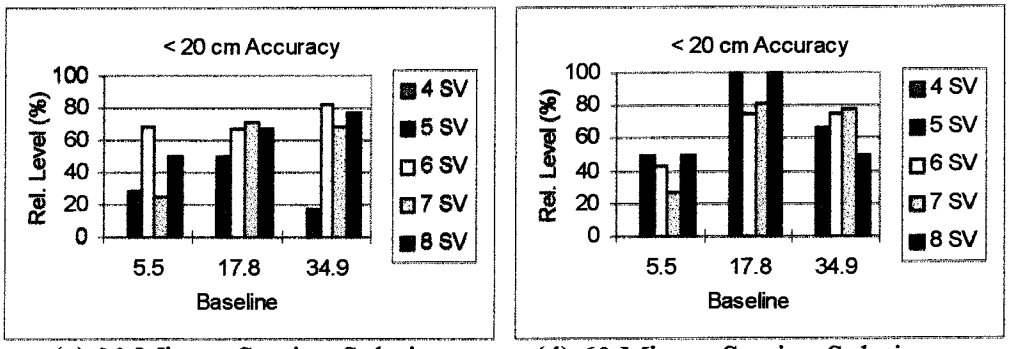

(c) 30 Minute Session Solutions (d) 60 Minute Session Solutions

Figure 8.28: Plots of Reliability Performance of the Triple-Difference L1 Carrier-Phase System vs Number of Satellites

Conclusions that can be drawn from these plots:

- In the case of the 5 minute session solutions, the normal trend of improved performance with more observed satellites is confirmed for the 17.8 and 34.9 km baselines. The change from five to six observed satellites is quite significant (about 20% for the 17.8 km baseline and 10% for the 34.9 km baseline).

- The 10 minute session solutions show the same trend, with the exception of the increase of five to six observed satellites in the 34.9 km baseline. The increase in performance from four to five observed satellites for the 17.8 km baseline is enormous, about 50%.
- The longer observation spans (30 and 60 minutes) also indicate the same trend, with some discrepancies, for example in Figure 8.28 (c) for the six to seven observed satellite for the 5.5 km and the 34.9 km baselines and Figure 8.28 (d) for the seven to eight observed satellites for the 34.9 km baseline.

8.3.4 System 6 - Mixed C/A-Code and L1 Phase System

All three baselines observed in this campaign (Table 8.17) were used in testing this system. The C/A-code pseudo-range and the L1 carrier-phase data are processed using the BASEPRPH program, utilising the mixed measurement algorithm described in Chapter 5. The results of the processing, in terms of the number of baseline solutions, are listed in Table 8.25. The same explanation concerning the number of solutions as tended for the earlier two systems also holds for this case.

Table 8.25: Total Baseline Solutions for Various Observation Sessions

Session length / Baseline (km)	1 min	2 min	5 min	10 min	30 min	60 min
5.5	1347	684	273	134	39	17
17.8	1334	650	234	137	42	19
34.9	1415	710	284	140	44	20

The reliability performance of the system, for various observation spans, is tabulated in Table 8.26.

It was noted earlier that the results for the 5.5 km baseline indicated a constant bias of about 1.1 m between the C/A-code and the L1 carrier-phase solutions. For this reason, the mixed C/A-code and L1 carrier-phase solutions would be subject to the same bias. Note the low reliability performance of this baseline in Figure 8.29 (c, d, e and f). Therefore, this baseline will not be included in the analyses.

Performance vs Observation Spans

The mixed C/A-code pseudo-range and L1 carrier-phase system is expected to have a lower performance compared to the mixed PC/A-code and L1 carrier-phase system tested in campaign I. This should be especially true for the shorter observation spans since with small amounts of data, the code measurements will dominate the results. Hence the result would basically reflect the difference in the noise level between the two types of pseudo-range measurements.

Table 8.26: Reliability Performance (in %) of the Mixed C/A-Code + L1 Carrier-Phase System for Different Observation Spans

	Baseline (km)		
Accuracy	5.5	17.8	34.9
< 1m	56	35	87
< 2m	88	68	99
< 5m	100	99	100

(a) 1 Minute Session Solutions

	Baseline (km)		
Accuracy	5.5	17.8	34.9
< 1m	76	63	89
< 2m	94	91	99
< 5m	99	100	100

(b) 2 Minute Session Solutions

	Baseline (km)		
Accuracy	5.5	17.8	34.9
< 50cm	53	71	70
< 1m	84	94	93
< 2m	97	99	99

(c) 5 Minute Session Solutions

	Baseline (km)		
Accuracy	5.5	17.8	34.9
< 50cm	63	87	83
< 1m	87	99	97
< 2m	96	100	99

(d) 10 Minute Session Solutions

	Baseline (km)		
Accuracy	5.5	17.8	34.9
< 20cm	38	60	73
< 50cm	87	100	93
< 1m	100	100	100

(e) 30 Minute Session Solutions

	Baseline (km)		
Accuracy	5.5	17.8	34.9
< 10cm	53	32	50
< 20cm	53	79	80
< 50cm	100	100	100

(f) 60 Minute Session Solutions

Studying the reliability performance in Table 8.26, the following conclusions are drawn:

- For the 1 and 2 minute session solutions, the 17.8 km baseline gives 2-5 m accuracy at the 95 % level of reliability, while the longer 34.9 km baseline gives 1-2 m accuracy.
- The 5 minute session solutions give less than 2 m accuracy, at a higher 99 % level of reliability.
- The 10 minute session solutions give submetre accuracy for both baselines.
- The 30 minute session solutions give an accuracy between 20-50 cm at the 95 % level for the 17.8 km baseline, while the 34.9 km baseline only gives 50 cm - 1 m accuracy.

- The results of the 60 minute session solutions were poorer than the 30 minute ones. No explanation can be given for this.

Performance vs Baseline Length

The reliability performance for specific accuracy bands in Table 8.26 were also plotted in Figure 8.20. Analysing the figures, the following conclusions are made (again, excluding the 5.5 km baseline):

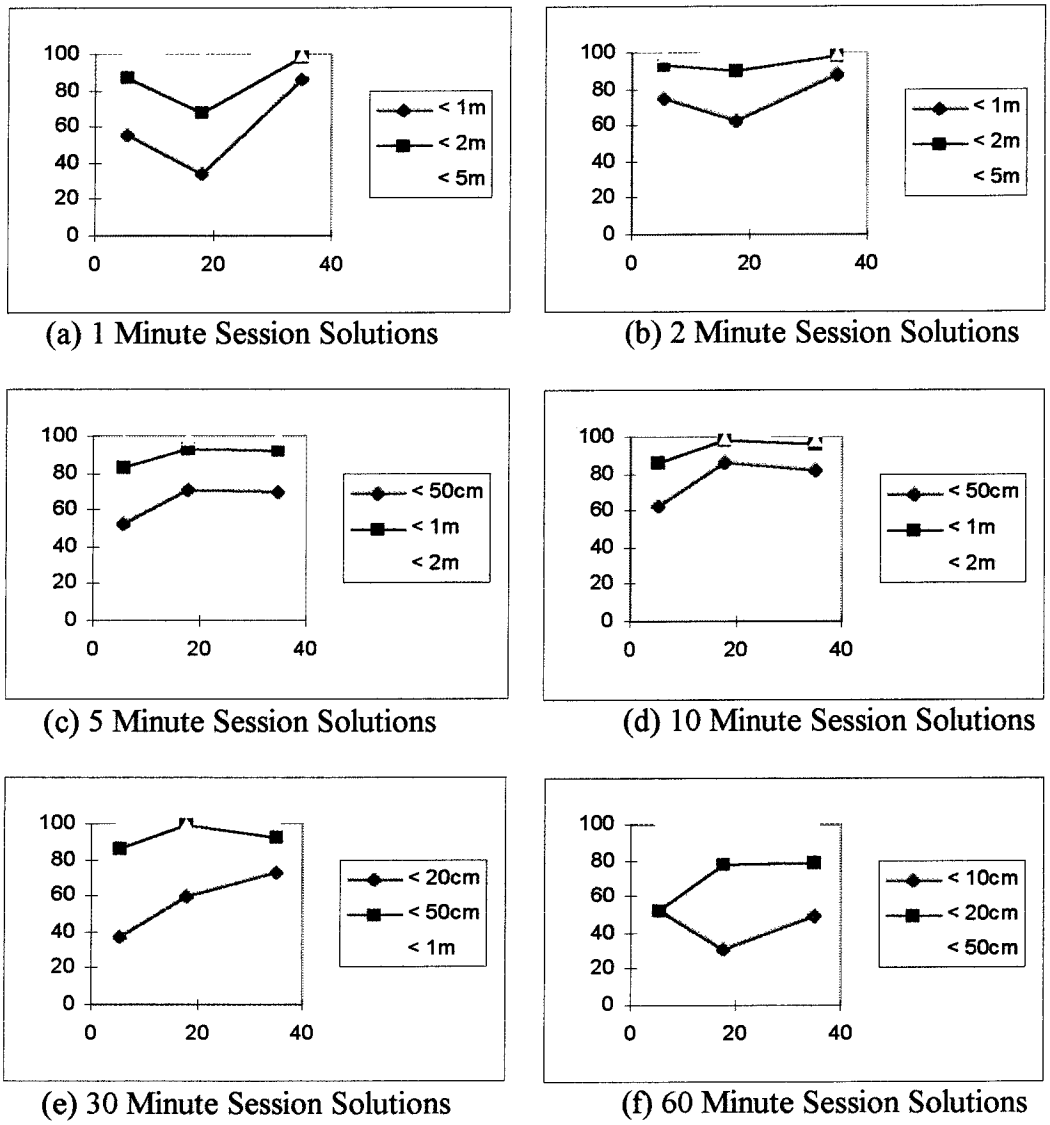

(a) 1 Minute Session Solutions

(b) 2 Minute Session Solutions

(c) 5 Minute Session Solutions

(d) 10 Minute Session Solutions

(e) 30 Minute Session Solutions

(f) 60 Minute Session Solutions

Figure 8.29: Plots of Reliability Performance (in %) of the Mixed C/A-Code + L1 Carrier-Phase System for Different Observation Spans

- The 1 and 2 minute session solutions indicate a poor result for the 17.8 km baseline, due perhaps to the strong multipath effecting the C/A-code measurements (see Figure 8.20).

- The 5 minute session solutions start to indicate a decrease in the performance with increasing baseline length, but only slightly.
- The 10 minute session solutions indicate a more distinct decreasing slope with increasing baseline length.
- The 30 and 60 minute session solutions also indicate this effect for the overall performance, except for the < 50 cm accuracy band in Figure 8.29 (e), and the < 20 cm accuracy band in Figure 8.29 (f).

Performance vs Different Ionospheric Influences

The 24 hour baseline solutions are grouped according to the DAY and NIGHT time

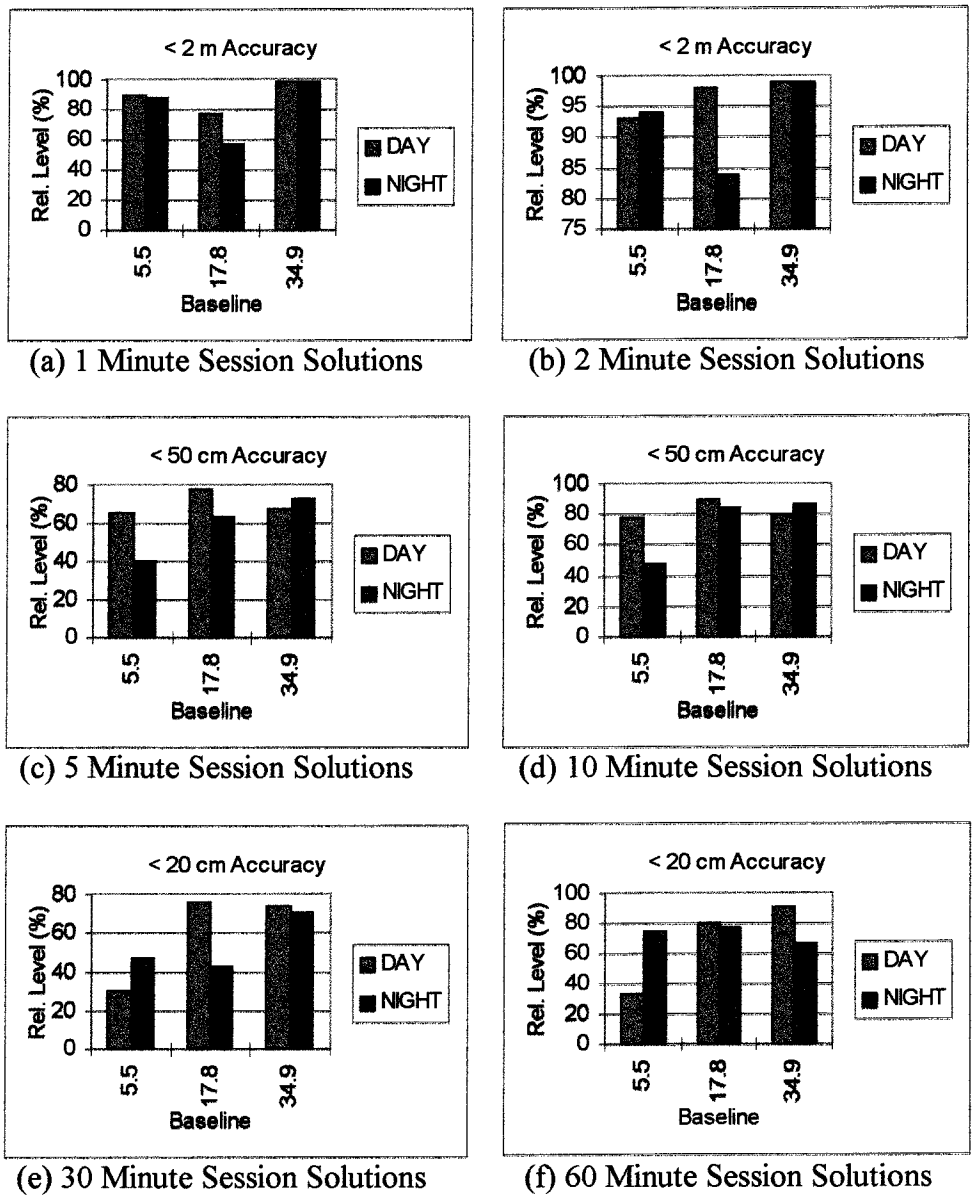

Figure 8.30: Plots of Reliability Performance (in %) of the Mixed C/A-Code + L1 Carrier-Phase System - Comparing DAY and NIGHT Sessions.

sessions in the procedure described earlier, with plots in Figure 8.30. Although the results of this system are expected to be similar to System 5 in the first campaign, it turns out that the performance was not so. For example:

- For the 17.8 km baseline, all the observation spans give a better DAY time performance than the NIGHT time performance. This might have been the result of multipath on the baseline solutions. Note in Figure 8.20, the DAY time multipath effect (first half of the plots) could have been minimised if the mean value is computed due to its sinusoidal nature, while the NIGHT time effect (the other half of the plots) cannot. Due to the long period of the multipath cycle in this baseline, longer observation spans (30 and 60 minutes) would have been effected as well as the short ones.
- The 34.9 km baseline gives equivalent DAY and NIGHT time performance for the 1 and 2 minute observation sessions, and better NIGHT time performance for the 5 and 10 minute session solutions as would be expected. However, the 30 and 60 minute session solutions imply the opposite! No explanation can be given for this anomalous result.

Performance vs Satellite Geometry

The 24 hour baseline solutions are then grouped according to the number of observed satellites. For each group of solutions the same analyses were carried out. Plots of the reliability level for specific accuracy bands are given in Figure 8.31.

The following conclusions are drawn (again, neglecting the results of the 5.5 km baseline):

- The short session solutions (1, 2, 5 and 10 minutes), indicate a trend of increasing reliability performance with the addition of observed satellite. The increase of five to six satellites is quite significant (Figure 8.31 (c and d)), up to about 25%.
- An increase from six to seven observed satellites, seems to be also quite significant, especially for the 17.8 km baseline with up to about a 10 % improvement.
- An increase from seven to eight observed satellites, however, gives a mixed performance result, sometimes better and sometimes worse (though the magnitude was only about few percent).

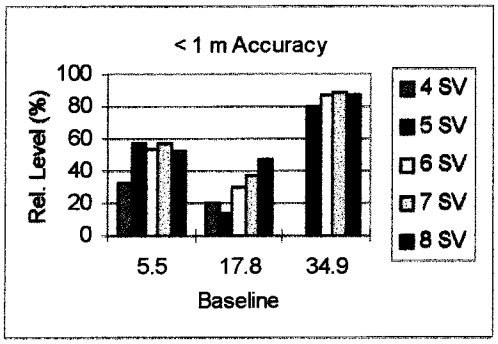

(a) 1 Minute Session Solutions

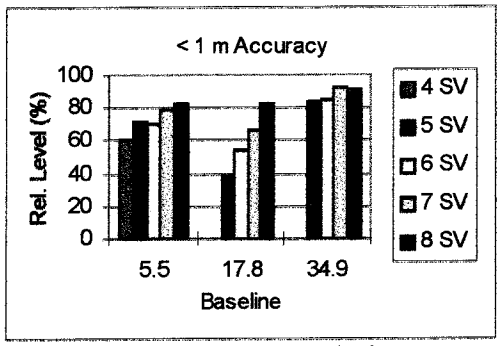

(b) 2 Minute Session Solutions

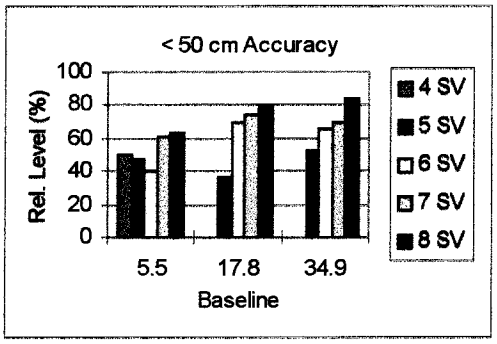

(c) 5 Minute Session Solutions

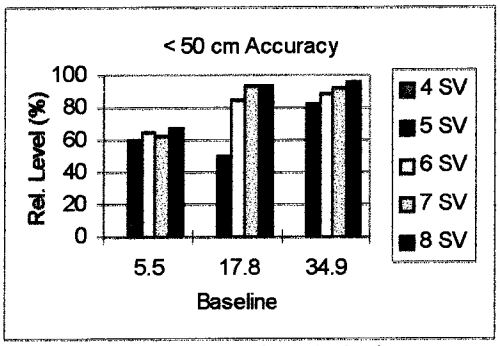

(d) 10 Minute Session Solutions

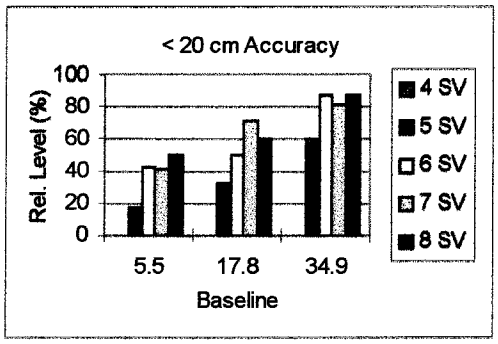

(e) 30 Minute Session Solutions

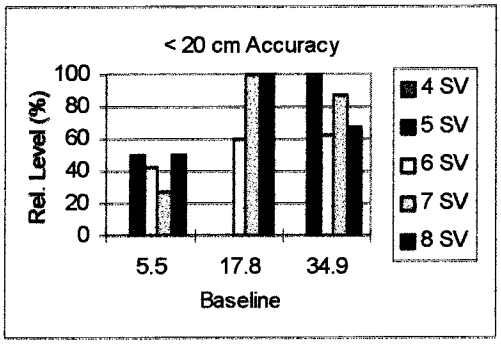

(f) 60 Minute Session Solutions

Figure 8.31: Plots of Reliability Performance of the Mixed C/A-Code + L1 Carrier-Phase System vs Number of Satellites

Chapter 9

SUMMARY, CONCLUSIONS, AND RECOMMENDATIONS

This chapter summarises the investigations, makes conclusions on the findings, and recommends topics for further investigations.

9.1 SUMMARY

GPS, as a new tool for surveying, has proven to be able to address all classes and types of surveying applications. The high and ultra-high surveying accuracy applications, which have driven phase-based GPS system development, are now addressed by mature and well-tested technologies. System requirements, field procedures and data processing algorithms to achieve these accuracies are generally well defined. However, in the case of intermediate to low-accuracy applications, which possibly represent the majority of GPS 'non-navigation' users, few guidelines or standards are available.

As a result there has been a tendency within the GPS surveying community to use dual-frequency receivers for all surveying tasks, regardless of the accuracy requirement. This practice implies high investment costs in GPS technology, even for medium accuracy surveying applications, and this may be hindering the adoption of GPS in many small survey practices.

Realising the importance of this issue, these investigations focused on the performance characteristics of several low-cost GPS system options (as discussed in Chapter 4) which are appropriate for moderate accuracy surveying and mapping applications. In particular, tests were carried out to bench-mark these systems in term of the achievable accuracy and the level of reliability associated with this accuracy.

The performance of any GPS system are also affected by observational conditions or constraints in its use. In these investigations, some of these constraints (which are further classified as being either under the influence of users, or not, as indicated in Figure 9.1) are also studied. The effect of these constraints on the performance of the GPS systems has been discussed in Chapter 8.

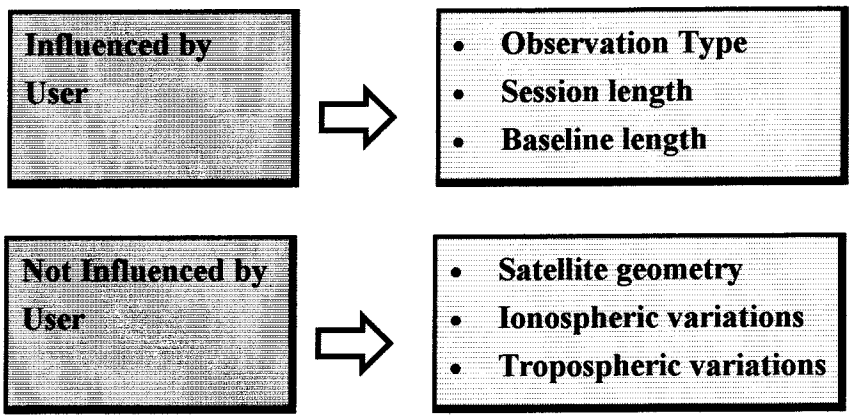

Figure 9.1 Observational Constraints Affecting System Performance

For the purpose of evaluating a low-cost GPS system a standardised test procedure has been designed and implemented in these investigations. Several baselines of varying length (representing the likely 'scale' of most medium accuracy mapping applications) have been observed for 24 hour periods in order to sample all possible satellite geometries and ionospheric influence. The test procedure is described in Chapter 7. The observed data has been processed with a variety of baseline computation. Multiple observation session spans of varying length have been processed. The results and their analysis for each system configuration (Chapter 7) are presented in Chapter 8.

9.2 CONCLUSIONS

ON SYSTEM PERFORMANCE CHARACTERISTICS

Based on the investigations carried out and the results obtained from the data processing associated with thousands of baseline solutions, the following conclusions can be drawn. (Note that some of these conclusions may not be 'universal', as not all possible system configurations, baseline lengths, locations and site factors could be tested.)

9.2.1 PC/A-Code System

- The PC/A-code system can deliver baseline accuracies under 2 m with single-epoch data, and submetre accuracy with 5-10 minute observation data. Hence this system could be use for rapid static positioning, or even 'kinematic' applications that are satisfied with such accuracy requirements.

- This performance is achieved at the 95% level of reliability any time of the day or night, with five or more observed satellites, for baseline lengths under 35 km.

- Multipath still hinders the full capabilities of this system. It is anticipated that Precise C/A-code system coupled with *multipath elimination technology* could provide higher levels of accuracy, e.g. single-epoch baseline determination with submeter accuracy and sub 50 cm accuracy with several epochs of data. Hence, rapid-positioning without the use of phase data would be possible.

9.2.2 C/A-Code System

- The C/A-code system could not deliver baseline accuracies below 5 m with single-epoch data. At least 1-2 minutes of data appears to be needed to achieve this accuracy. An accuracy of 1-2 m can only be achieved with at least 10 minutes of observations.

- This performance is achieved at the 95% level of reliability any time of the day or night, with five or more observed satellites, for baseline lengths under 35 km.

- Multipath affected this system worst than any other. It is believed that under benign multipath conditions, 1 m accuracy could be achieved with 5-10 minutes of observations.

9.2.3 L1 Carrier-Phase Double-Difference (Ambiguity Float) System

- With 5-10 minutes of L1 carrier-phase data, the performance of this system is similar to that of the PC/A-code system. However, because of the susceptibility to phase-type biases such as cycle slips, this system is less robust than pseudo-range systems. With 30 minutes or more data this system delivers baseline accuracies under 50 cm, and of the order of 10-20 cm with 60 minutes of data.

- This performance is achieved at the 95% level of reliability any time of the day or night, with five or more observed satellites, for baseline lengths under 15 km. It is believed that higher accuracies can be achieved for shorter baselines, and for night time observations where ionospheric bias is less severe.

- For short baseline applications (under 15 km), the data double-differencing mode employed virtually cancels the ionospheric biases. However, as the baseline length increases, the accuracy of the double-difference carrier-phase solution appears to degrade. This degradation can also be related to the amount of data being processed. In general, the longer the baseline, the greater amount of data needed in order to achieve the same level of accuracy as for short baselines.

9.2.4 L1 Carrier-Phase Triple Difference System

- The phase triple-difference system delivers submetre baseline accuracy using 5-10 minutes of data, under 50 cm accuracy with 30 minutes of data, and between 20-50 cm with 60 minutes of observations.

- This performance is achieved at the 95% level of reliability any time of the day or night, with five or more observed satellites, for baselines under 15 km in length.

- The performance of this system also degrades with increasing baseline length, though not as obviously as the L1 carrier-phase double-difference (ambiguity float) system.

9.2.5 The mixed PC/A-Code and L1 Carrier-Phase System

- The mixed PC/A-code + L1 carrier-phase system delivers baseline accuracies under 2 m with single-epoch data, submetre accuracy with 2 minutes data, under 50 cm with 10 minutes of data, and around 10-20 cm with 60 minutes of data.

- This performance is achieved at the 95% level of reliability any time of the day or night, with five or more observed satellites, for baselines under 15 km in length.

- The mixed code + carrier-phase system gives the most stable solutions. The fact that it is a combination of unambiguous, but coarse, code-derived range measurements and the precise, but ambiguous, carrier-phase measurements, means that stable baseline accuracies are achievable with a minimum of observations. This would be the ideal system to use for those rapid static positioning applications that do not require ambiguity resolution. The mixed PC/A-code + L1 carrier-phase system can be used for applications requiring under 50 cm accuracy with 5-10 minutes of data, or for submetre accuracy with as little as 1 or 2 minutes of data.

9.2.6 The mixed C/A-Code and L1 Carrier-Phase System

- The mixed C/A-code + L1 carrier-phase system could only deliver baseline accuracies around 2-5 m with 1-2 minutes data, under 2 m accuracy with 5 minutes data, submetre accuracy with 10 minutes data, and between 20-50 cm accuracy with 30 minutes of data.

- This performance is achieved at the 95% level of reliability any time of the day or night, with five or more observed satellites, for baselines under 15 km in length.

- The mixed C/A-code + L1 carrier-phase system can be used for applications requiring better than 1 m accuracy, with 5-10 minutes of data. Under benign multipath conditions, a higher level of performance can be expected.

9.2.7 Rapid-Static Positioning with L1-Phase (RSP-L1) System

- This system gave reliable results (i.e. correct ambiguity resolution) with more than 30 minutes of data, with five or more observed satellites, for baselines under 10 km in length. Night time observations would increase the reliability level. For baselines longer than 10 km, one hour or more of data are needed.

- The performance of this system is strongly influenced by the quality of the observations, with multipath (assuming that the cycle slips have been repaired) appearing to be the major contributor to poor data quality. Since the LAMBDA method utilises the VCV information to resolve the ambiguities, the cyclical nature of multipath by introducing further between-epoch data correlation, results in overly optimistic covariance information being provided to the ambiguity resolution algorithm.

- Multipath may also have periods extending for over than an hour and although averaging across the full observation period tends to mitigate the influence, the longer observation spans cannot be considered as being suitable for "rapid" positioning.

- In circumstances when ambiguity resolution is not reliable, solutions using mixed observation type should be use instead.

9.2.8 Low-Cost GPS System Positioning Accuracy Spectrum

A general indication of the performance in terms of achievable accuracy (at the one sigma level - as computed using equation 8.1), for all low-cost system algorithms, utilising five or more observed satellites, is illustrated in Figure 9.2, for baselines under 15 km in length.

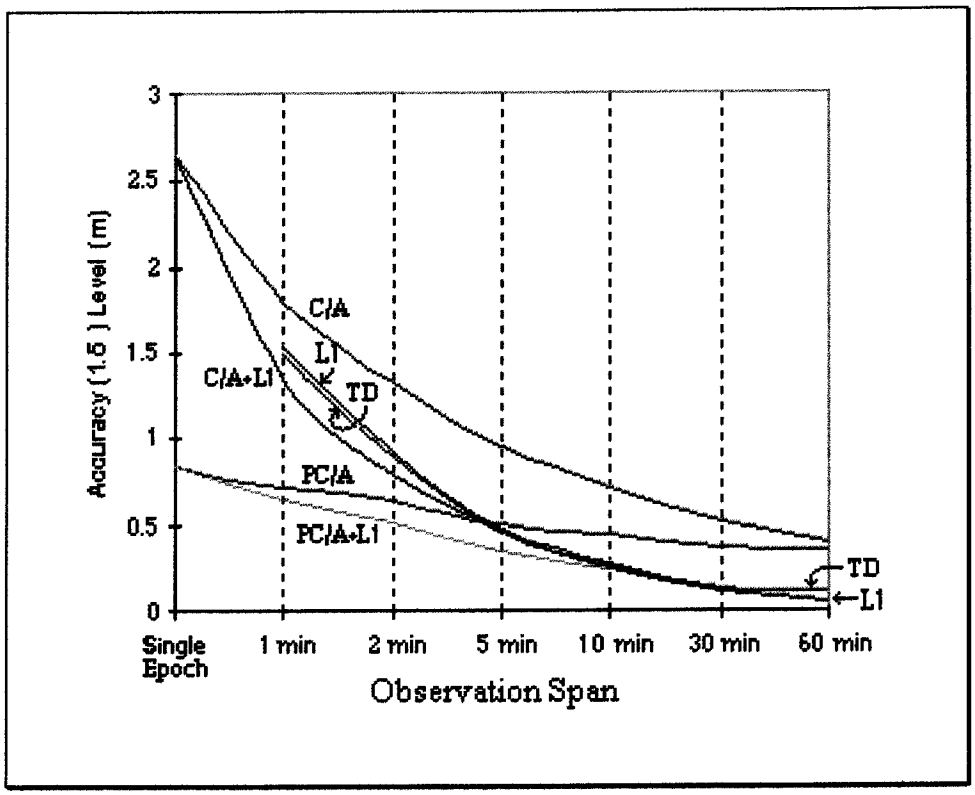

Figure 9.2: Plot of Baseline Solution Accuracy for Various Measurement Types at one sigma level of Reliability (TD - triple-difference; L1 - L1 double-difference ambiguity float; PC/A- precise C/A double-difference; PC/A + L1 - mixed precise C/A-code and L1 carrier-phase double-difference ambiguity float; C/A - standard C/A-code double-difference; C/A + L1 - mixed C/A-code + L1 carrier-phase double-difference ambiguity float)

9.3 RECOMMENDATIONS

Although efforts have been made to ensure that the tests carried out in these investigations are as representative as possible, unforeseen technical and logistic problems have limited the total number of baselines that could be tested. Nevertheless, the conclusions drawn from the analyses have identified several clear performance characteristics of the low-cost GPS system configurations studied. Further bench-marking tests could be done to confirm and extend the relevance of the results of these investigations (remember, all tests were carried out in tropical environments).

The following recommendations are made;

A. ON LOW-COST GPS SYSTEM OPTIONS

A.1 The low-cost GPS systems proposed in these investigations have been restricted to traditional surveying applications. However, there is, in principle, no reason why such systems cannot also be applied to kinematic applications.

A.2 Real-time applications could be addressed with appropriate radio communication links between 'rover' and the 'master' GPS receivers. An example of such a system implementation would an 'alarm-system' for volcano deformation monitoring (Rizos et al., 1996).

A.3 'Ultra-low-cost' GPS sensors could be tested to identify other more cost-effective low-cost GPS system configurations.

B. ON GPS SYSTEM TESTING

B.1 Multipath elimination techniques should be employed - either in hardware or firmware. Alternatively, the multipath signature of the test sites should be studied and somehow filtered-out from the observational data (to ensure 'multipath-free' sites).

B.2 In GPS system performance testing, it is necessary to differentiate between the performance of the GPS system as a whole, and that of the GPS user system. However, at this stage, how this can be done and how to quantify these differences, is still not known.

C. ON STANDARDS AND SPECIFICATIONS FOR MODERATE ACCURACY APPLICATIONS

C.1 For moderate accuracy surveying and mapping applications, various low-cost GPS system configurations are recommended, with matching position accuracy performance summarised in Table 9.1.

Table 9.1: Matching Positioning Accuracy With Low-Cost GPS Systems (at 95% Reliability Level)

Positional Accuracy	Low-Cost GPS System	Observation span
5 m	C/A-code	Single-epoch
2.5 m	PC/A-code C/A-code	Single-epoch 5-10 minutes
1.0 m	PC/A-code Mixed PC/A-code+L1 phase	5-10 minutes 1-2 minutes
0.5 m	Mixed PC/A-code+L1 phase DD or TD L1 phase	5-10 minutes 10-30 minutes
10-30 cm	DD L1 phase (ambiguity float)	60 minutes
<10 cm	DD L1 phase (ambiguity fixed)	60 minutes

Allahu a'lam bis sowab

REFERENCES

Abidin, H. Z., 1993. Computational and geometrical aspects of on-the-fly ambiguity resolution, Ph.D. dissertation, Department of Surveying Engineering Technical Report No. 164, University of New Brunswick, Fredericton, New Brunswick, Canada, 314 pp.

Abidin, H. Z., and M. Subari, 1994. On the discernibility of the ambiguity sets during on-the-fly ambiguity resolution, *Australian Journal of Geodesy, Photogrammetry and Survey*, No. 61, December, pp. 17-40.

Ackroyd, N., and R. Lorimer, 1990. Global navigation: A GPS's user's guide, Lloyd's of London Press Ltd., 202 pp.

Barboux, J.P., 1995. Use of KART principles for real time centimetre surveys, Paper presented at the DSNS 95, Bergen, Norway, April 24-28.

Beutler, G., I. Bauersima, W. Gurtner, and M. Rothacher, 1987a. Correlations between simultaneous GPS double-difference carrier phase observations in the multistation mode: Implementation considerations and first experiences, *Manuscripta Geodaetica*, Vol. 12, pp. 40-44.

Beutler, G., I. Bauersima, W. Gurtner, M. Rothacher, T. Schildknecht, G. L. Mader, M. D. Abell, 1987b. Evaluation of the 1984 Alaska Global Positioning System campaign with Bernese GPS Software, *Journal of Geophysical Research*, 90, pp. 1295-1303.

Beutler, G., W. Gurtner, M. Rothacher, U. Wild, 1989. Relative static positioning with the Global Positioning System: Basic technical considerations, in "Global Positioning System: An Overview", (Bock, Y., and N. Leppard, Eds.), International Association of Geodesy Symposium No. 120, Edinburgh, Scotland, August 7-8, pp. 1-23.

Blewitt, G., 1989. Carrier phase ambiguity resolution for the Global Positioning System applied in geodetic baselines up to 2000km, *Journal of Geophysical Research*, 94, pp. 10,187-10,203.

Bock, Y., R. I. Abbot, C. C. Counselman, S. A. Gourevitch, and R. W. King, 1985. Establishment of three-dimensional geodetic control by interferometry with the Global Positioning System, *Journal of Geophysical Research*, 90 (B9), pp. 7689-7703.

Bock, Y., et al., 1986. Interferometric analysis of GPS phase observation, *Manuscripta Geodaetica*, Vol. 11, No. 4, pp. 282-288.

Braasch, M., 1995. GPS and DGPS multipath effects and modelling, Navtech Seminars Inc. ION GPS-95 Tutorial, September 11, 118 pp.

Braasch, M., 1994-1995. Isolation of GPS multipath and receiver tracking errors, *Navigation*, Journal of the Institute of Navigation, Vol.41, No.4, Winter 1994-1995, pp. 415-434.

Brunner, F. K., and W. M. Welsch, 1993. Effect of the troposphere on GPS measurements. *GPS World*, Volume 4, No. 1, pp. 42-51.

Cannon, M. E., J. F. McLellan, and J. B. Schleppe, 1992. High accuracy static GPS surveys with low-cost receivers, *CISM Journal* ACSGC, Vol.46, No.1, Spring, pp. 9-16.

Cannon, M. E., and G. Lachapelle, 1992. Analysis of a high performance C/A code GPS receiver in kinematic mode, *Navigation*, Journal of the Institute of Navigation, Vol. 39, No. 3, Fall, pp. 285-300.

Chen, D., 1993. Fast Ambiguity Filter (FASF): A novel concept for GPS ambiguity resolution, Proceedings of the ION GPS-93, Salt Lake City, Utah, September 22-24, pp. 781-787.

Clark, D., 1963. Plane and geodetic surveying, Vol.2 - Higher Surveying, Constable & Company Ltd., London, 685 pp.

Conley, R., M. Fryt, and S. Scott, 1995. GPS performance characteristics and trends, Proceedings of ION GPS-95, 8th International Technical Meeting of The Satellite Division of the Institute of Navigation, Palm Springs, USA, September 12-15, pp. 1363-1371.

Danna, P.H, 1996. An overview of the Global Positioning System (GPS), Department of Geography, University of Texas at Austin HomePage at *http://www.utexas.edu/depts/grg/gcraft/notes/gps/gps.html*

Dierendonck, A.J.V., 1995. Understanding GPS receiver terminology: A tutorial, Innovation, *GPS World*, Vol. 6, No. 1, pp. 34-44.

El-Rabbany, A. E-S., 1994. The effect of physical correlations on the ambiguity resolution and accuracy estimation in GPS differential positioning, Ph.D dissertation, Department of Surveying Engineering Technical Report No. 170, University of New Brunswick, Fredericton, New Brunswick, Canada, 161 pp.

Erickson, C., 1992a. An analysis of ambiguity resolution techniques for rapid static GPS surveys using single frequency data, Proceedings of ION GPS-92, Fifth International Technical Meeting of the Satellite Division of The Institute of Navigation, Albuquerque, New Mexico, September 16-18, pp. 453-462.

Erickson, C., 1992b. Investigations of C/A-code and carrier measurements and techniques for rapid static GPS surveys. UCGE Reports Number 20044, The University of Calgary, Canada, 180 pp.

Erickson, C., 1995. GPS positioning guide: A user's guide to the Global Positioning System, Geodetic Survey Division, Geomatics Canada, 110 pp.

Euler, H., and H. Landau, 1992. Fast GPS ambiguity resolution on-the-fly for real-time applications, Proceedings of the 6th International Symposium on Satellite Positioning, Columbus, Ohio, 17-20 March, pp. 650-659.

Federal Geodetic Control Committee (FGCC), 1989. Geometric Geodetic Accuracy Standards and Specifications for Using GPS Relative Positioning Techniques, National Geodetic Survey, United States of America, 48 pp.

Fenton, P., W. Falkenberg, T. Ford, K. Ng, and A. J. Van Dierendonck, 1991. NovAtel's GPS receiver, the high performance OEM sensor of the future, Proceedings of ION GPS-91, The Institute of Navigation, Washington DC, pp. 49-58.

Frei, E. and G. Beutler, 1990. Rapid static positioning based on the Fast Ambiguity Resolution Approach "FARA": Theory and first results, *Manuscripta Geodaetica*, Vol. 15, pp. 325-356.

Fu, W., 1996. A study of GPS and other navigation systems for high precision navigation and attitude determination, PhD dissertation, the School of Geomatic Engineering, University of New South Wales, 333 pp.

Georgiadou, Y., and K.D. Doucet, 1990. The Issue of selective availability. *GPS World*, Sept/Oct. 1990, pp. 53-56.

Goad, C. C., 1985. Precise relative position determination using Global Positioning System carrier phase measurements in nondifferenced mode, Proceedings of the 1st International Symposium on Precise Positioning with Global Position System, April 15-19, Rockville, Maryland, pp. 347-356.

Goad, C. C., 1995. Short distance GPS models, *Lecture Notes*, International School GPS For Geodesy, Delf, The Netherlands, March 26-April 1.

Goodchild, M. F., 1993 An Overview of GPS/GIS Integration, Proceedings of ION GPS-93, Sixth International Technical Meeting of the Satellite Division of The Institute of Navigation, Salt Lake City, Utah, September 22-24, pp. 79 - 83.

GPS World, 1995a. Editorial, Vol. 6, No. 10, October, pp. 10.

GPS World, 1995b. Newsfront, Vol. 6, No. 6, June, pp. 20.

Grant, D. B., C. Rizos, and A. Stolz, 1990. Dealing with GPS biases: Some theoretical and software considerations, in "Contributions to GPS Studies", (Rizos, C., Ed.), UNISURV S-38, the School of Surveying, the University of New South Wales, pp. 1-43.

Green, I. R., C. Smith, and E. J. Tuhoy, 1992. Some applications of GPS position fixing in a resource industry, paper presented at the 18th National Surveying Conference, Cairns, pp. 31-35.

Gurtner, W., G. Mader, and D. Mac Athur, 1989a. A common exchange format for GPS data, in Proceedings of the Fifth International Symposium on Satellite Positioning, Las Cruces, New Mexico, 13-17 March, pp 920-931.

Gurtner, W., W, Beutler, M. Rothacher, 1989b. Combinations of GPS observations made with different receiver types, in Proceedings of the Fifth International Symposium on Satellite Positioning, Las Cruces, New Mexico, 13-17 March, pp 362-374.

Han, S., and C. Rizos, 1995a. Standardisation of the variance-covariance matrix for GPS rapid static positioning, *Geomatic Research Australasia*, No.62, June, pp. 37-54.

Han, S. 1995. Ambiguity resolution techniques using least squares estimation for rapid static or kinematic positioning, paper presented at the Satellite Navigation Technology: 1995 and Beyond, Brisbane, Queensland, June 26-28.

Han, S., and C. Rizos, 1995b. A new method for constructing multi-satellite ambiguity combinations for improved ambiguity resolution, Proceedings of ION GPS-95, 8th International Technical Meeting of The Satellite Division of the Institute of Navigation, Palm Springs, USA, September 12-15.

Han, S., and C. Rizos, 1996. Integrated method for instantaneous ambiguity resolution using new generation GPS receivers, Proceedings of the IEEE PLANS'96, Atlanta, 22-26 April, pp. 254-261.

Harvey, B. R., 1994. Practical Least Squares and Statistics for Surveyors, Monograph 13, School of Surveying, The University of New South Wales, Australia, 319 pp.

Hatch, R., 1982. The synergism of GPS code and carrier measurements, Proceedings the Third International Geodetic Symposium on Satellite Doppler Positioning, Las Cruces, New Mexico, February 8-12, pp. 1213-1231.

Hatch, R., 1986. Dynamic differential GPS at the centimeter level. Proceedings of the Fourth International Geodetic Symposium on Satellite Positioning, Austin, Texas, April 28 - May 2, pp. 1287-1298.

Hatch, R., 1990. Instantaneous ambiguity resolution, in Kinematic systems in Geodesy, Surveying and Remote Sensing, IAG Symposium No. 107, Banff, Alberta, Canada, September 10-13, pp. 299-308.

Heroux, P., and A. Kluesberg, 1989. GPS precise relative positioning and ionosphere in auroral regions, in Proceedings of the Fifth International Symposium on Satellite Positioning, Las Cruces, New Mexico, 13-17 March, pp 475-486.

Hofmann-Wellenhof, B., H. Lichtenegger, and J. Collins, 1994. *GPS Theory and Practice*, Springer-Verlag, Vienna, New York, 3rd Ed., 355 pp.

Inter-Governmental Advisory Committee on Surveying and Mapping (IGACSM), 1994. Standards and Specifications for Control Surveys, Publication No.1, July.

ION Newsletter, 1995. The Quarterly Newsletter of The Institute of Navigation, Vol. 5, No. 3, Fall. 12 pp.

Jin, XX. 1995. The relationship between satellite elevation and the accuracy of GPS code observations, the 4th International Conference on Differential Satellite Navigation Systems, Bergen, Norway. April 24-28.

Johns, J.C., and R. Conley, 1994. A summary of GPS SPS performance as observed by the FAA's GPS Performance Analysis Network, Proceedings of ION GPS-94, Seventh International Technical Meeting of the Satellite Division of The Institute of Navigation, Salt Lake City, Utah, September 20-23, pp. 1117-1125.

Kalafus, R. M., 1991. Elevating differential GPS to practice, First International Symposium Real Time Differential Applications of the Global Positioning system, Braunschweig, FRG, September 16-20, pp. 476-483.

Klobuchar, J.A., 1987. Ionospheric time-delay algorithm for single-frequency GPS users, IEEE Transactions on Aerospace and Electronic Systems, Vol. AES-23 No. 2, pp. 325-331.

Klobuchar, J. A., 1991. Ionospheric effects on GPS, *GPS World*, Vol. 2 No. 4 April, reprint.

Lachapelle, G., M. E. Cannon, and G. Lu, 1992. Ambiguity resolution on-the-fly - A comparison of P-code and high performance C/A-code receiver technologies, Proceedings of ION GPS-92, Fifth International Technical Meeting of the Satellite Division of The Institute of Navigation, Albuquerque, New Mexico, September 16-18, pp. 1025-1032.

Lachapelle, G., C. Liu, and G. Lu, 1993. Quadraple single frequency receiver system for ambiguity resolution on the fly. Proceedings of ION GPS-93, Sixth International Technical Meeting of the Satellite Division of The Institute of Navigation, Salt Lake City, Utah, September 22-24, pp. 1167-1172.

Landau, H., and H. J. Euler, 1992. On-the-fly ambiguity resolution for precise differential positioning, Proceedings of ION GPS-92. Fifth International Technical Meeting of the Satellite Division of The Institute of Navigation, Albuquerque, New Mexico, September 16-18, pp. 607-613.

Langley, R.B., 1991. The GPS receiver: An Introduction, *GPS World*, Vol. 2, No. 1, January, reprint.

Leick, A. 1995. *GPS Satellite Surveying*, Second Edition, John Wiley and Sons, New York. 560 pp.

Lin, L. S., and C. Rizos, 1996. Real-time estimation of ionospheric delays using GPS. Paper presented at the International Conference on GPS, Paper No. 10., Taipei, Taiwan, June 12-15.

Lu, G., 1995. Development of a GPS multi-antenna system for attitude determination, UCGE Report No. 20073. Department of Geomatics Engineering, the University of Calgary, Canada, 185 pp.

Lukac, C. F., and Q. Zhuang, 1989. Comparison between geodetic survey results and GPS positioning using C/A code receiver, Proceedings of the 5th International Geodetic Symposium on Satellite Positioning, Las Cruces, New Mexico, March 13-17, pp. 1083-1089.

Mader, G. L., 1990. Ambiguity Function Technique for GPS phase initialization and kinematic solutions. Proceedings of Second International Symposium on Precise Positioning with the Global Positioning System, Ottawa, Canada, September 3-7, pp. 1233-1247.

Masters, E. G., C. Rizos, and B. Hirsch, 1993. GPS for GIS, Proceedings of the Land Information Management and Geographic Information Systems, Monograph 15, Vol. 1, School of Surveying, The University of New South Wales, pp. 157-163.

Masters, E.G., C. Rizos, and B. Hirsch, 1994. GPS...More than a real world digitizer, Proceedings of the IEEE PLANS'94, Las Vegas, Nevada, April 11-15, pp. 381-387.

Mekenkamp, P. G. M., 1994. Global changes and GIS accuracy, XX Congress, International Federation of Surveyors, Commission 3, Melbourne, Australia, March 5-12.

Merminod, B., 1990. Resolution of the cycle ambiguities, in "Contributions to GPS Studies", (Rizos, C., Ed.), UNISURV S-38, the School of Surveying, the University of New South Wales, pp. 103-154.

Merminod, B., and C. Rizos, 1994. Optimization of rapid static GPS surveys, *Manuscripta Geodaetica*, Vol.19,, pp. 231-246.

Mourad, A. G, and D. M. J. Fubara, 1974. Requirements and applications of marine geodesy and satellite technology to operations in the oceans, Proceedings of International Symposium on Applications of Marine Geodesy, pp 15-27.

Nolan, J. M., I. R. Webster, S. A. Gourevitch and J. W. Ladd, 1992. Rapid static surveying with an operational GPS system, Proceedings of ION GPS-92. Fifth International Technical Meeting of the Satellite Division of The Institute of Navigation, Albuquerque, New Mexico, September 16-18, pp. 453-462.

NovAtel, 1994. GPSCard OEM Series Installation and Operating Manual, OM-20000007 Rev. 1.0, NovAtel Communications Ltd., Canada, 39 pp.

Ostensen, O., 1994. Framework of European standardisation in the field of geographic information, XX Congress, International Federation of Surveyors, Commission 3, Melbourne, Australia, March 5-12.

Philip Business Information, 1995, GPS Directory, Fall, Seventh Edition, Philip Business Information Inc., 220 pp.

Qiu, W., 1993. An analysis of some critical errors sources in static GPS surveying, UCGE Reports Number 20054, Department of Geomatic Engineering, University of Calgary, 102 pp.

Remondi, B. J., 1984. Using the Global Positioning System (GPS) phase observable for relative geodesy: Modeling, processing, and results, Ph.D dissertation, Center for Space Research, The University of Texas at Austin, 360 pp.

Rizos, C., R. Galas, and C. Reigber, 1996. Design challenges in the development of a GPS-based volcano monitoring system. Paper presented in The 8th FIG International Symposium on Deformation Measurements, Hong Kong, June 25-28.

Rizos, C., M. Subari, and W.X. Fu, 1994. The use of low-cost GPS navigation receivers for survey applications, XX Congress, International Federation of Surveyors, Commission 5, Melbourne, Australia, March 5-12.

Rizos, C., M. Subari, and W.X. Fu, 1995. Appropriate GPS technology for sub-half-metre accuracy applications: Observation modelling for low-cost receiver hardware, Paper presented in The 5th South East Asian and 36th Australian Surveyors Congress, Singapore, July 16-20.

Rizos, C., 1996. Principles and Practice of GPS Surveying, *Lecture Notes*, School of Geomatic Engineering, the University of New South Wales, Australia.

Rizos, C. M. Subari, and W. Fu, 1995. Appropriate GPS technology for sub-half-metre accuracy applications: Observation modelling for low-cost receiver hardware, paper presented at the 5th SEA and 36th Australian Surveyors Conference, Singapore, July 16-20.

Seeber, G. 1993. *Satellite Geodesy, Foundations, Methods and Applications*, Walter de Gruyter, Berlin. New York, 531 pp.

Shrestha, R. L, Dewitt, B. A., and Wilson, M. M., 1995. Consideration and effect of a local base station range in horizontal position determination by GPS techniques, in Surveying and Land Information Systems, Vol. 55, No. 1, pp. 39-49.

Subari, M.,1996. Mixing low-cost GPS receiver with a standard surveying receiver, Paper submitted to the Buletin Ukur, Universiti Teknologi Malaysia.

Subari, M., and C. Rizos, 1995a. Low-cost GPS surveying package, *The Surveyors*, Institute of Surveyors Malaysia, Malaysia, Vol. , No. 4, pp. 27-33.

Subari, M., and C. Rizos, 1995b. Addressing surveying and mapping:- Economical considerations vis-a-vis the use of Global Positioning System, Technical Proceedings of The 5th South East Asian and 36th Australian Surveyors Congress, Singapore, July 16-20, pp. 383-394.

Subari, M., and C. Rizos, 1995c. Weighting costs and profits of GPS system, *GIM*, Vol.9, No.12, December, pp. 53-59.

Subsuantaeng, S., 1990. A PC-based GPS data processing software package, Masters Thesis, School of Surveying, The University of New South Wales, 136 pp.

Teunissen, P. J. G., 1994. A new method for fast carrier phase ambiguity estimation, IEEE PLANS'94, Las Vegas, Nevada, April 11-15, pp. 562-573.

Thompson, D. B, D. E. Wells, and W. H. Falkenberg, 1983. Hydrographic Surveying, UCSE Report No. 10002. Department of Surveying Engineering, the University of Calgary, Canada, 257 pp.

Tolman, B. W., J. R. Clynch, D. S. Coco, and M. P. Leach, 1990. The effect of Selective Availability on Differential GPS positioning, Proceedings of The Second International Symposium on Precise Positioning with the Global Positioning System, Ottawa, Canada, September 3-7, pp. 34-49.

Torge, W., 1980. Geodesy, Walter de Gruyter, Berlin . New York, 254 pp.

Townsend, B., and P. Fenton. 1994. A practical approach to the reduction of pseudorange multipath errors in a L1 GPS receiver, Proceedings of ION GPS-94, Seventh International Technical Meeting of the Satellite Division of The Institute of Navigation, Salt Lake City, Utah, September 20-23, pp. 143-148.

Trimble, 1990. SVeeSix Manual, Revision D, Trimble Navigation Ltd., USA.

Uotila, U, 1985. Adjustment Computations, *Lecture Note*, Department of Geodetic Science, the Ohio State University.

Van Dierendonck, A.J., P. Fenton, and T. Ford, 1992. Theory and performance of narrow correlator spacing in a GPS receiver, ION National Technical Meeting, San Diego, California, January 27.

Wang, Y.J., 1995. Monitoring ionospheric TEC using GPS, IPS Radio and Space Services Internal Report, Department of Administrative Services, Australia, 33 pp.

Wassef, A. M., 1986. Bias in GPS positioning by improper weighting of data, Proceedings of the Fourth International Geodetic Symposium on Satellite Positioning, Austin, Texas, April 28 - May 2, pp. 705-719.

Weill, L.R, 1992. Submeter positioning with a low-cost hand-held receiver, Proceedings of the 5th International Technical Meeting, Satellite Division of The Institute of Navigation, Albuquerque, New Mexico, September 16-18, pp. 647-653.

Wells, D. E., N. Beck, D. Delikaraoglou, A. Kleusberg, E. J. Krakiwsky, G. Lachapelle, R. B. Langley, M. Nakiboglu, K. P. Schwarz, J. M. Tranquilla, P. Vanicek, 1986. *Guide to GPS Positioning*, Canadian GPS Associates, Fredericton, N. B., Canada.

Publications from

THE SCHOOL OF GEOMATIC ENGINEERING

(Formerly School of Surveying)

THE UNIVERSITY OF NEW SOUTH WALES

All prices include postage by surface mail. Air mail rates on application. (Effective August 1997)

To order, write to Publications Officer, School of Geomatic Engineering
The University of New South Wales, Sydney 2052, AUSTRALIA

NOTE: ALL ORDERS MUST BE PREPAID

UNISURV REPORTS - S SERIES

S8 - S20	Price (including postage) :		$10.00
S29 onwards	Price (including postage) :	Individuals	$25.00
		Institutions	$30.00

S8 A. Stolz, "Three-D Cartesian co-ordinates of part of the Australian geodetic network by the use of local astronomic vector systems", Unisurv Rep. S8, 182 pp, 1972.

S10 A.J. Robinson, "Study of zero error & ground swing of the model MRA101 tellurometer", Unisurv Rep. S10, 200 pp, 1973.

S12. G.J.F. Holden, "An evaluation of orthophotography in an integrated mapping system", Unisurv Rep. S12, 232 pp, 1974.

S14. Edward G. Anderson, "The Effect of Topography on Solutions of Stokes` Problem", Unisurv Rep. S14, 252 pp, 1976.

S16. K. Bretreger, "Earth Tide Effects on Geodetic Observations", Unisurv S16, 173 pp, 1978.

S17. C. Rizos, "The role of the gravity field in sea surface topography studies", Unisurv S17, 299 pp, 1980.

S18. B.C. Forster, "Some measures of urban residential quality from LANDSAT multi-spectral data", Unisurv S18, 223 pp, 1981.

S19. Richard Coleman, "A Geodetic Basis for recovering Ocean Dynamic Information from Satellite Altimetry", Unisurv S19,332 pp, 1981.

S20. Douglas R. Larden, "Monitoring the Earth's Rotation by Lunar Laser Ranging", Unisurv Report S20, 280 pp, 1982.

S29 Gary S Chisholm, "Integration of GPS into hydrographic survey operations", Unisurv S29, 190 pp, 1987.

S30. Gary Alan Jeffress, "An investigation of Doppler satellite positioning multi-station software", Unisurv S30, 118 pp, 1987.

S31. Jahja Soetandi, "A model for a cadastral land information system for Indonesia", Unisurv S31, 168 pp, 1988.

S33. R. D. Holloway, "The integration of GPS heights into the Australian Height Datum", Unisurv S33, 151 pp.,1988.

S34. Robin C. Mullin, "Data update in a Land Information Network", Unisurv S34, 168 pp. 1988.

S35. Bertrand Merminod, "The use of Kalman filters in GPS Navigation", Unisurv S35, 203 pp., 1989.

S36. Andrew R. Marshall, "Network design and optimisation in close range Photogrammetry", Unisurv S36, 249 pp., 1989.

S37. Wattana Jaroondhampinij, "A model of Computerised parcel-based Land Information System for the Department of Lands, Thailand," Unisurv S37, 281 pp., 1989.

S38. C. Rizos (Ed.), D.B. Grant, A. Stolz, B. Merminod, C.C. Mazur "Contributions to GPS Studies", Unisurv S38, 204 pp., 1990.

S39. C. Bosloper, "Multipath and GPS short periodic components of the time variation of the differential dispersive delay", Unisurv S39, 214 pp., 1990.

S40. John Michael Nolan, "Development of a Navigational System utilizing the Global Positioning System in a real time, differential mode", Unisurv S40, 163 pp., 1990.

S41. Roderick T. Macleod, "The resolution of Mean Sea Level anomalies along the NSW coastline using the Global Positioning System", 278 pp., 1990.

S42. Douglas A. Kinlyside, "Densification Surveys in New South Wales - coping with distortions", 209 pp., 1992.

S43. A. H. W. Kearsley (ed.), Z. Ahmad, B. R. Harvey and A. Kasenda, "Contributions to Geoid Evaluations and GPS Heighting", 209 pp., 1993.

S44. Paul Tregoning, "GPS Measurements in the Australian and Indonesian Regions (1989-1993)", 134 + xiii pp, 1996.

S45. Wan-Xuan Fu, "A study of GPS and other navigation systems for high precision navigation and attitude determinations", 332pp, 1996.

S46. Peter Morgan et al, "A zero order GPS network for the Australia region", 187 + xii pp, 1996.

S47. Yongru Huang, "A digital photogrammetry system for industrial monitoring", 145 + xiv pp, 1997.

S48. Kim Mobbs, "Tectonic interpretation of the Papua New Guine Region from repeat satellite measurements", 256 + xc pp, 1997.

S49. Shaowei Han, "Carrier phase-based long-range GPS kinematic positioning", 185 + xi pp, 1997.

S50. Mustafa D Subari, "Low-cost GPS systems for intermediate surveying and mapping accuracy applications", 179 + xiii pp, 1997.

MONOGRAPHS

Prices include postage by surface mail

		Price
M1.	R.S. Mather, "The theory and geodetic use of some common projections", (2nd edition), 125 pp., 1978.	$15.00
M2.	R.S. Mather, "The analysis of the earth's gravity field", 172 pp., 1971.	$8.00
M3.	G.G. Bennett, "Tables for prediction of daylight stars", 24 pp.,1974.	$5.00
M4.	G.G. Bennett, J.G. Freislich & M. Maughan, "Star prediction tables for the fixing of position", 200 pp., 1974.	$8.00
M8.	A.H.W. Kearsley, "Geodetic Surveying", 96 pp, (revised) 1988.	$12.00
M11.	W.F. Caspary, "Concepts of Network and Deformation Analysis",183 pp., 1988.	$25.00
M12.	F.K. Brunner, "Atmospheric Effects on Geodetic Space Measurements", 110 pp., 1988.	$16.00
M13.	Bruce R. Harvey, "Practical Least Squares and Statistics for Surveyors", (2nd edition), 319 pp., 1994.	$30.00
M14.	Ewan G. Masters & John R. Pollard (Ed.), "Land Information Management", 269 pp., 1991. (Proceedings LIM Conference, July 1991).	$20.00
M15/1	Ewan G. Masters & John R. Pollard (Ed.), "Land Information Management - Geographic Information Systems - Advance Remote Sensing Vol 1" 295 pp., 1993 (Proceedings of LIM & GIS Conference, July 1993).	$30.00
M15/2	Ewan G. Masters & John R. Pollard (Ed.), "Land Information Management - Geographic Information Systems - Advance Remote Sensing Vol 2" 376 pp., 1993 (Proceedings of Advanced Remote Sensing Conference, July 1993).	$30.00
M16.	A. Stolz, "An Introduction to Geodesy", 112 pp., 1994.	$20.00
M17	Chris Rizos, "Principles and Practice of GPS Surveying", 565 pp., 1997.	$50.00